Mississippi Mound Trail:

Phase III Investigations

Report prepared by:
Jay K. Johnson
Samuel Butz
Gabriel Coggin
Todd McLeod

The Center for Archaeological Research
University of Mississippi
December 2016

Contents

List of Figures

List of Tables

Introduction

As a final phase of the Mound Trail Project, the Center for Archaeological Research at the University of Mississippi conducted geophysical survey of nine selected Mound Trail sites. The contract called for the downhole magnetic susceptibility exploration of nine mounds along the route, three in each of the three segments of the route. In addition, gradiometer survey was to be conducted at three sites located in the middle and southern segments of the route. As always, when you're doing archaeological research, plans change. For example, we had hoped to do a downhole survey on the Johnson Cemetery mound in order to add to the very interesting mound strata that we exposed in the slope trench. However, uneasy about having auger holes placed in a mound with historic burials, the property owner, who is a descendant of the people buried on the mound, decided that she did not want us to disturb the top of the mound. In another example, we had planned to do a gradiometer survey at Smith Creek but John O'Hear, in consultation with Meg Kassabaum, determined that the open areas at the site appear to have been badly disturbed so we settled for just downhole survey at that site. Similar decisions made in consultation with the archaeologists working in the three portions of the Mound Trail survey led to a list of sites which differs from the original list but did produce important results on many of the sites (Table 1). With a few notable exceptions, the downhole magnetic susceptibility survey was disappointing. However, negative results are important also. We did demonstrate in all but one case that intact burned surfaces were not present, at least in the center of the mounds. As usual, the gradiometer surveys were more satisfying in that we found evidence for relatively intact structures on exactly half of the sites we surveyed.

We began the fieldwork on Mound A at Hollywood on October 9, 2014 and concluded the fieldwork at the Dunn Mound on June 30, 2015 which was Johnson's last day before he retired. The initial field crew consisted of Jay Johnson, Sam Butz, Todd McLoud, and Gabby Coggin. This was the crew that joined Jessica Kowalski at Arcola late in October of 2014. We stayed in a cabin at Leroy Percy State Park and drove into Greenwood to watch the Ole Miss and LSU game. We also recorded some very informative gradiometer imagery in the fields surrounding the mounds at Arcola. Sam graduated and took a job in May, leaving the reduced crew to complete the project. In addition to helping us lay grid and pull ropes at Arcola, Jessica and Ed Jackson joined us at Aden. Both provided general advice on the central section of the Mound Trail. John O'Hear served as overall coordinator on the project as well as joining us in January and June of 2015 in Natchez to do the fieldwork on the southern section of the project. As usual, Jay and John took advantage of Lee and Sherry Jones' hospitality in Natchez and stayed in their guest house.

Table 1 Sites tested.

Site No.	Name	National Register Status	Period	Gradiometer	Downhole
22Tu500	Hollywood	NHRP 1982	Mississippian		X
22Tu513	Beaverdam	NHRP 1972	Mississippian		X
22Co632	Dunn	Eligible	Mississippian		X
22Ws500	Winterville	NHRP 1973	Mississippian		X
22Ws516	Arcola	NHRP 1991	Mississippian	X	X
22Is509	Aden	NHRP 1988	Woodland	X	
22Ad503	Foster	NHRP 1982	Mississippian	X	
22Wk504	Lessley	Eligible	Mississippian	X	X
22Wk526	Smith Creek	NHRP 1978	Woodland		X

Gradiometer Survey

Field methods

If archaeologists had to pick only one geophysical survey instrument to use, most would pick a magnetic gradiometer. On many sites, it provides what amounts to a map showing structures, berms, ditches, and mound remnants. On early contact period sites as well as historic sites, the distribution of metal artifacts and bricks make it possible to locate structures and activity areas. The gradiometer measures two kinds of magnetic information, remnant magnetism and magnetic susceptibility (Clark 1996; Gafney and Gater 2003; Kvamme 2006). On archaeological sites, remnant magnetism occurs when material which contains iron is heated above 575-675 degrees Celsius. At that point the iron molecules align with the magnetic poles of the earth and retain that alignment after cooling. This is why gradiometer surveys on Mississippian period sites in the Yazoo Basin have been so successful (e.g. Haley 2014; Nelson 2014; Reynolds 2002). When wall trench structures burn, their clay floors are often heated sufficiently to become magnetic.

Magnetic susceptibility is measured by introducing a magnetic field and recording the response. The most common instrument used on archaeological sites to measure susceptibility is the Geonics EM38. This instrument uses a magnetic coil to project a magnetic field into the soil and records the results. However, metal artifacts containing iron respond so well that the Earth’s magnetic field is sufficient to provide a signal that can be measured using a gradiometer. Soils that are rich in organic material also develop magnetic susceptibility as they age (Dahlin 2006). So, midden, for example, can also be detected using a gradiometer.

Because gradiometer surveys are conducted by walking the instrument back and forth across an area in a regular pattern, they work best on sites where there are few obstructions since every time you come to a tree, you have to stop the instrument, record the portion of the survey line blocked by the tree, and start the instrument over again on the other side of the tree. Fortunately, the plaza and village areas of most of the Mound Trail sites are in cultivation or pasture. We began each survey by laying out a 20m grid using a Leica total station. The grids were oriented as close as possible to the cardinal directions but we have learned that the instrument we use, the Bartington Grad601-2, is not particularly sensitive to the orientation of the traverse as long as that orientation is consistent. Therefore, whenever possible, the grids were oriented to align with fences and field roads so that there would be as few partial grids as possible. Each grid is recorded by walking parallel transects at fixed intervals in a zig zag pattern along plastic lines with colored marks at each meter commonly called ropes by archaeologists. The marks allow the operator to set a regular pace so that readings are recorded at fixed intervals. Since we were looking for large things like burned structures, we used a one meter line interval and recorded measurements at every 25cm along those lines.

The resultant data were downloaded to a computer and processed using Geoscan Research's Geoplot 3.0, a software that was created to deal with archaeological remote sensing data. Geoplot provides several processing options which smooth and enhance the data as well as stitch the several 20m grids used to cover the survey area into a single image. This image was then exported as a Surfer grid file and processed using Golden Software's Surfer 10 mapping program to further process the data and produce a file which could be imported into ESRI's ArcGIS 10.3 GIS software and integrated with other spatial data. The gradiometer imagery was georeferences using ground control point, usually the corners of the overall survey grid that were recorded in the field using a Trimble GPS. The final step in the processing consisted of creating a data layer in the GIS on which probable archaeological features were identified.

Arcola

When we met Jessica at Arcola on the first day of the survey, we were presented with a particular challenge. The fields surrounding the mounds had been recently disced, leaving long, deep east-west furrows. It is critical to keep the elevation of the instrument about the surface of the survey area constant while surveying which is one of the reasons that the Bartington gradiometer comes with a harness. If we had run north-south transected, crossing the furrows, that would have been impossible. Therefore, we decided to set up the survey so that the transects ran east-west, following the furrows (fig. 1). There was, however another problem. Not surprisingly, the farm machinery used in discing the field was not metric. The rows were space approximately 96cm apart. However, they were absolutely straight. Therefore, we set up the grid corners so that each grid measured 20m east-west and 19.2m north-south. The ropes were run east-west along the tops of the furrows and the surveyor walked in the valleys between the ropes (fig. 2). We shot the corners of each survey area in using a Trimble GPS and used those points to georeferenced the gradiometer image. Using this strategy, we covered 1.65ha (4.08 acres) in two survey blocks surrounding the mounds on either side of the field road that separates Mounds A and B from Mound C (fig. 3). We covered the spread of the distribution of artifacts on the surface of the fields.

Although the survey to the east of the road and south of Mound C failed to recorded and evident prehistoric features, the survey that included the fields north, east, and south of Mound was more successful (figs. 3-5). The most obvious feature is the dense scatter of metal debris north of Mound B. This was likely the location of a tenant house. There are, however, several features evident in the imagery of the areas north of Mound A and between Mounds A and B. The ones that are easiest to identify are rectangular patterns of low amplitude positive return often surrounded by low negative values (figs 5, 6, Table 2). These rectangles are similar in size to Mississippian period house structures and several years of testing these features on Mississippian sites in the northern Yazoo Basin (Haley 2014; Nelson 2014; Reynolds 2002) make it clear that these are the remains of burned Mississippian structures, probably domestic houses based on their size. We have uncovered similar structures on the tops of Mississippian mounds which are generally larger in size and are likely the remains of more specialized ritual or status habitation (Stevens 2006). The second class of probable prehistoric features are relatively small areas of low amplitude, positive return. These could be midden pits, large post holes, or fragments of structures disturbed by more than a century of cultivation (figs.5, 6, Table 2). The gradiometer imagery was provided to Kowalski prior to the beginning of her dissertation field work. We also did a downhole magnetic susceptibility survey of the top of Mound A at Arcola. Those results will be presented in the section on that instrument.

Figure 1 Gradiometer survey at Arcola, Mound A in the background, Sam Butz, Todd McLoud, and Jessica Kowalski, view to the northwest.

Figure 2 Gradiometer survey to the south of Mound A at Arcola, Sam Butz and Jessica Kowalski, view to the west.

Figure 3 Arcola, gradiometer image and recent aerial image.

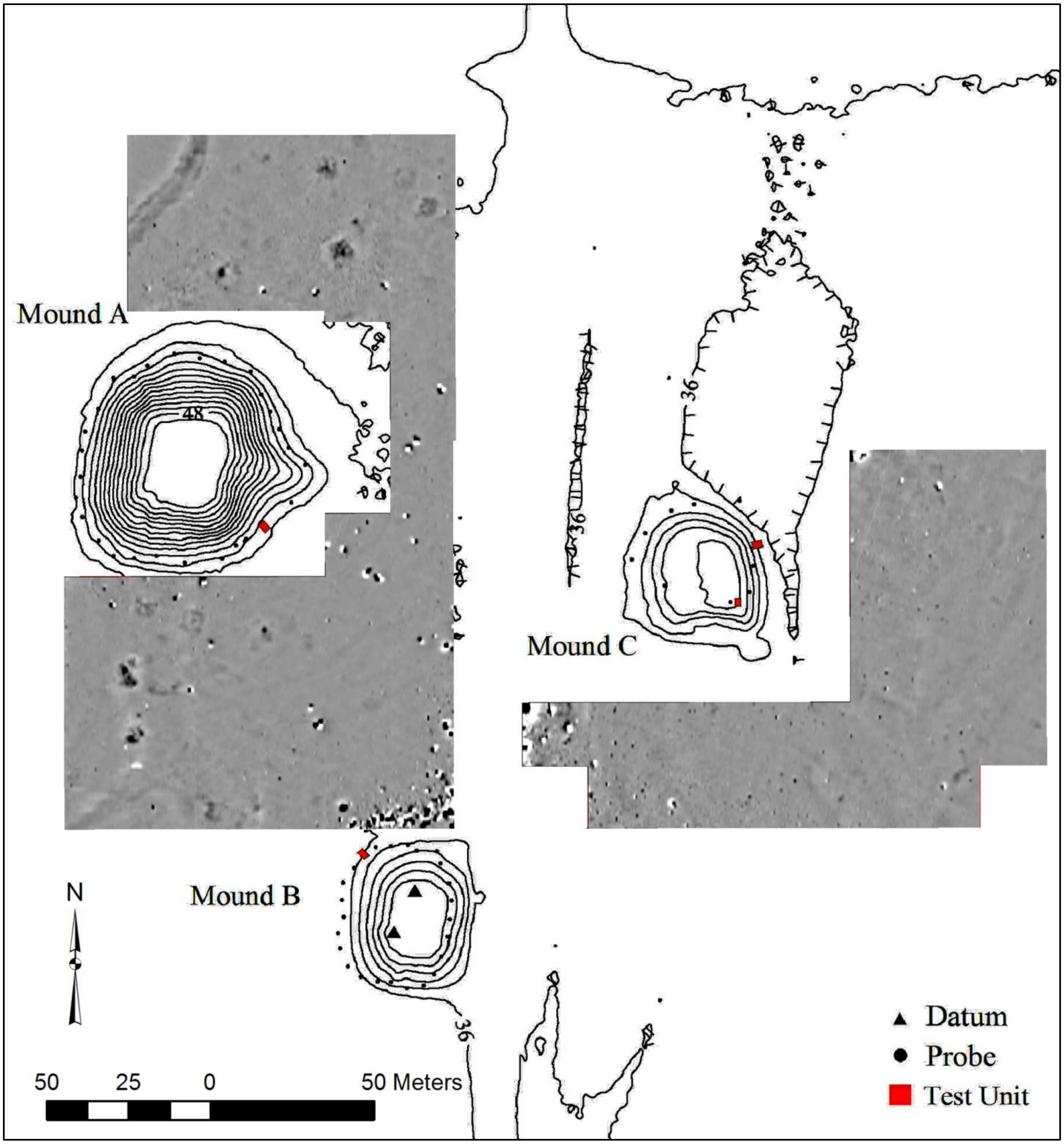

Figure 4 Arcola, gradiometer image, LiDAR generated contour map, and Phase II test pit locations (after Jackson and Kowalski 2015:fig. 2.1).

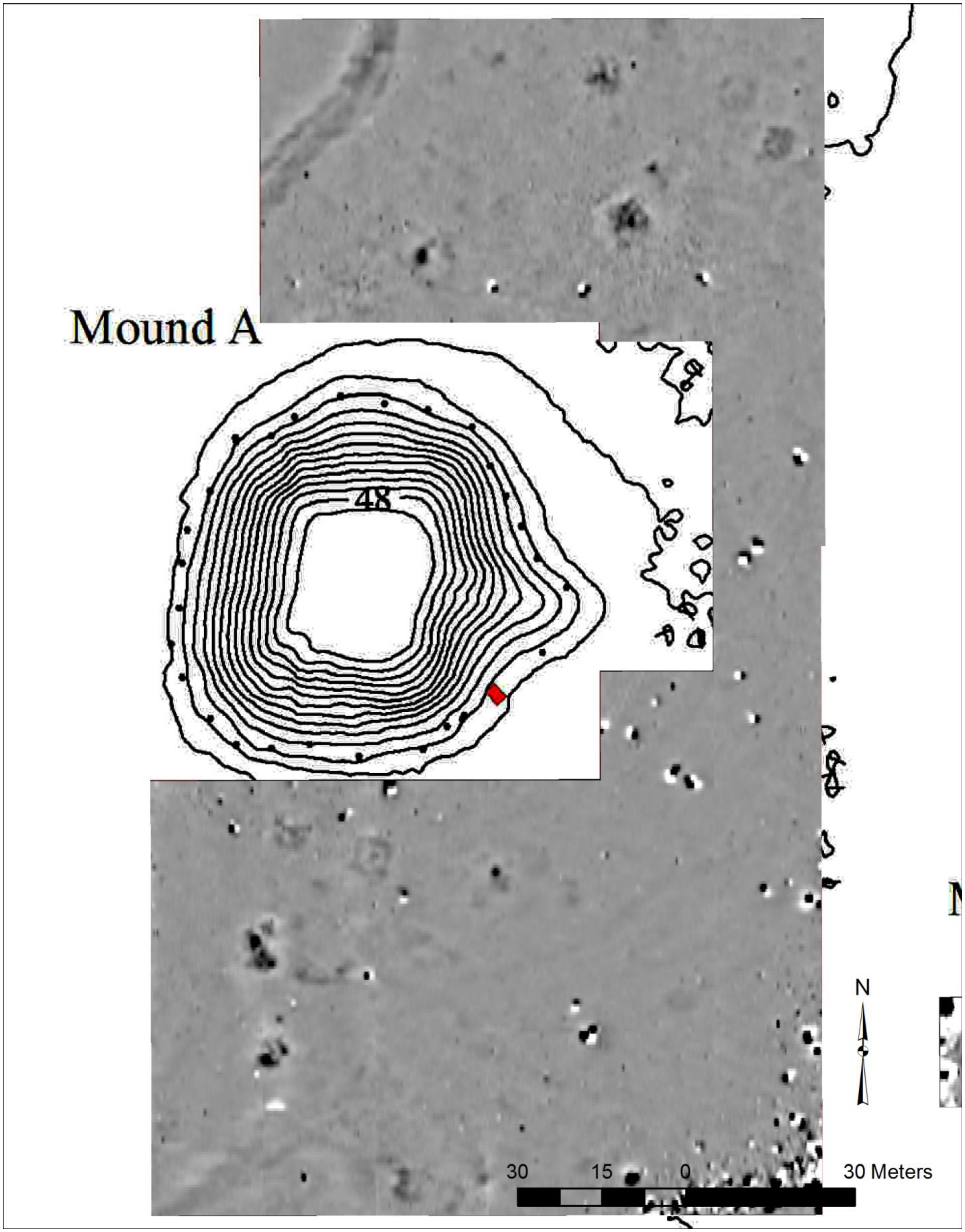

Figure 5 Arcola, gradiometer image near Mound A.

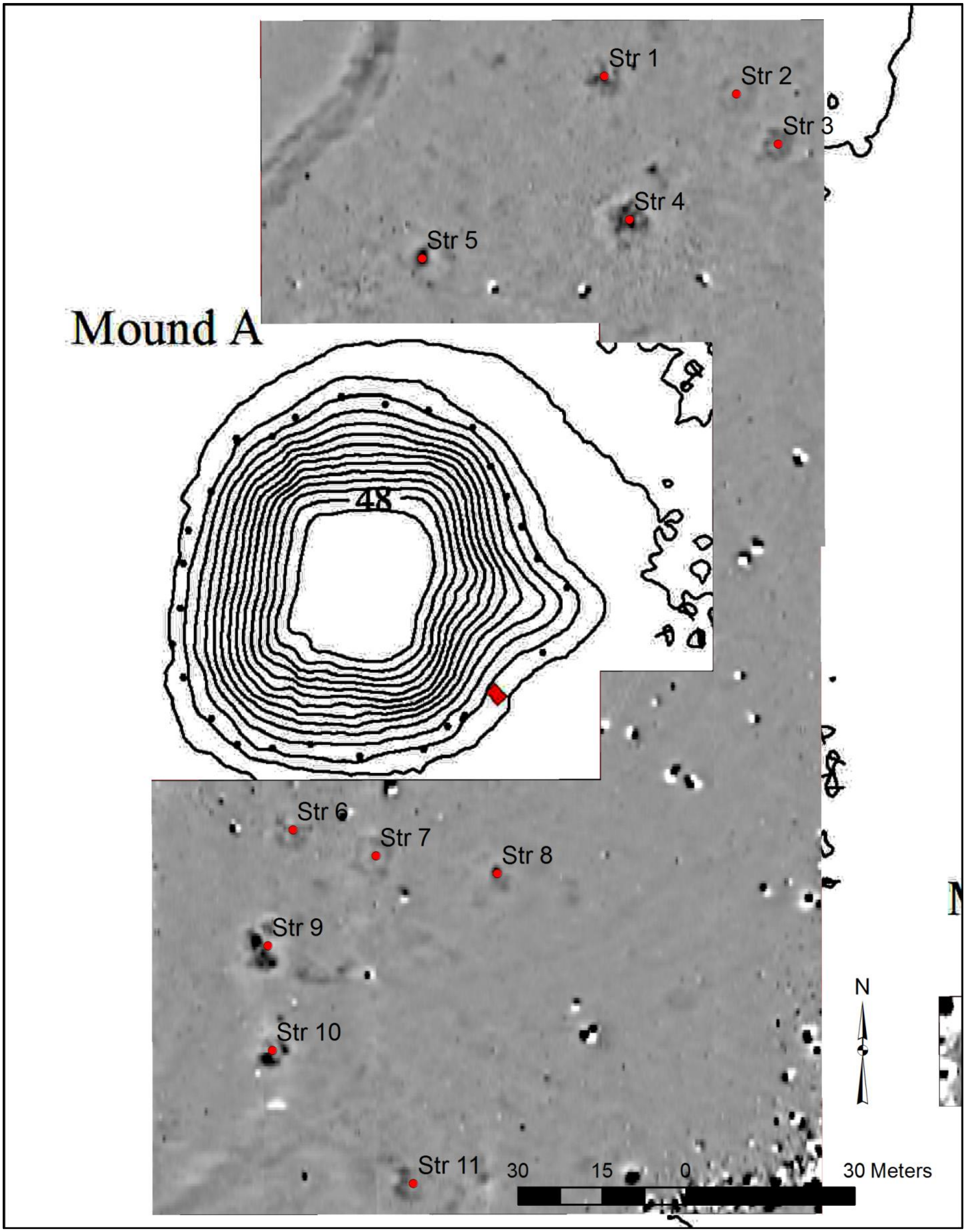

Figure 6 Arcola, gradiometer image near Mound A with possible structure locations marked.

Table 2 Possible structure locations at Arcola.

Label	Easting	Northing	Description
Str 1	697,273.88	3,680,548.85	low amplitude positive feature
Str 2	697,297.37	3,680,545.68	rectangular pattern
Str 3	697,304.83	3,680,536.79	rectangular pattern
Str 4	697,278.32	3,680,523.29	rectangular pattern
Str 5	697,241.49	3,680,516.47	low amplitude positive feature
Str 6	697,218.47	3,680,414.87	rectangular pattern
Str 7	697,233.24	3,680,410.26	rectangular pattern
Str 8	697,254.83	3,680,407.09	low amplitude positive feature
Str 9	697,214.03	3,680,394.23	low amplitude positive feature
Str 10	697,214.82	3,680,375.65	low amplitude positive feature
Str 11	697,239.90	3,680,352.00	rectangular pattern

Aden

We met Ed Jackson and Jessica Kowalski at the Aden mounds in early June, 2015. The area between the mounds had been planted in corn which was about knee high and we used a survey technique similar to the one we developed at Arcola. That is, the transects followed the rows which ran in an east, southeast direction (fig. 7). Each grid was 20 rows wide and 20m long. We recorded the UTM coordinates of the corners of the survey area using a GPS and used those coordinates to georeference the imagery. A 1.65ha (4.08 acres) block located east of Mound B and north of Mound A was surveyed. We would have liked to extend the survey into the area north of Mound B and west of Mound A but the corn was planted in rows that curved around both mounds, making it impossible to walk straight lines.

Aden is a Woodland period site without daub or other evidence of burned structures on the surface. We were uncertain about what we would find.   Many strong, small dipoles (a negative return immediately adjacent to a positive return) were recorded. These are undoubtedly pieces of ferrous metal scattered across the site during the course of the decades of cultivation of the site. There was one clearly cultural feature located to the east of Mound B. This is a large circular pattern delineated by low amplitude, positive values, particularly in the northwest and northeast quadrants (figs. 7-10). These could be shallow ditches that had filled with organic deposits which characteristically have an enhanced magnetic susceptibility. Similar, much larger features have been recorded using a gradiometer at the Shady Grove site in the northern Yazoo Basin (Harris 2011), at Little Spanish Fort in the southern Yazoo Basin (Clay 2001) and at Woodland sites in the Ohio River Valley (Burks and Cook 2011; Henry 2011). The feature has a diameter of approximately 15m depending on where you measure its boundaries. The UTM coordinates of its center point are approximately 702,960E and 3,613,076N, Zone 15, NAD83.

Figure 7 Aden, gradiometer image and recent aerial image.

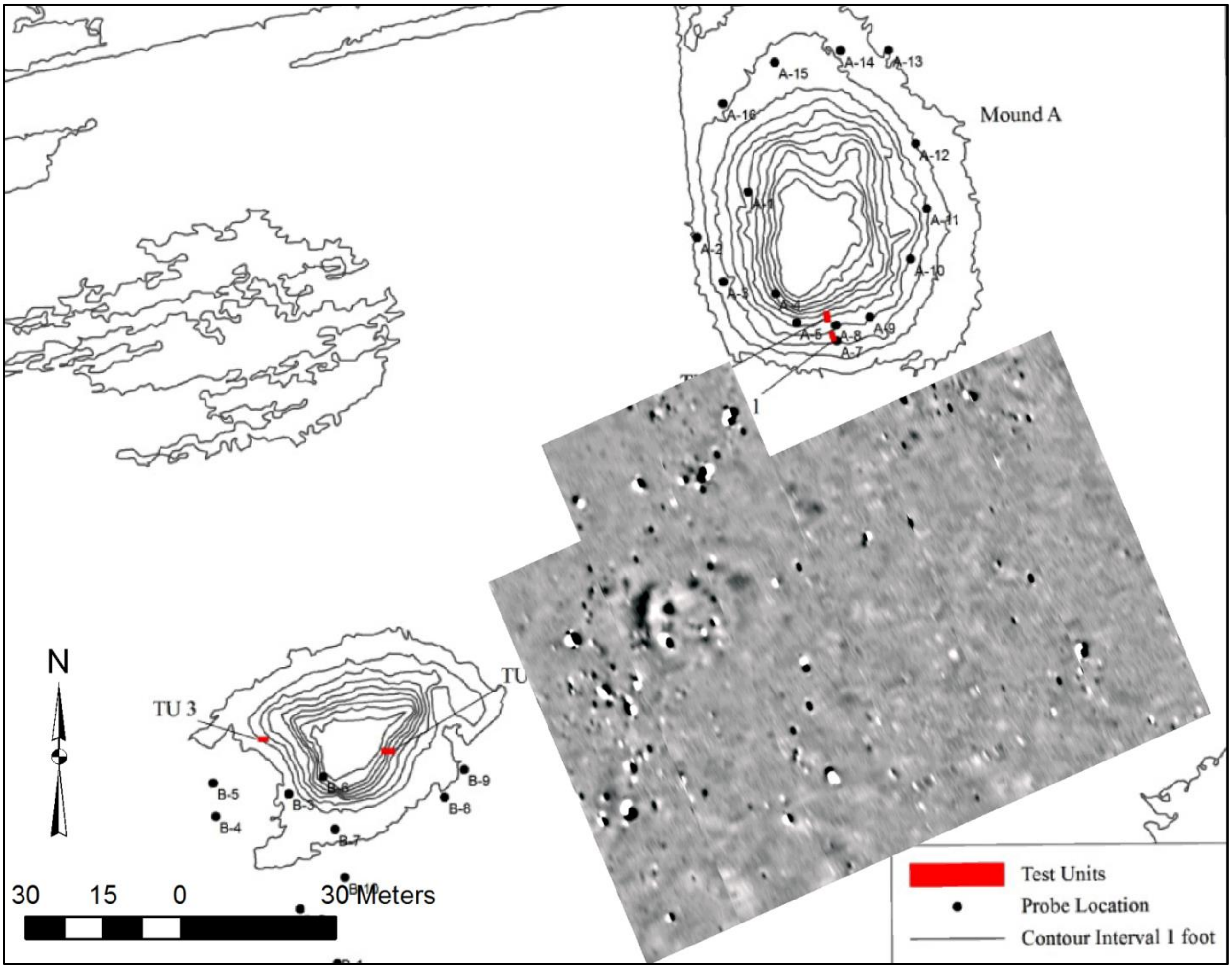

Figure 8 Aden, gradiometer image, LiDAR generated contour map, and Phase II test pit locations (after Jackson and Kowalski 2015:fig. 4.3).

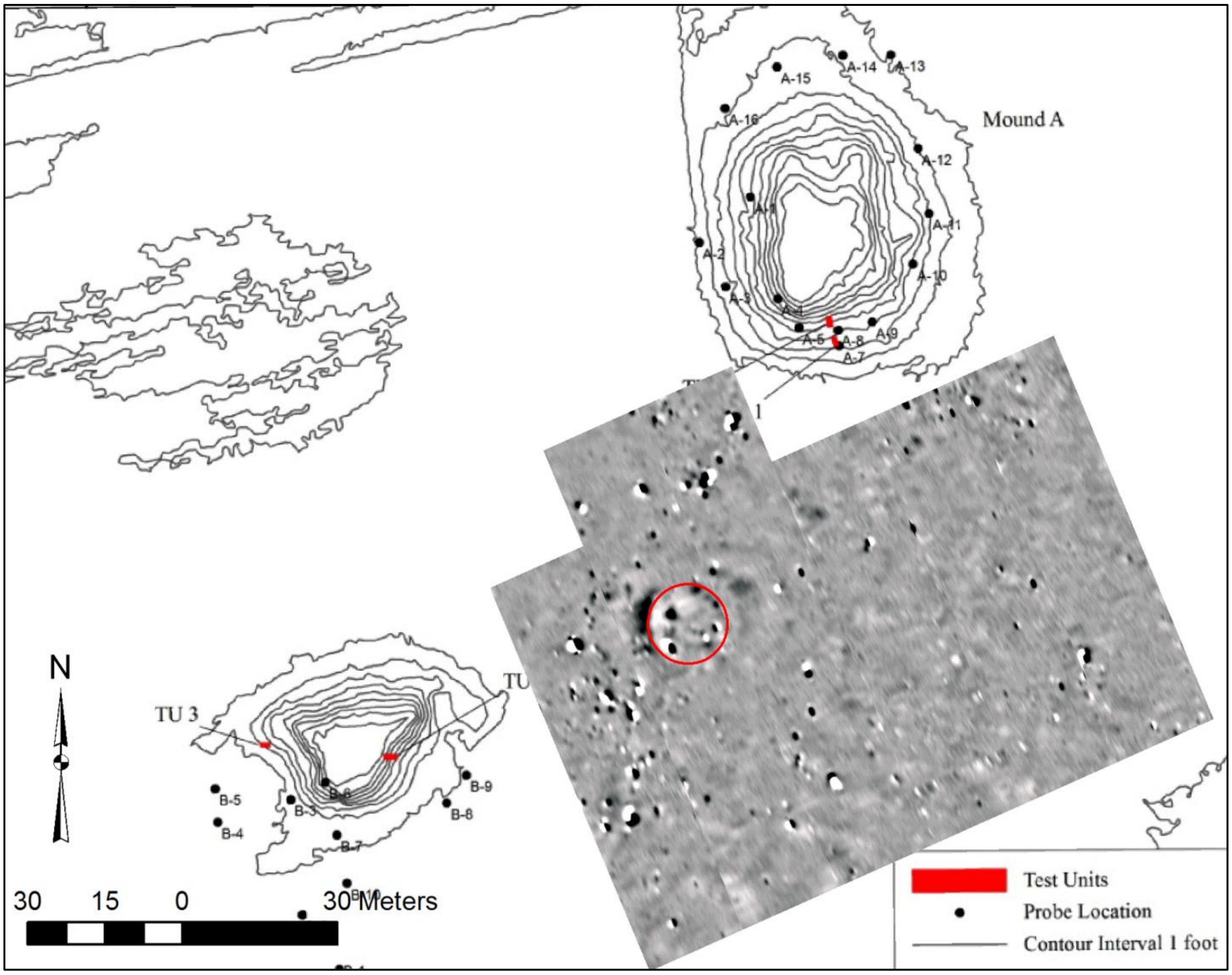

Figure 9 Aden, gradiometer image, LiDAR generated contour intervals and Phase II test pit locations with circular feature outlined (after Jackson and Kowalski 2015:fig. 4.3).

Figure 10 Aden, close up of gradiometer image.

Foster

We did a gradiometer survey at Foster during our first visit to the Southern Segment of the Mound Trail in January of 2015. All of the Mound Trail sites in this segment are in the uplands where there is less land in cultivation and fields tend to be smaller. This had a direct impact on the gradiometer imagery where it is often easier to see patterns in images that cover larger areas. At Foster, for example, we were only able to fit in four 20 by 20m grids in the field north of Mound B (figs. 11-14). Mound B has been badly degraded by cultivation and there is little change in elevation evident on the north side of the mound. We were able, therefore to located the south edge of the survey on the mound itself, limited only by our need to keep some distance from the fence along the south side of the mound in order to avoid the impact that the metal would have on the measurements, effectively masking in of the more subtle patterns that would likely reveal prehistoric features. We used the east fence line of the pasture to orient the survey grid. The north limit was determined by another fence line.

Although there are a few dipoles created by the scattering of metal you expect in a field that has been cultivated and the barbed wire of the fence caused interference on the west, south, and east sides, there was little else in the data that could be interpreted as cultural.

Figure 11 Gradiometer survey on Mound B at Foster, Sam Butz, view to the south.

Figure 12 Foster Mounds, gradiometer image and recent aerial image.

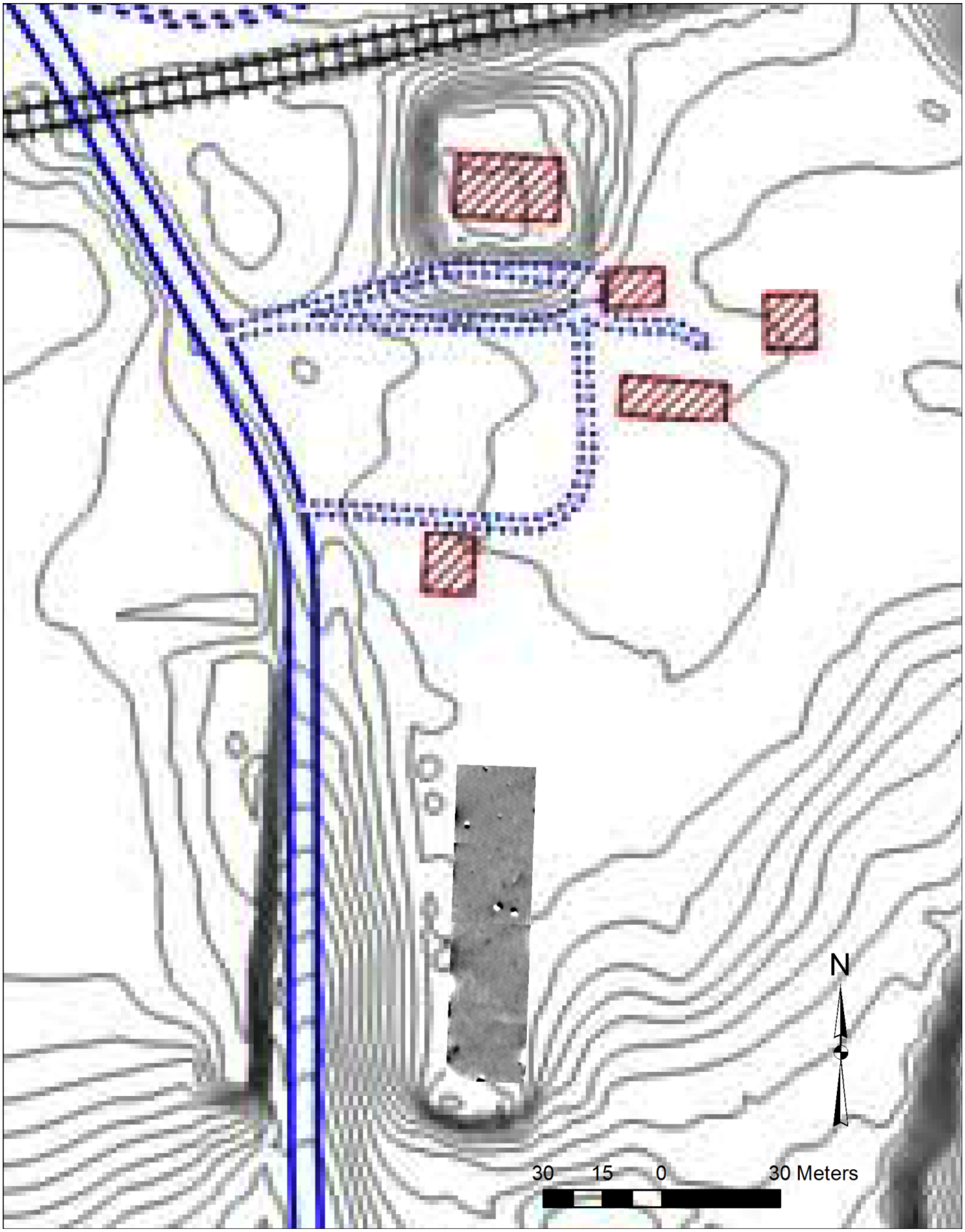

Figure 13 Foster Mounds, LiDAR derived contours and gradiometer image (after Nelson et. al 2013:136).

Figure 14 Foster Mounds, close up of Mound B area and gradiometer image.

Lessley

The gradiometer survey of the Lessley Mound site was also conducted during our first visit to the Natchez Bluff region in January of 2015. Once again there was only a limited amount of area in which we could do the gradiometer survey, a small pasture north of the mound. We were able to fit six 20 by 20m grids between the mound and the fence lines covering a total area of 0.24ha (0.59 acres). Other than scattered metal artifacts showing up as dipoles, there is nothing in the imagery that can be related to cultural activity (figs. 15-18). We also conducted a downhole susceptibility survey of the mound at Lessley.

Figure 15 Gradiometer survey area at Lessley, Mound A in the background, view to the south.

Figure 16 Lessley Mound, gradiometer image and recent aerial image.

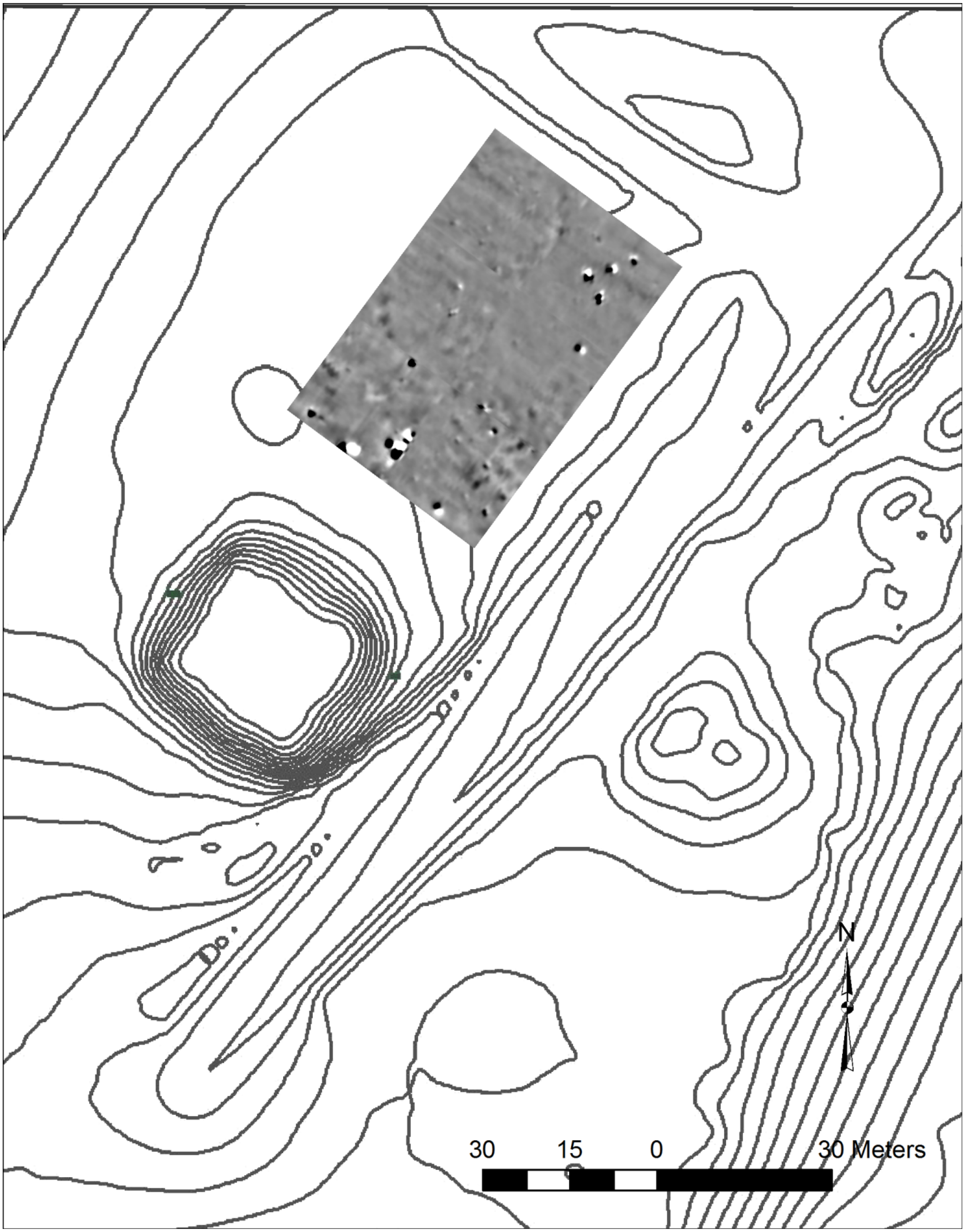

Figure 17 Lessley Mound, LiDAR derived contours and gradiometer image (after Nelson et. al 2013:170).

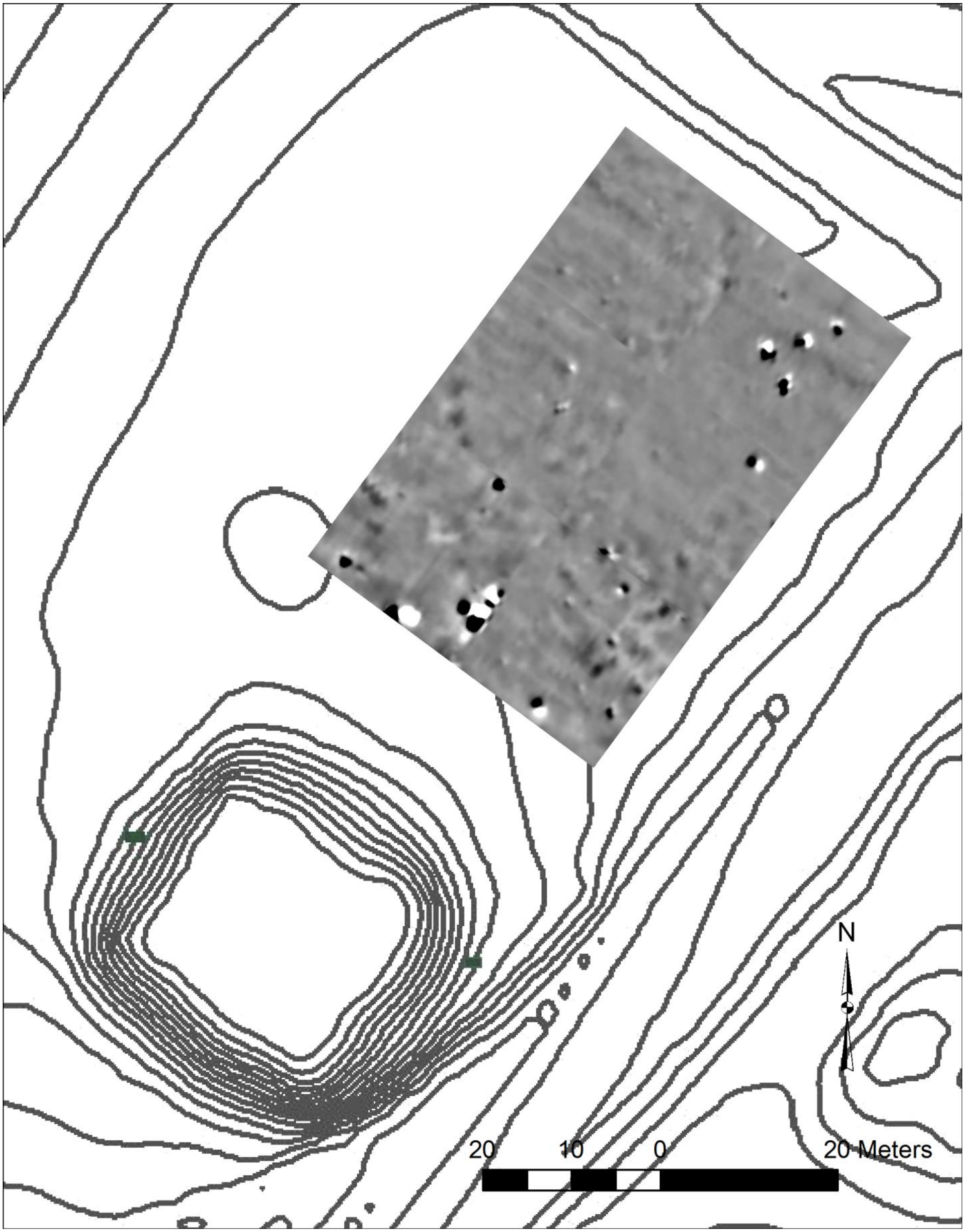

Figure 18 Lessley Mound, LiDAR derived contours and gradiometer image (after Nelson et. al 2013:170).

Downhole Susceptibility Results

Field methods

Inspired in part by Ed Henry's (Henry and Johnson 2012) success in using down susceptibility in exploring Mound A at the Feltus site, we decided to explore the summits of a sample of the Mound Trails sites using this technique. The primary goal was to discover and map mound top structures by searching for burned surfaces which would have an enhanced magnetic susceptibility. The use of downhole measurements to record magnetic characteristics of cultural deposits was pioneered by Ranita Dalin (2001, 2006) in collaboration with Bartington Instruments, a major manufacturer of geophysical survey equipment. She began with the Bartington MS2 magnetic susceptibility meter and developed a downhole sensor and appropriate software to use in the field. Bartington subsequently marketed the MS2H downhole sensor. In the field, the probe is attached to the meter and both are controlled by a notebook computer running, in our case, Multsus Fieldpro, a beta version of the software that is currently distributed by Bartington. The survey data were exported as a Microsoft Excel files which were used to create broken line profiles of the downhole.

We began each survey by determining the approximate center of the mound top using metric tapes. Two transects following the long axis and short axis of the mound were then established using a total station. The transects intersected at right angles at the mound center and pin flags were located at 3m intervals along each transect. We began the survey using an Oakfield tube sampler soil probe with a ¾ inch diameter to establish probe holes. The goal was to measure susceptibility at 2cm intervals for the first 2m of mound fill. In practice, we were rarely able to go that deep with the Oakfield even when using a foot jack or by pounding on the top of the shaft which eventually destroyed the handle. About halfway through the project, we discovered a second manufacturer of soil probes, JMC, which makes a probe that was designed to be driven into the ground using a mallet. We were much more successful in reaching the 2m depth on subsequent mound explorations. The 2cm increment in the depth measurements was established by using the metric scale etched on the rods of the probe and maintained by setting the software to increase the Z value of the readings by 2cm each time. The probe operator and the instrument operator would periodically check to see that they were at the same depth. Susceptibility readings were recorded in SI units.

Winterville

Mound B at Winterville was not the first mound we tested but it would have been useful if it had been. This was the only mound on which the summit was sufficiently intact that we were able to clearly map a burned surface. Actually, we knew going in that there was a burned surface on Mound B because Ed Jackson had dug a trench along the southwest edge of the mound top during one of his field schools at Winterville. Among other things, the trench exposed a well-defined, relatively shallow burned surface.

As always, we began by clearing the top of the mound. Mound B at Winterville was covered in chest high grass (figs. 19, 20). The long axis of Mound B runs southwest to northeast. That became our grid north line with the first grid east line crossing it at the grid E10N13 point. Once we completed the downhole readings along these lines, we decided to place another grid east-west line at the N6 point in order to delineate the two burned surfaces we'd discovered (fig. 21; Table 3).

The very first core we took exposed what we have come to recognize through experience in mound excavation in the northern Yazoo Basin as the classic profile for a burned surface (fig. 22). That is, an abrupt upper boundary with the mound fill followed by the hard, orange burned clay which grades into a black, oxidized layer, then unmodified mound fill. It is that orange surface where the magnetic susceptibility reading peaks and we expected that peak to be asymmetric, skewed to the right. That is, as you go down there would be a rapid increase in reading as you encountered the burned surface followed by a graduate decrease in readings as you move away from the burned surface. That is exactly what we got. The SI value in the E10N0 core first exceeded 100 at 34cmbs, peaked at 379 SI at 44cmbs and didn't drop below 100 SI until 64cmbs (fig. 23). However, the curve is flatter than we expected, particularly on upper tail where, apparently, the burned surface is detected in the susceptibility reading before it is actually reached. There is a second, much lower peak of 132 SI at 1.49mbs in the E10N0 core (fig. 23) which we interpret to be a second burned surface. Some core show only the lower surface, E4N6 for example (fig. 24). Others show only the upper surface, E1N13 (fig. 25).

There is some variation in the depth at which these surfaces appear in the cores. Undulations in the mound surface could account for some of this. Disturbance of the surface itself could also be a factor. When the cores are used to plot the horizontal distribution of the surfaces using the downhole readings (fig. 27), it appears that there has been substantial disturbance. While the lower surface appears to have survived well in the northwest and southwest quadrants of the mound top, the upper surface has a much more restricted distribution. Incidentally, although in profile these burned surfaces look exactly like the floors of burned mound top structures at the Parchman Mounds in the northern Yazoo Basin (Stevens 2006), we have been careful to call them surfaces because it seems unlikely, given their distribution on Mound B and Winterville, that they are floors.

Beyond the information on the distribution of burned surfaces on the top of Mound B at Winterville, the downhole survey at that site provides a model of what to expect a burned surface to look like in the susceptibility profile. In the best examples, there is an asymmetric peak of between 300 and 400 SI units which shows up at similar depth in adjacent core holes. This latter criterion is fundamental. Most of the lower burned surfaces on Mound B are in the 200 SI range but they stand out from the background and appear at about the same depth. We will use the Winterville data in interpreting the downhole susceptibility profiles from the rest of the downhole surveys. The remaining mound surveys will be present in order from north to south.


Figure 19 Mound B at Winterville.

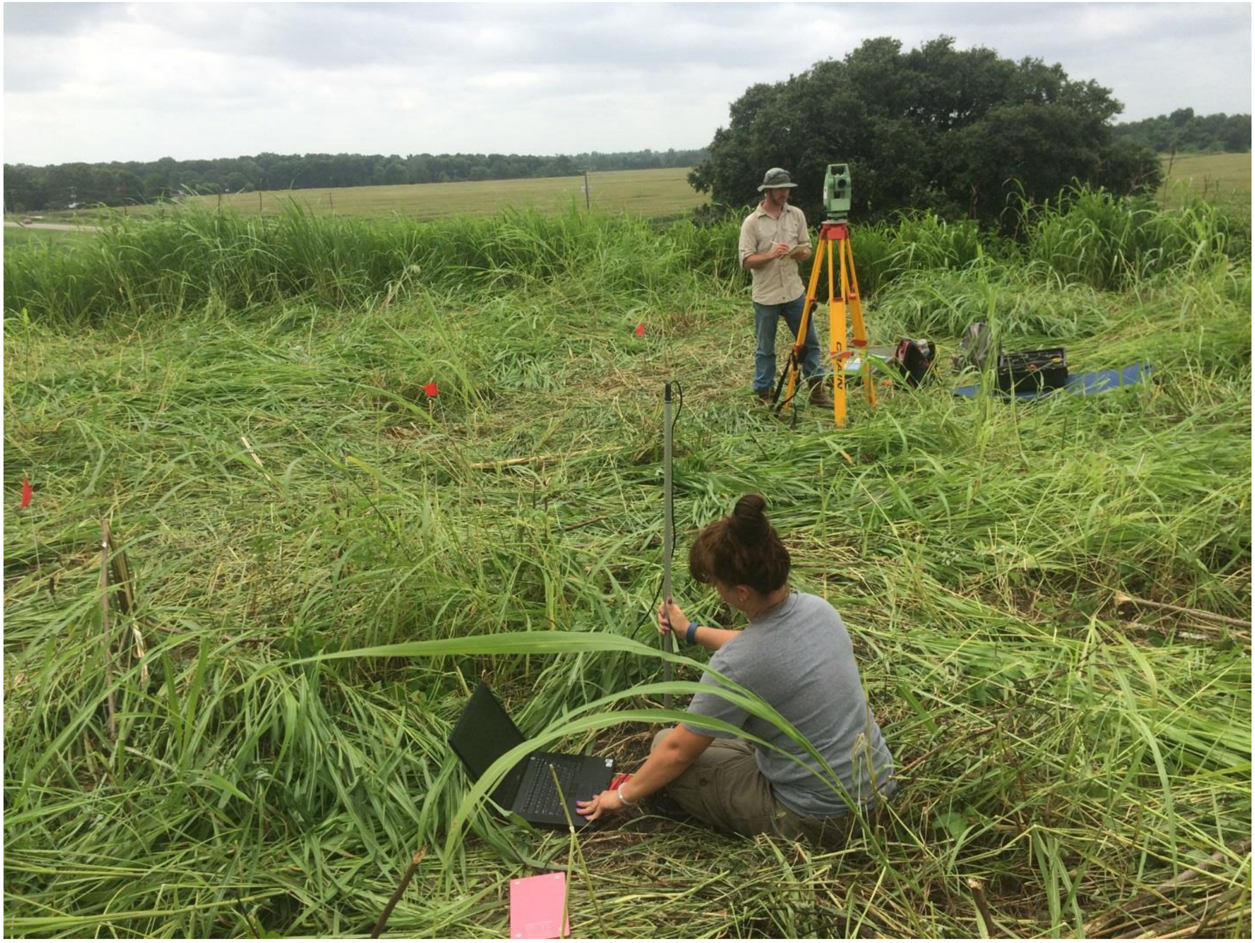

Figure 20 Laying grid and recording downhole readings on Mound B at Winterville, Gabby Coggin and Todd McLeod.

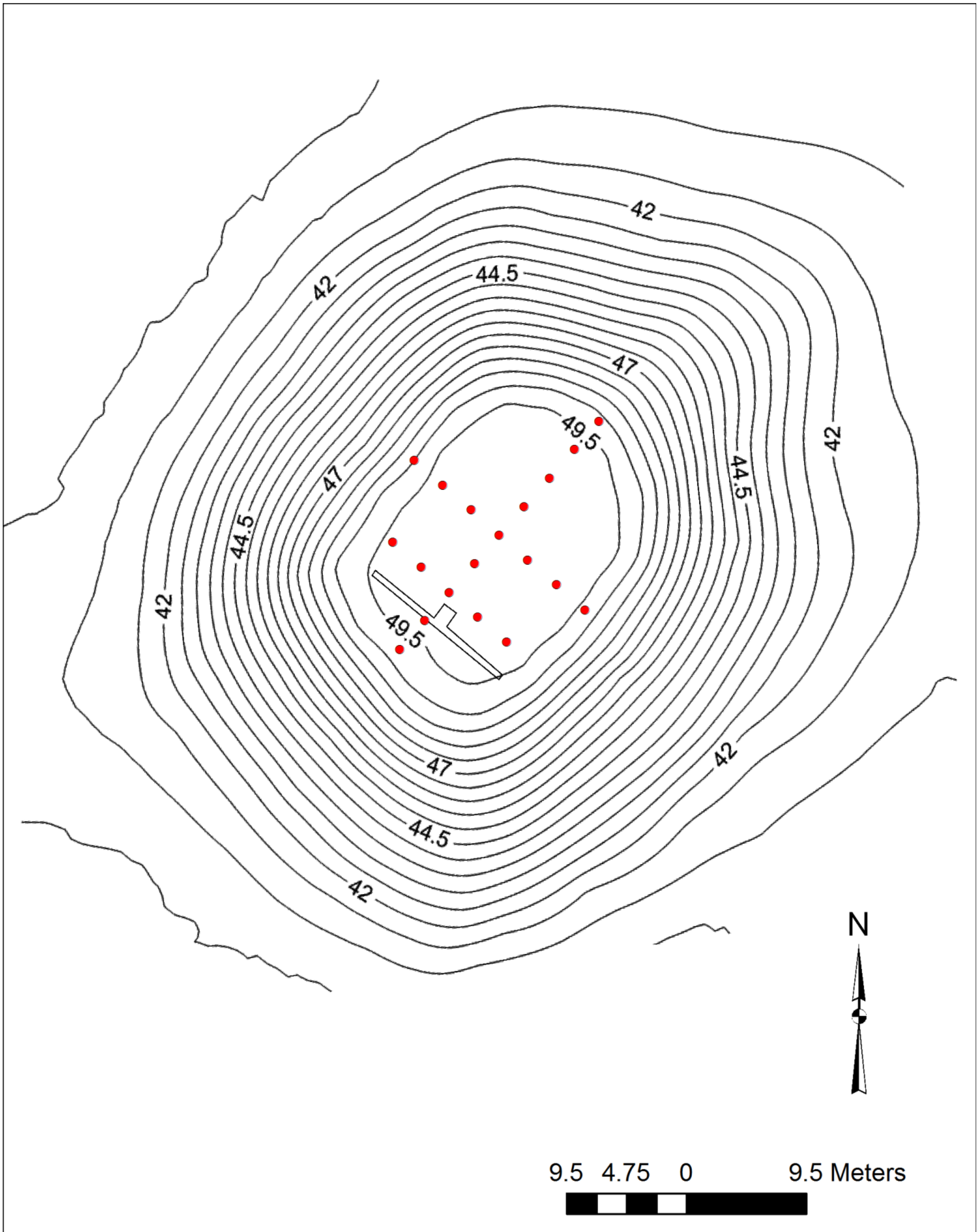

Figure 21 Downhole locations on Mound B at Winterville (topographic map provided by Ed Jackson and Jessica Kowalski).

Figure 22 Typical burned surface as expose in the core tube.

Table 3 Downhole coordinates on Mound B at Winterville, NAD83.

ID	Easting	Northing
E10N0	680,012.95	3,706,649.72
E10N3	680,014.92	3,706,651.98
E10N6	680,016.89	3,706,654.22
E10N9	680,018.88	3,706,656.50
E10N12	680,020.85	3,706,658.76
E10N15	680,022.82	3,706,661.02
E10N18	680,024.81	3,706,663.28
E10N21	680,026.80	3,706,665.54
E10N24	680,028.74	3,706,667.75
E1N12	680,014.12	3,706,664.66
E4N12	680,016.35	3,706,662.72
E7N12	680,018.61	3,706,660.75
E13N12	680,023.08	3,706,656.79
E16N12	680,025.37	3,706,654.82
E19N12	680,027.63	3,706,652.83
E4N6	680,012.42	3,706,658.20
E7N6	680,014.65	3,706,656.21
E13N6	680,019.15	3,706,652.27
E16N6	680,021.43	3,706,650.28

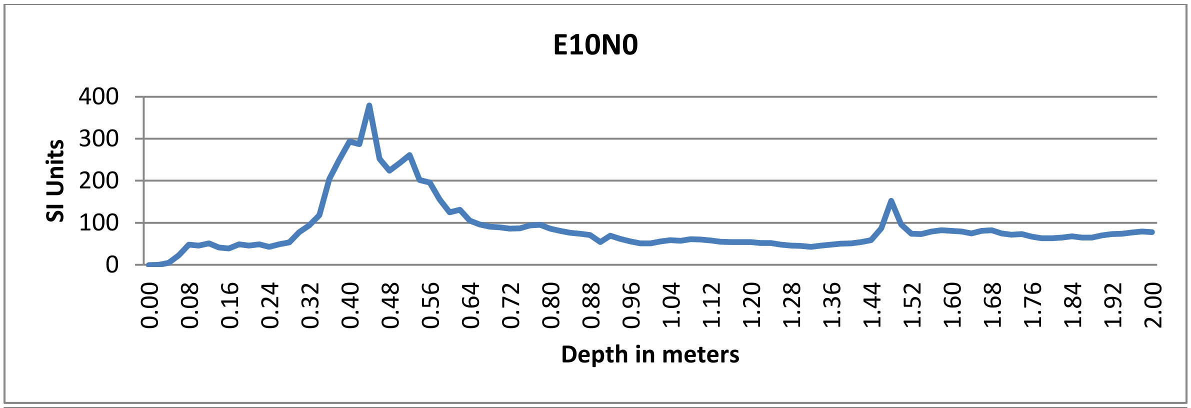
E10N0
SI Units
400
300
200
100
0
0.00 0.08 0.16 0.24 0.32 0.40 0.48 0.56 0.64 0.72 0.80 0.88 0.96 1.04 1.12 1.20 1.28 1.36 1.44 1.52 1.60 1.68 1.76 1.84 1.92 2.00
Depth in meters

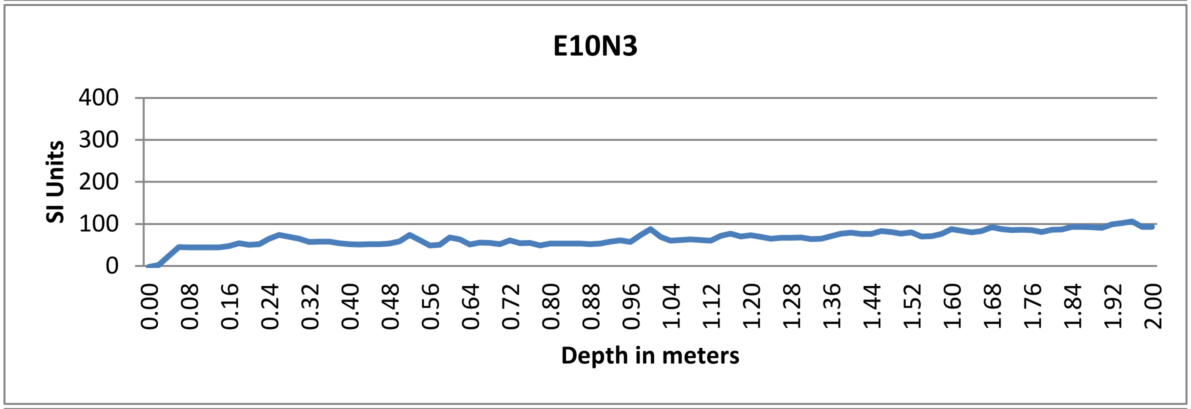
E10N3
SI Units
400
300
200
100
0
0.00 0.08 0.16 0.24 0.32 0.40 0.48 0.56 0.64 0.72 0.80 0.88 0.96 1.04 1.12 1.20 1.28 1.36 1.44 1.52 1.60 1.68 1.76 1.84 1.92 2.00
Depth in meters

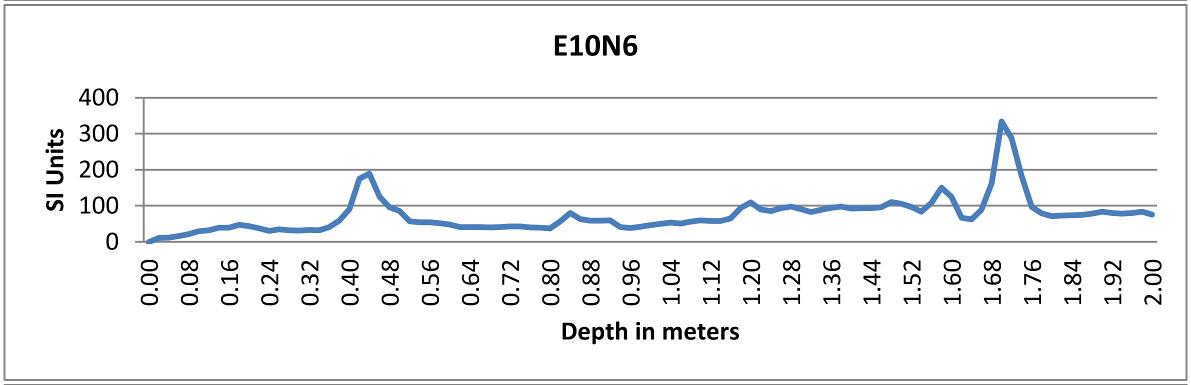
E10N6
SI Units
400
300
200
100
0
0.00 0.08 0.16 0.24 0.32 0.40 0.48 0.56 0.64 0.72 0.80 0.88 0.96 1.04 1.12 1.20 1.28 1.36 1.44 1.52 1.60 1.68 1.76 1.84 1.92 2.00
Depth in meters

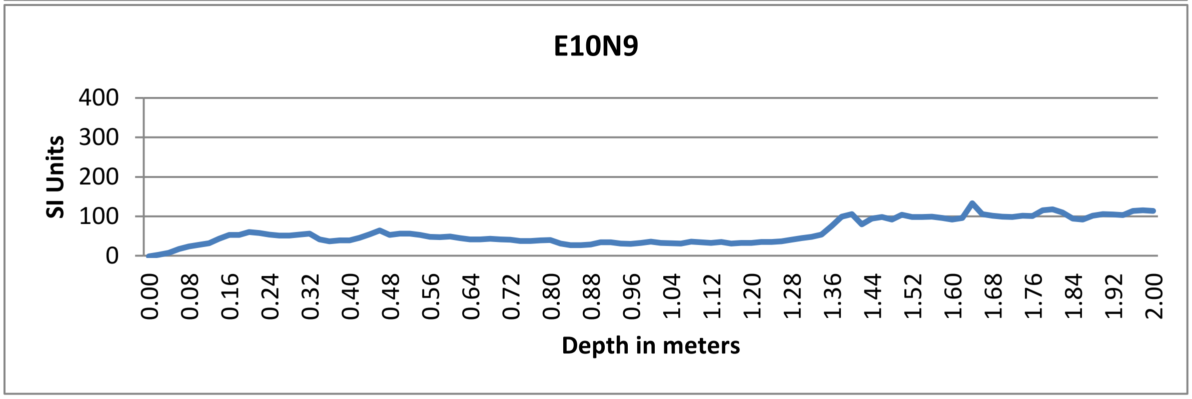
E10N9
SI Units
400
300
200
100
0
0.00 0.08 0.16 0.24 0.32 0.40 0.48 0.56 0.64 0.72 0.80 0.88 0.96 1.04 1.12 1.20 1.28 1.36 1.44 1.52 1.60 1.68 1.76 1.84 1.92 2.00
Depth in meters

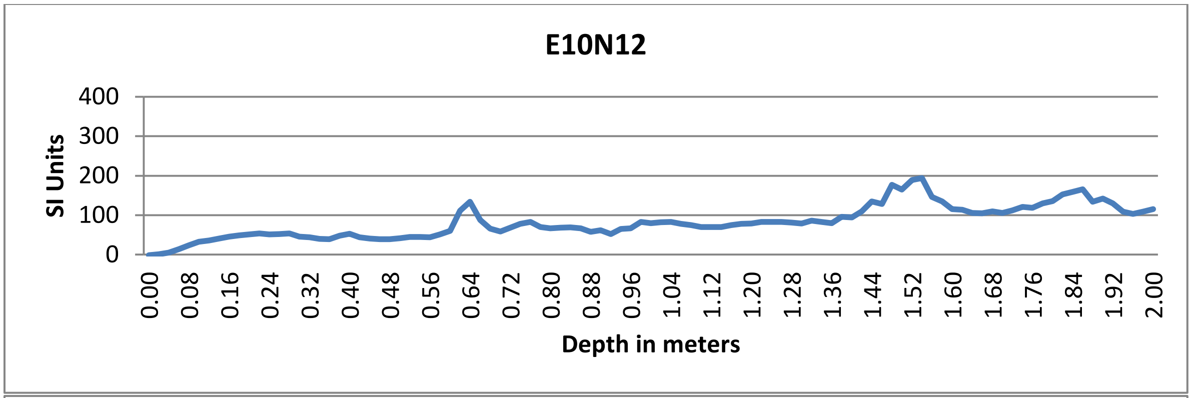
E10N12
SI Units
400
300
200
100
0
0.00 0.08 0.16 0.24 0.32 0.40 0.48 0.56 0.64 0.72 0.80 0.88 0.96 1.04 1.12 1.20 1.28 1.36 1.44 1.52 1.60 1.68 1.76 1.84 1.92 2.00
Depth in meters

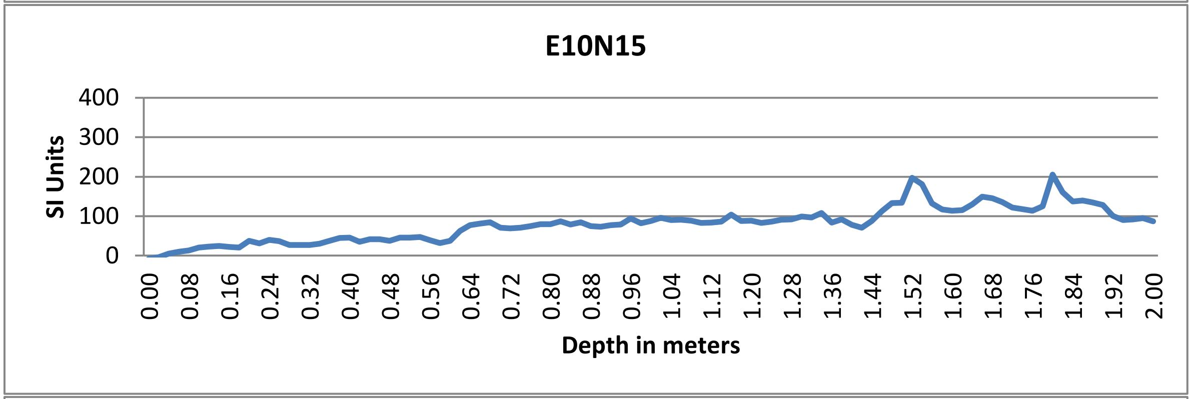
E10N15
SI Units
400
300
200
100
0
0.00 0.08 0.16 0.24 0.32 0.40 0.48 0.56 0.64 0.72 0.80 0.88 0.96 1.04 1.12 1.20 1.28 1.36 1.44 1.52 1.60 1.68 1.76 1.84 1.92 2.00
Depth in meters

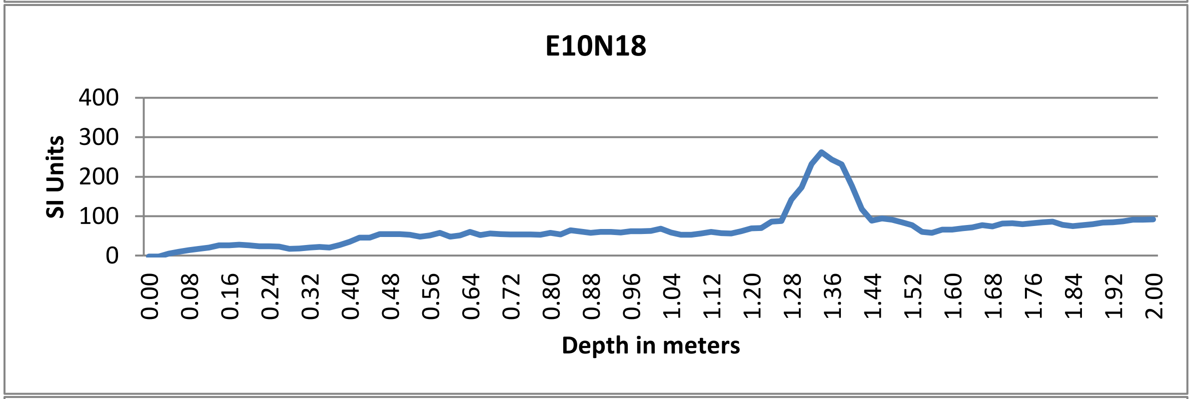
E10N18
SI Units
400
300
200
100
0
0.00 0.08 0.16 0.24 0.32 0.40 0.48 0.56 0.64 0.72 0.80 0.88 0.96 1.04 1.12 1.20 1.28 1.36 1.44 1.52 1.60 1.68 1.76 1.84 1.92 2.00
Depth in meters

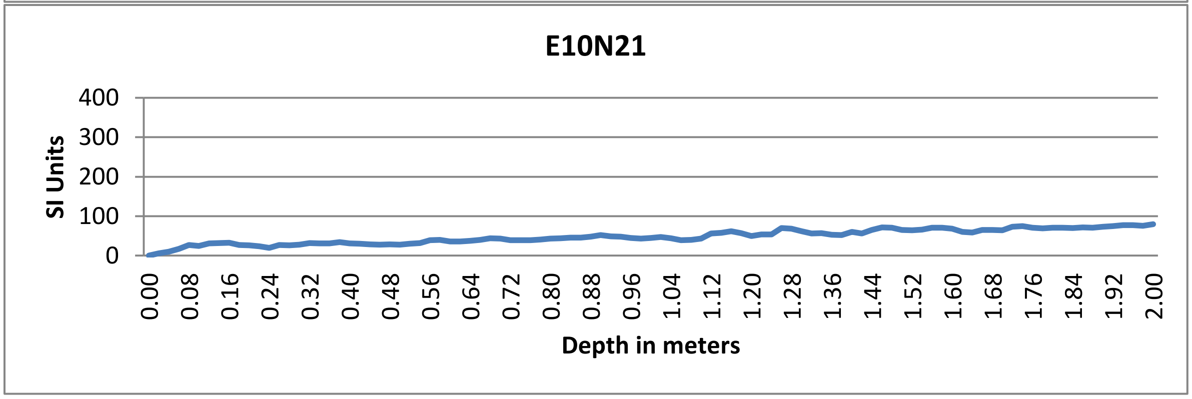
E10N21
SI Units
400
300
200
100
0
0.00 0.08 0.16 0.24 0.32 0.40 0.48 0.56 0.64 0.72 0.80 0.88 0.96 1.04 1.12 1.20 1.28 1.36 1.44 1.52 1.60 1.68 1.76 1.84 1.92 2.00
Depth in meters

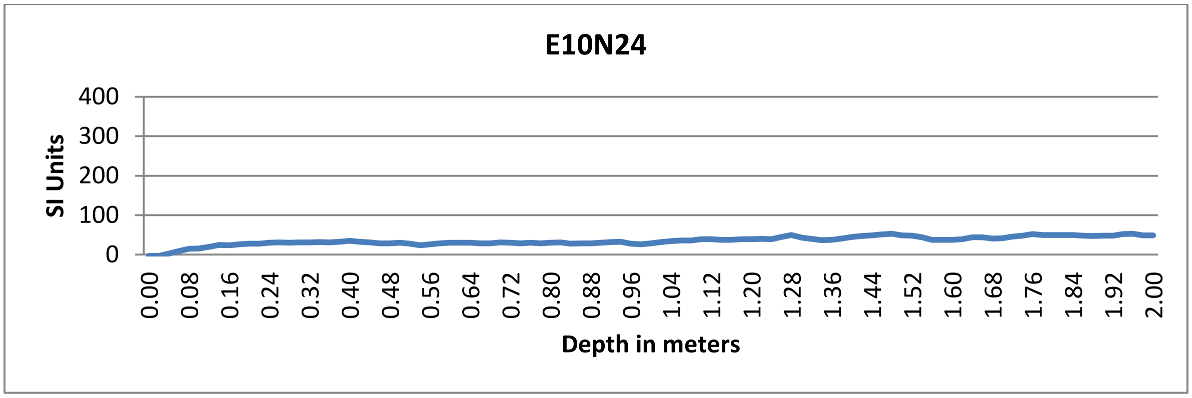

Figure 23 Winterville downhole profiles, E10 line.

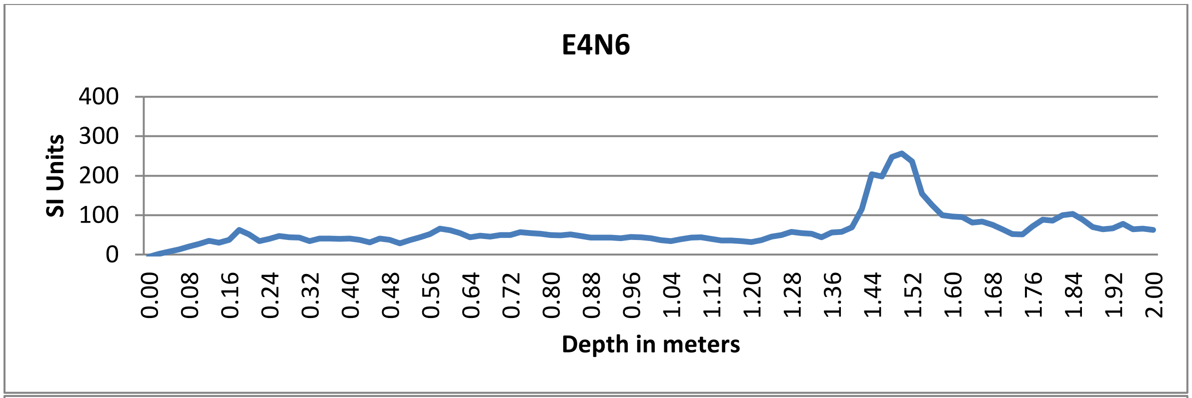
E4N6
SI Units
400
300
200
100
0
0.00
0.08
0.16
0.24
0.32
0.40
0.48
0.56
0.64
0.72
0.80
0.88
0.96
1.04
1.12
1.20
1.28
1.36
1.44
1.52
1.60
1.68
1.76
1.84
1.92
2.00
Depth in meters

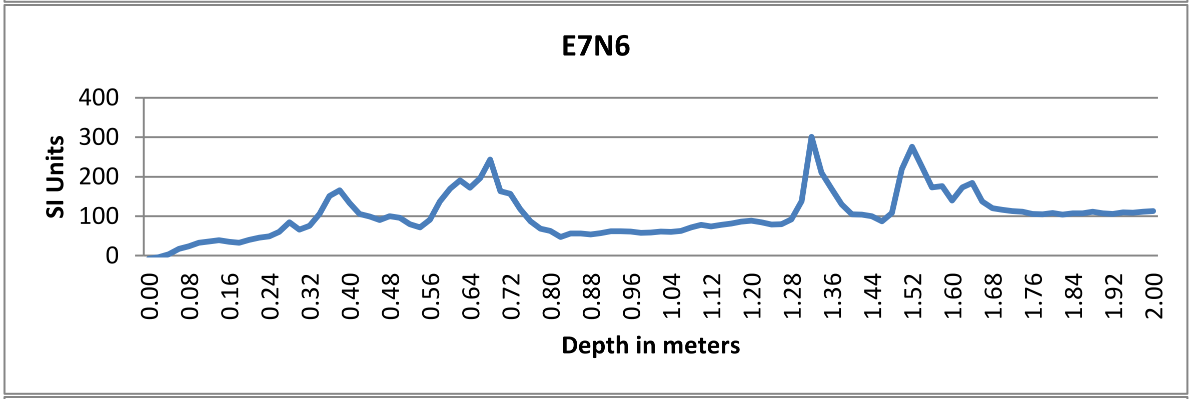
E7N6
SI Units
400
300
200
100
0
0.00
0.08
0.16
0.24
0.32
0.40
0.48
0.56
0.64
0.72
0.80
0.88
0.96
1.04
1.12
1.20
1.28
1.36
1.44
1.52
1.60
1.68
1.76
1.84
1.92
2.00
Depth in meters

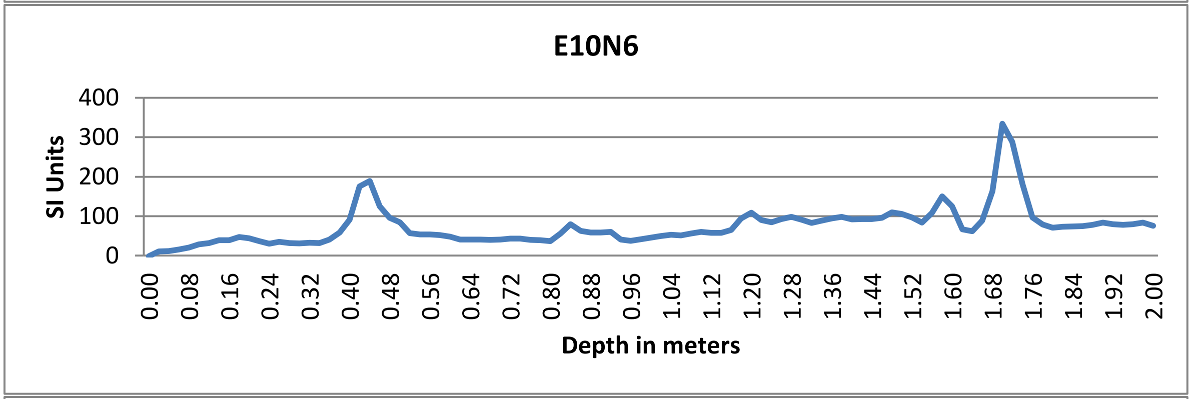
E10N6
SI Units
400
300
200
100
0
0.00
0.08
0.16
0.24
0.32
0.40
0.48
0.56
0.64
0.72
0.80
0.88
0.96
1.04
1.12
1.20
1.28
1.36
1.44
1.52
1.60
1.68
1.76
1.84
1.92
2.00
Depth in meters

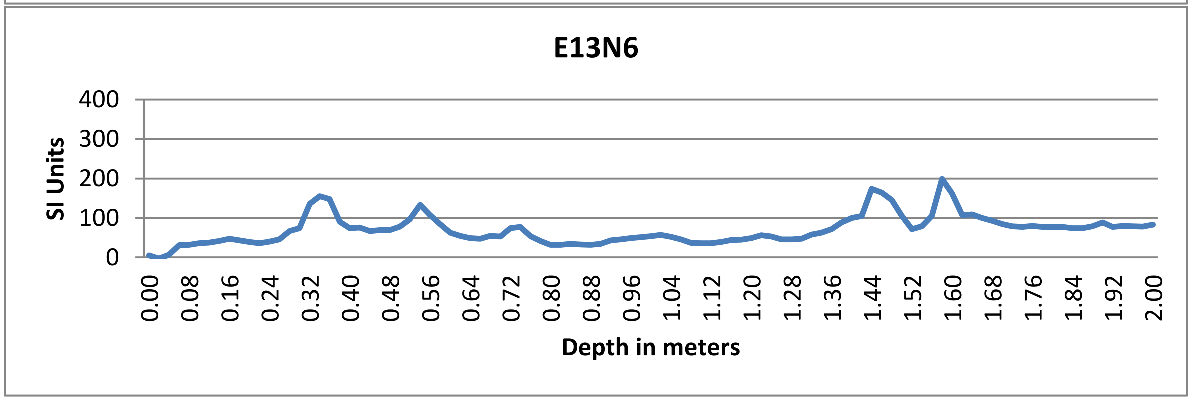
E13N6
SI Units
400
300
200
100
0
0.00
0.08
0.16
0.24
0.32
0.40
0.48
0.56
0.64
0.72
0.80
0.88
0.96
1.04
1.12
1.20
1.28
1.36
1.44
1.52
1.60
1.68
1.76
1.84
1.92
2.00
Depth in meters

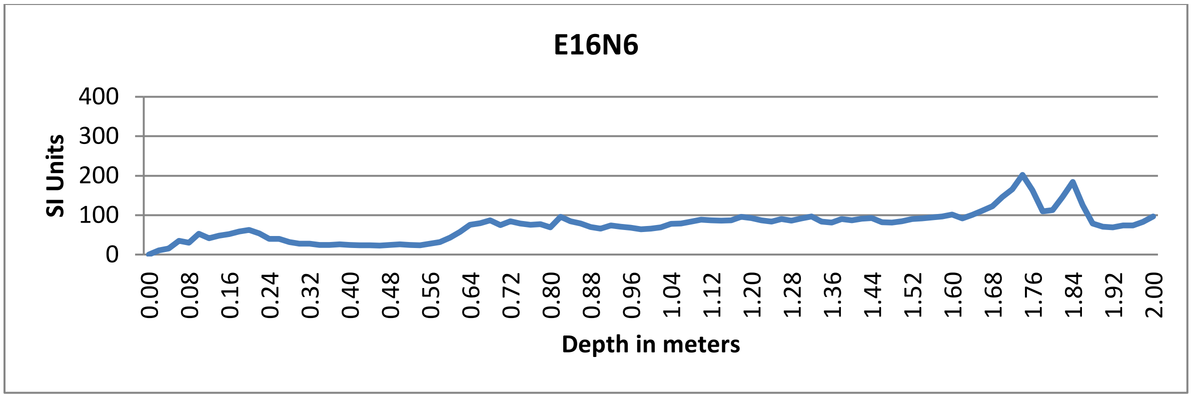

Figure 24 Winterville downhole profiles, N6 line.

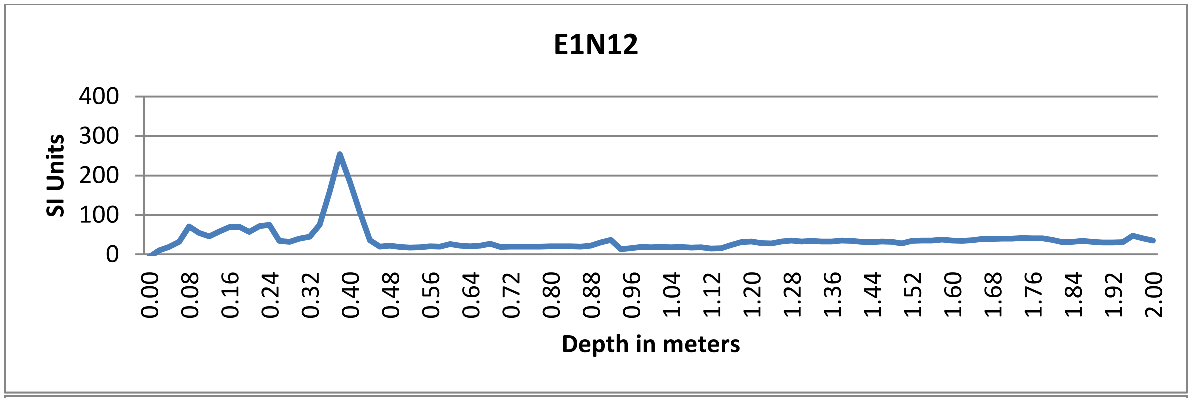
E1N12
SI Units
400
300
200
100
0
0.00
0.08
0.16
0.24
0.32
0.40
0.48
0.56
0.64
0.72
0.80
0.88
0.96
1.04
1.12
1.20
1.28
1.36
1.44
1.52
1.60
1.68
1.76
1.84
1.92
2.00
Depth in meters

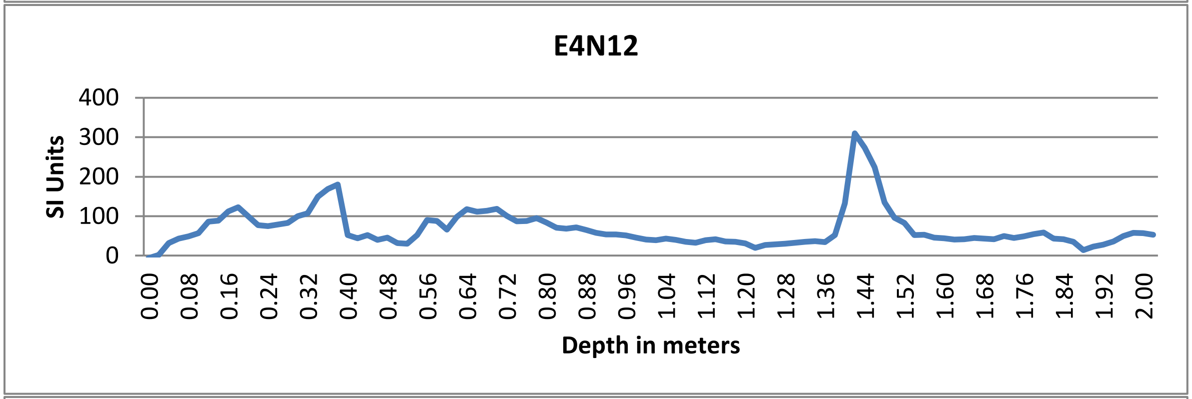
E4N12
SI Units
400
300
200
100
0
0.00
0.08
0.16
0.24
0.32
0.40
0.48
0.56
0.64
0.72
0.80
0.88
0.96
1.04
1.12
1.20
1.28
1.36
1.44
1.52
1.60
1.68
1.76
1.84
1.92
2.00
Depth in meters

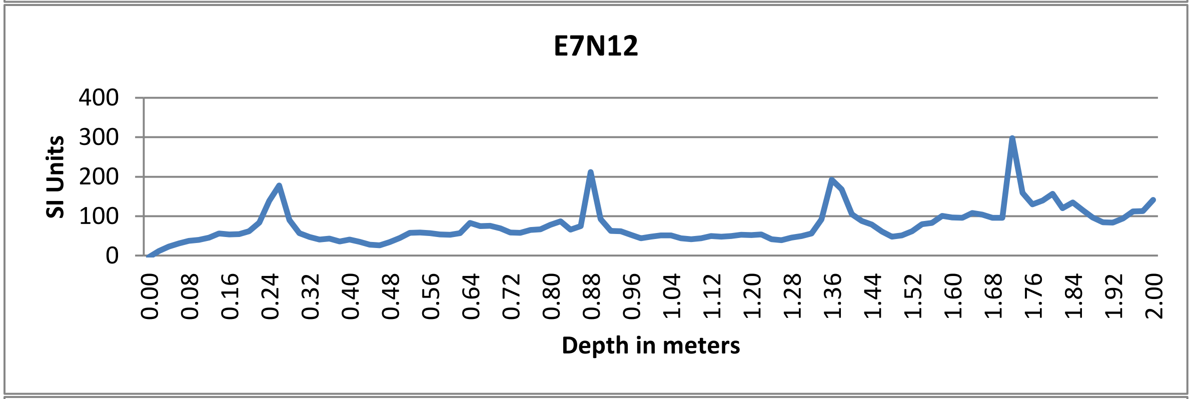
E7N12
SI Units
400
300
200
100
0
0.00
0.08
0.16
0.24
0.32
0.40
0.48
0.56
0.64
0.72
0.80
0.88
0.96
1.04
1.12
1.20
1.28
1.36
1.44
1.52
1.60
1.68
1.76
1.84
1.92
2.00
Depth in meters

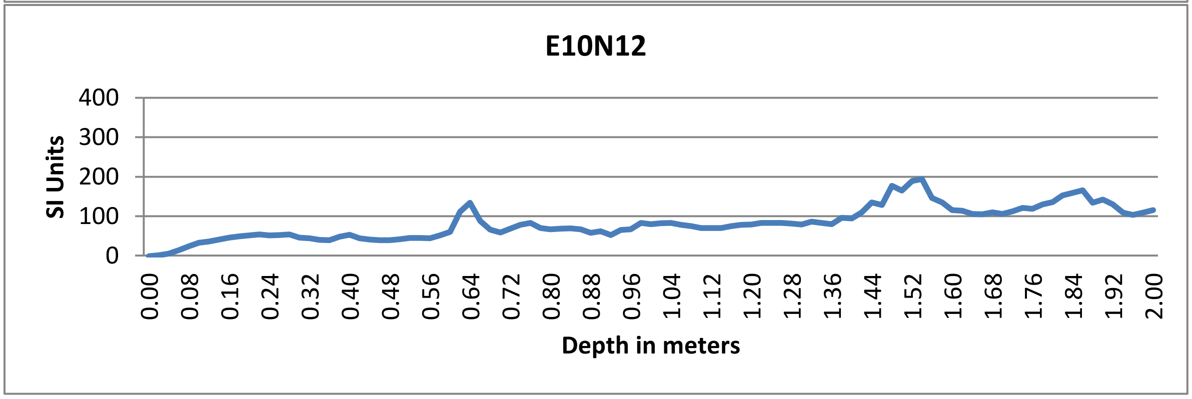
E10N12
SI Units
400
300
200
100
0
0.00
0.08
0.16
0.24
0.32
0.40
0.48
0.56
0.64
0.72
0.80
0.88
0.96
1.04
1.12
1.20
1.28
1.36
1.44
1.52
1.60
1.68
1.76
1.84
1.92
2.00
Depth in meters

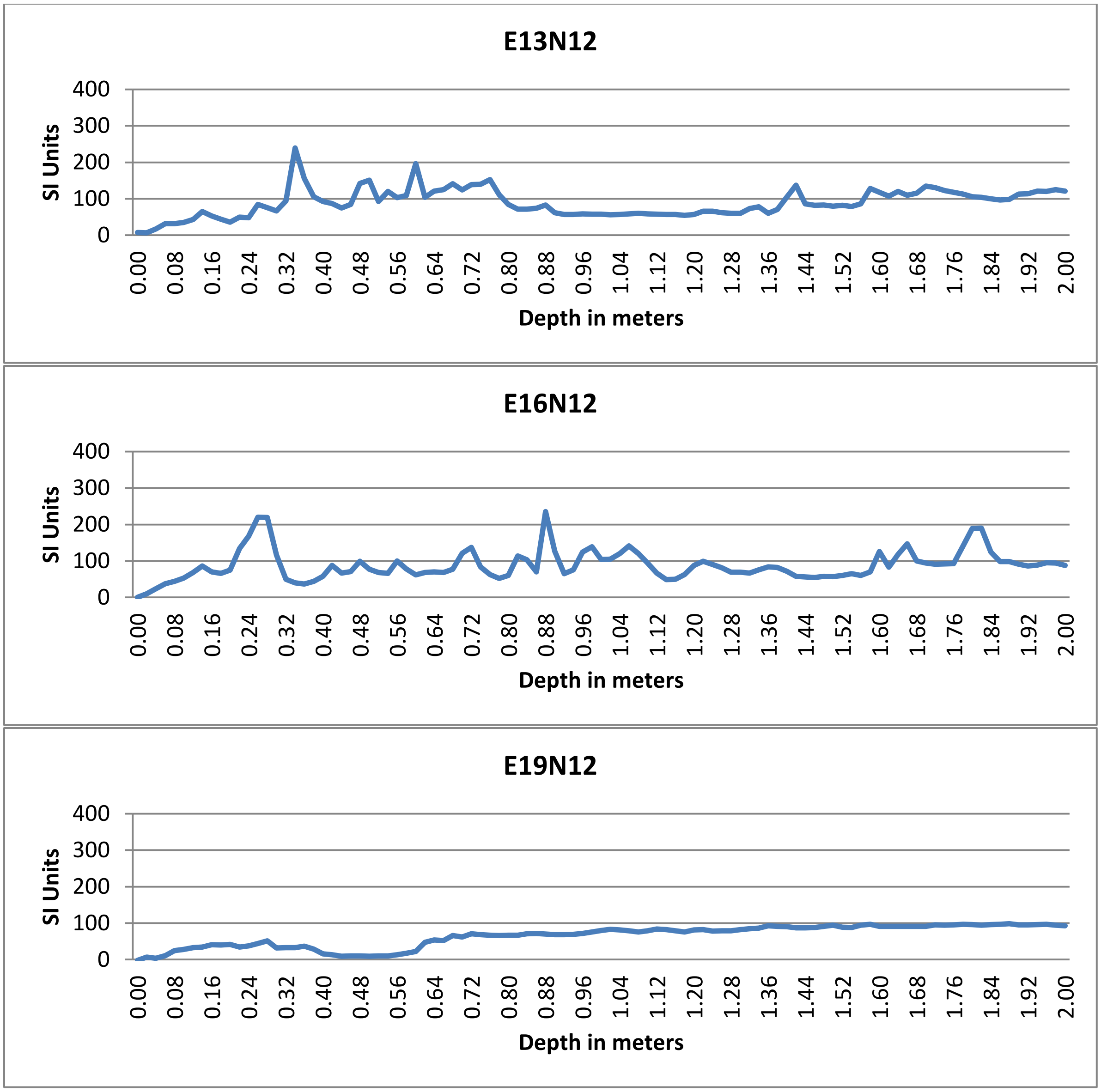

Figure 25 Winterville downhole profiles, N13 line.

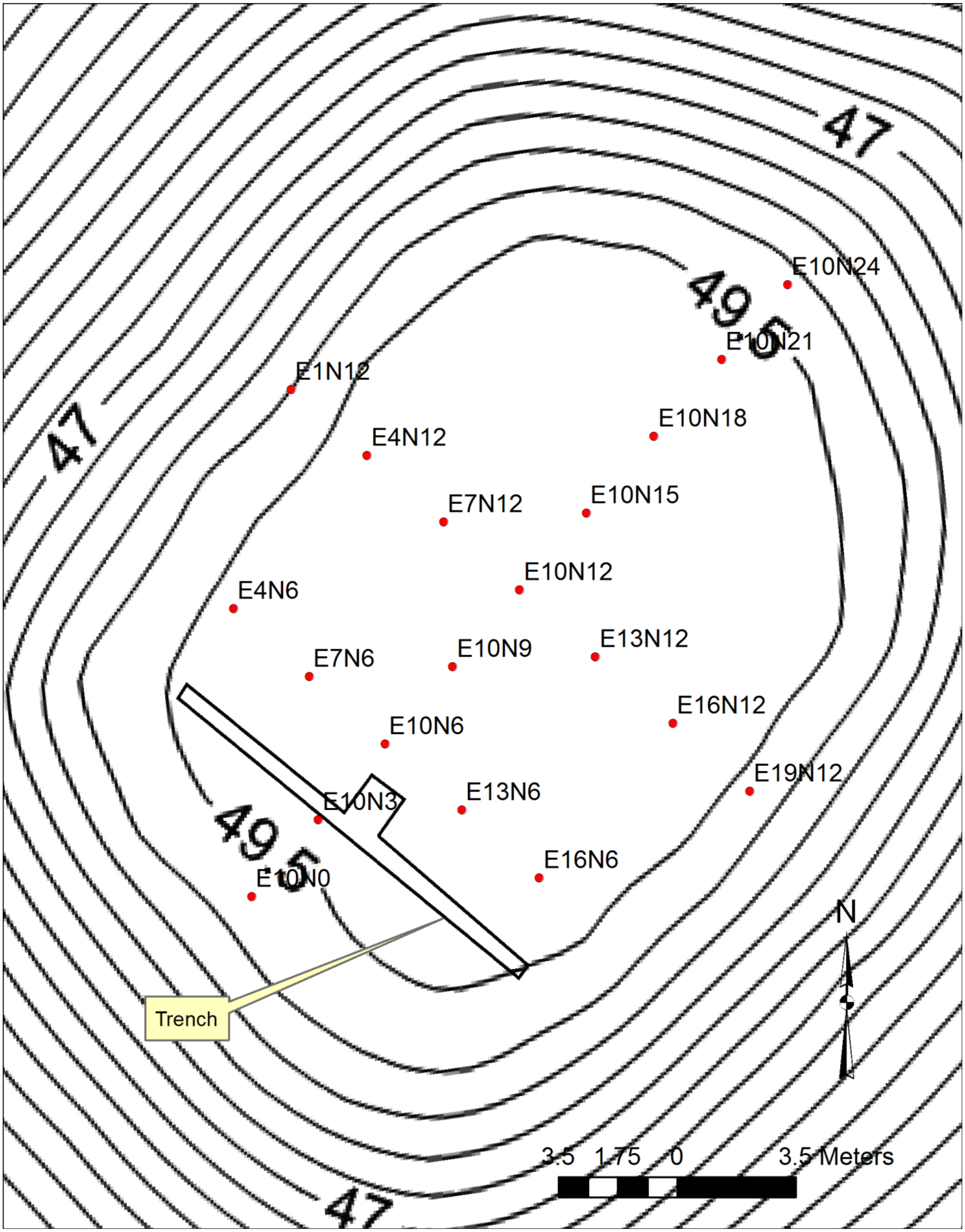

Figure 26 Labelled downhole locations on the top of Mound B at Winterville.

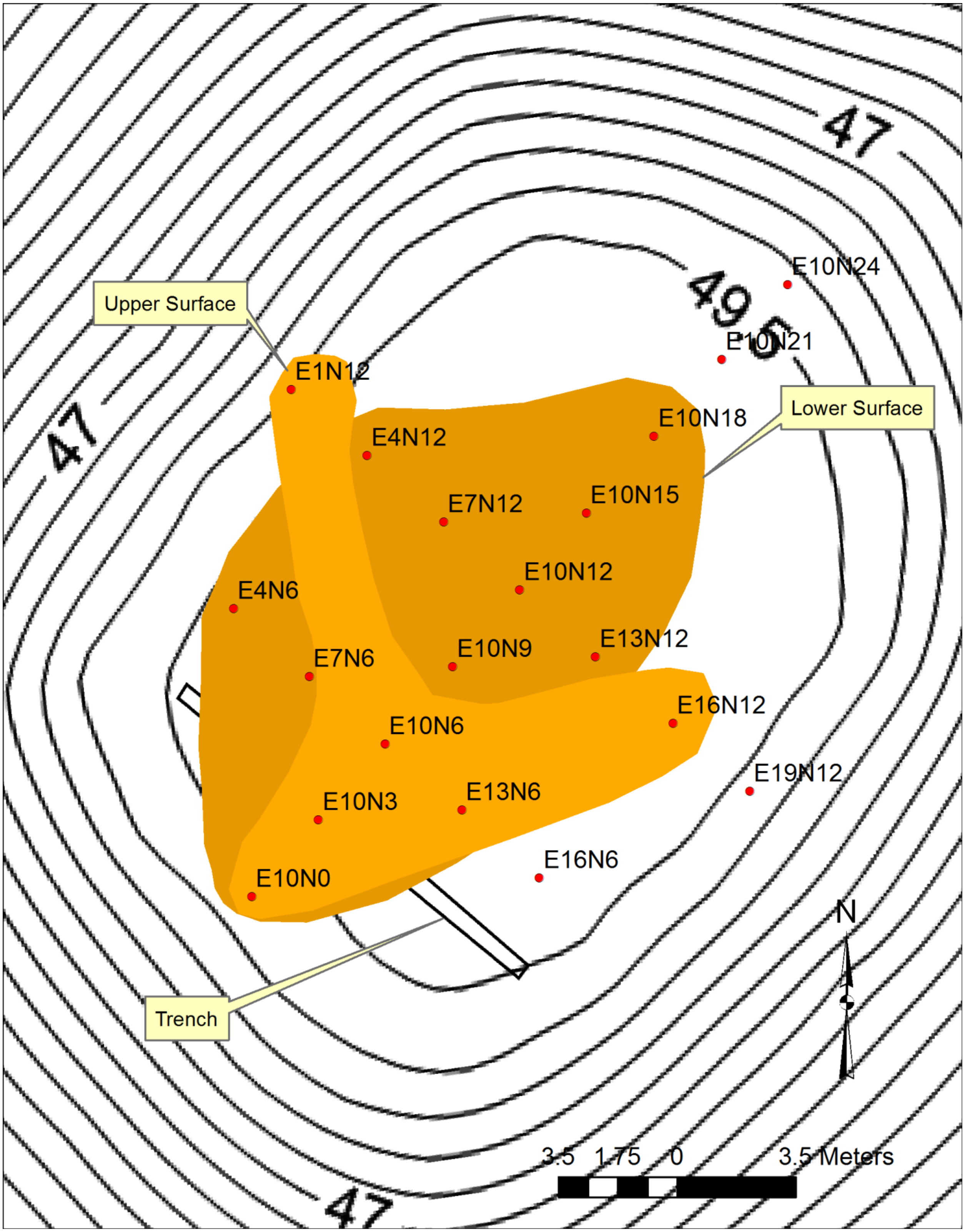

Figure 27 Extent of upper and lower burned surfaces as determined by downhole data.

Hollywood

Mound A at the Hollywood Mounds was the first mound on which we conducted a downhole susceptibility survey. We learned a good deal about what works and what doesn't. In particular, we began using an Oakfield probe with a foot jack. This was particularly important because we began the survey in October of 2015 and there had been relatively little rain. It was impossible to push a core very deep into the heavy clays of the top of Mound A. The foot jack helped some but even using the jack and a seven pound hammer, we were never able to reach the two meter depth was had intended to use in the survey. The pounding on the foot jack also resulted in bent shafts.

Given that this was our first downhole survey of the Mound Trail project, the results were disappointing. The susceptibility profiles for most of the downholes were relatively flat with readings that were generally below 100 SI units. While there were a few profiles showing peaks in the 200 to 300 SI unit range, the adjacent downhole profiles showed an entirely different pattern. Only two of the downholes, located at the north end of the north line show roughly similar profiles with possible floors at 0.70 and 0.90m below surface and these are located at the north edge of the mound. In fact, while our survey failed to detect any burned surfaces in the center of the mound, this possible edge location may be significant. Bryan Haley used a gradiometer survey of the top of Mound A to situate a test excavation which uncovered a burned floor and sheet midden deposit near the edge of the mound in its northwest quadrant. Similarly, the structures that we located in the remote sensing and test excavations at the Parchman Mounds (22Co511) to the south of Hollywood found structures located at the edge of the Mound A but not in the center (Nelson 2016). Finally, the only structure that Mehta (2016) was able to locate on the top of Mound D at the Carson Mounds site (22Co505) was located at the edge of the mound. It may be that mound center structures are unusual on Mississippian mounds in the northern Yazoo Basin. The sample is, of course, small.

Figure 28 Downhole survey on the top of Mound A at the Hollywood site, Sam Butz and Todd McLeod.

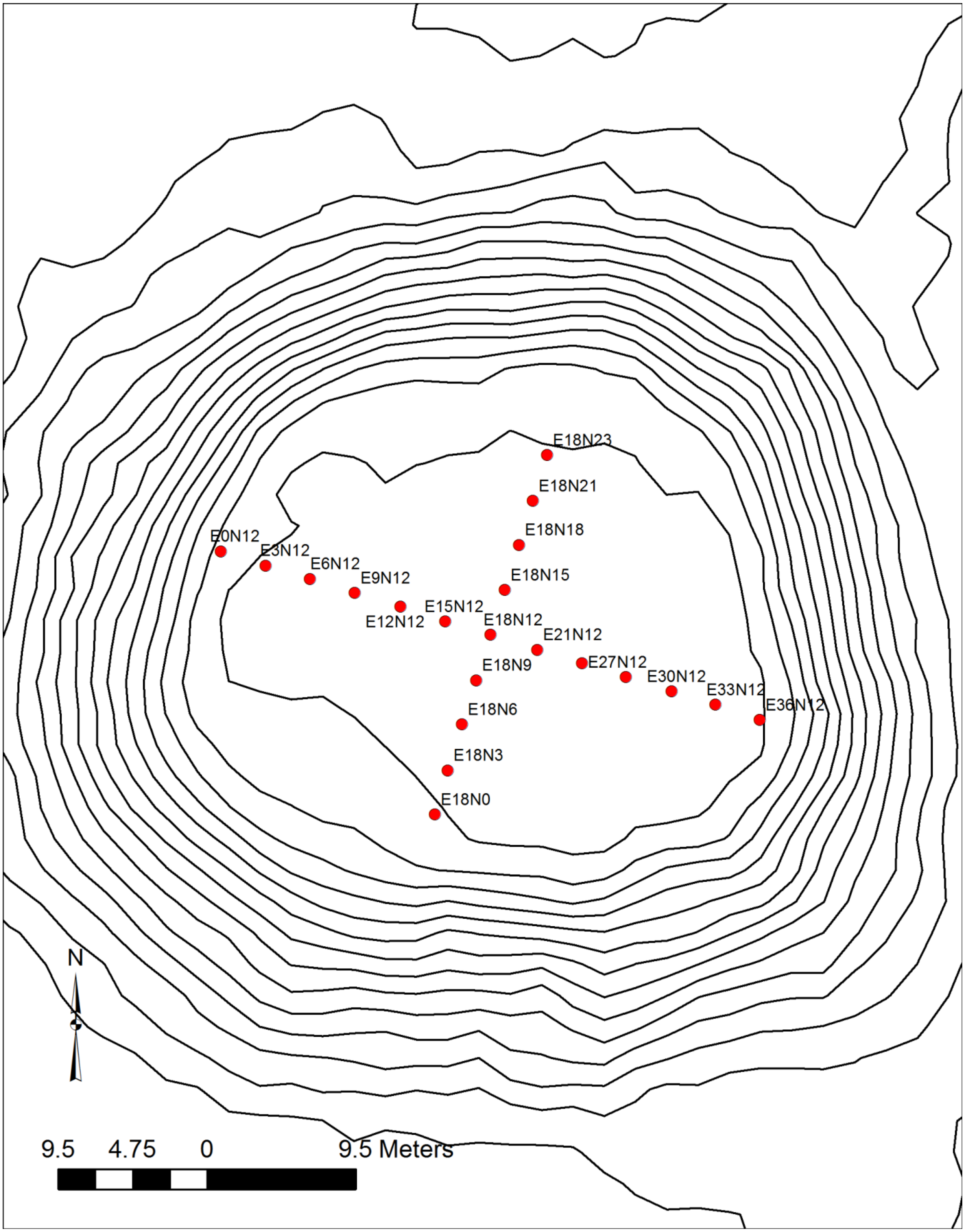

Figure 29 Downhole location on Mound A at Hollywood.

Table 4 Downhole coordinates on Mound A at Hollywood, NAD 83.

Coordinates	Easting	Northing
E0N12	740,596.51	3,851,512.35
E3N12	740,599.38	3,851,511.44
E6N12	740,602.19	3,851,510.59
E9N12	740,605.06	3,851,509.68
E12N12	740,607.97	3,851,508.83
E15N12	740,610.84	3,851,507.88
E18N12	740,613.75	3,851,507.02
E21N12	740,616.72	3,851,506.07
E24N12	740,619.58	3,851,505.21
E27N12	740,622.40	3,851,504.31
E30N12	740,625.31	3,851,503.40
E33N12	740,628.13	3,851,502.55
E36N12	740,630.93	3,851,501.58
E18N0	740,610.17	3,851,495.53
E18N3	740,611.01	3,851,498.35
E18N6	740,611.92	3,851,501.29
E18N9	740,612.83	3,851,504.11
E18N15	740,614.66	3,851,509.88
E18N18	740,615.57	3,851,512.76
E18N21	740,616.44	3,851,515.57
E18N24	740,617.36	3,851,518.50

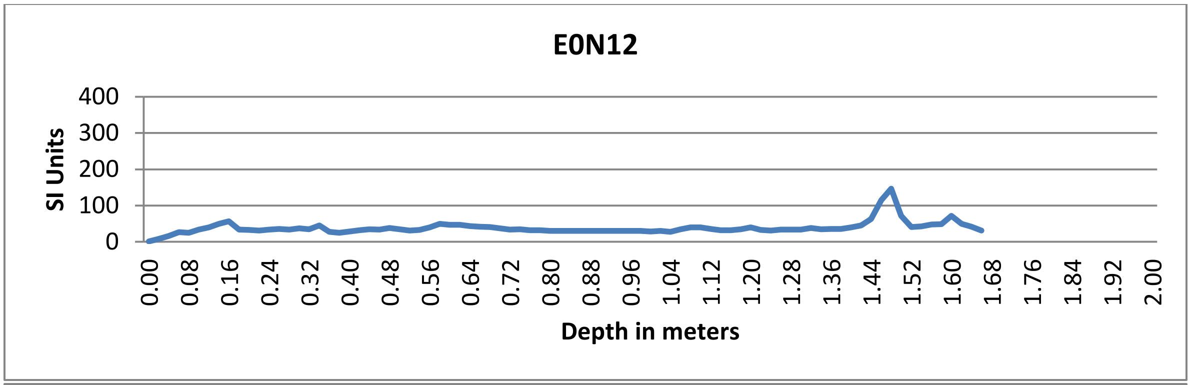
E0N12
SI Units
400
300
200
100
0
0.00
0.08
0.16
0.24
0.32
0.40
0.48
0.56
0.64
0.72
0.80
0.88
0.96
1.04
1.12
1.20
1.28
1.36
1.44
1.52
1.60
1.68
1.76
1.84
1.92
2.00
Depth in meters

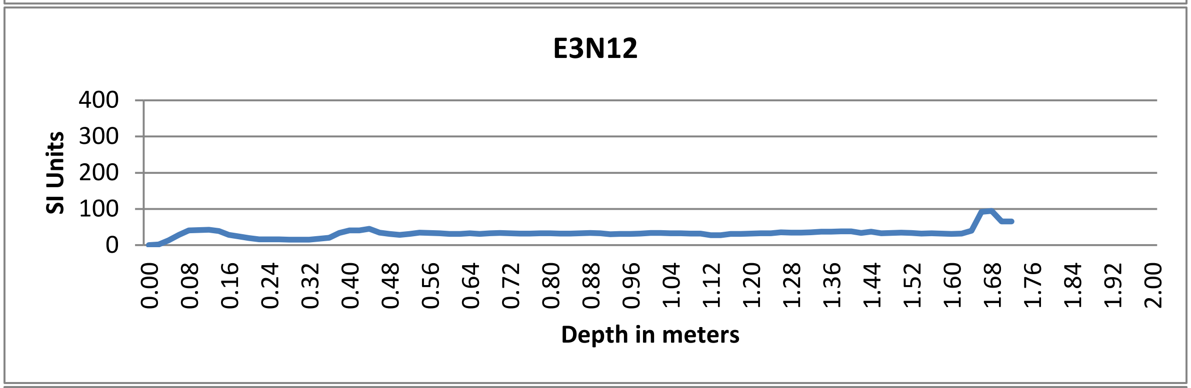
E3N12
SI Units
400
300
200
100
0
0.00
0.08
0.16
0.24
0.32
0.40
0.48
0.56
0.64
0.72
0.80
0.88
0.96
1.04
1.12
1.20
1.28
1.36
1.44
1.52
1.60
1.68
1.76
1.84
1.92
2.00
Depth in meters

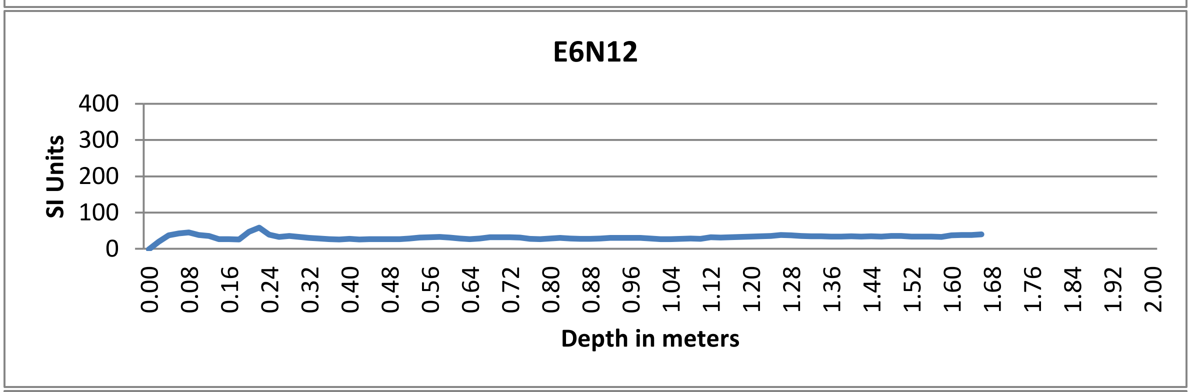
E6N12
SI Units
400
300
200
100
0
0.00
0.08
0.16
0.24
0.32
0.40
0.48
0.56
0.64
0.72
0.80
0.88
0.96
1.04
1.12
1.20
1.28
1.36
1.44
1.52
1.60
1.68
1.76
1.84
1.92
2.00
Depth in meters

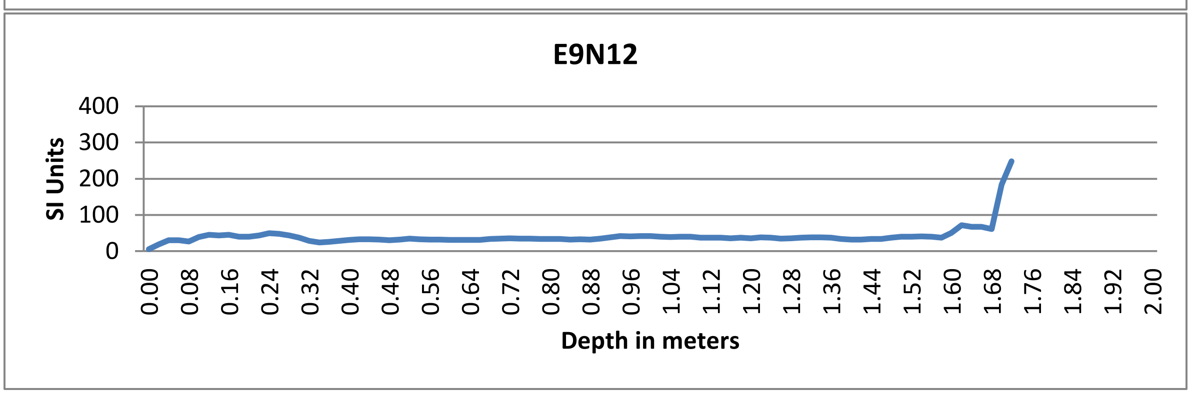
E9N12
SI Units
400
300
200
100
0
0.00
0.08
0.16
0.24
0.32
0.40
0.48
0.56
0.64
0.72
0.80
0.88
0.96
1.04
1.12
1.20
1.28
1.36
1.44
1.52
1.60
1.68
1.76
1.84
1.92
2.00
Depth in meters

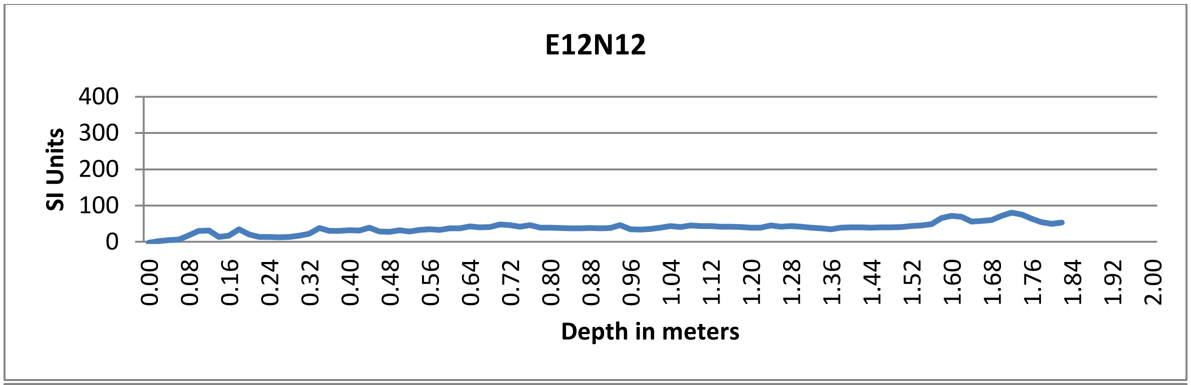
E12N12
SI Units
0
100
200
300
400
0.00
0.08
0.16
0.24
0.32
0.40
0.48
0.56
0.64
0.72
0.80
0.88
0.96
1.04
1.12
1.20
1.28
1.36
1.44
1.52
1.60
1.68
1.76
1.84
1.92
2.00
Depth in meters

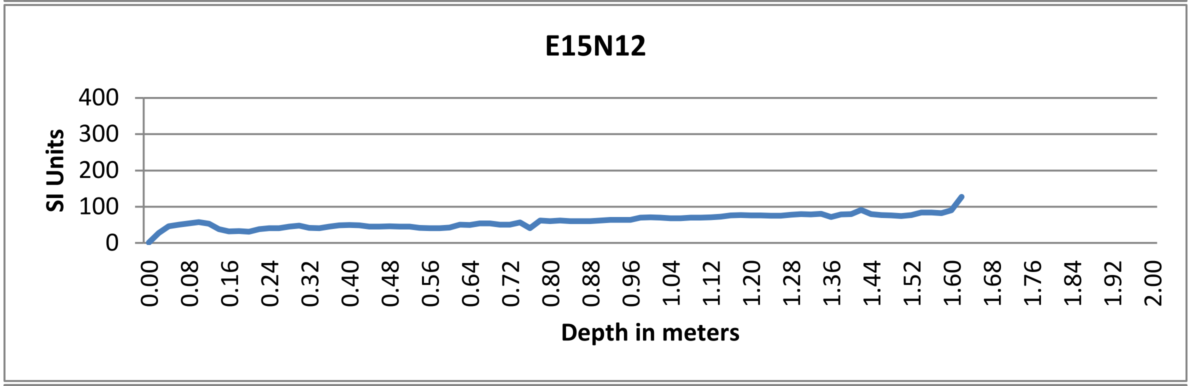
E15N12
SI Units
0
100
200
300
400
0.00
0.08
0.16
0.24
0.32
0.40
0.48
0.56
0.64
0.72
0.80
0.88
0.96
1.04
1.12
1.20
1.28
1.36
1.44
1.52
1.60
1.68
1.76
1.84
1.92
2.00
Depth in meters

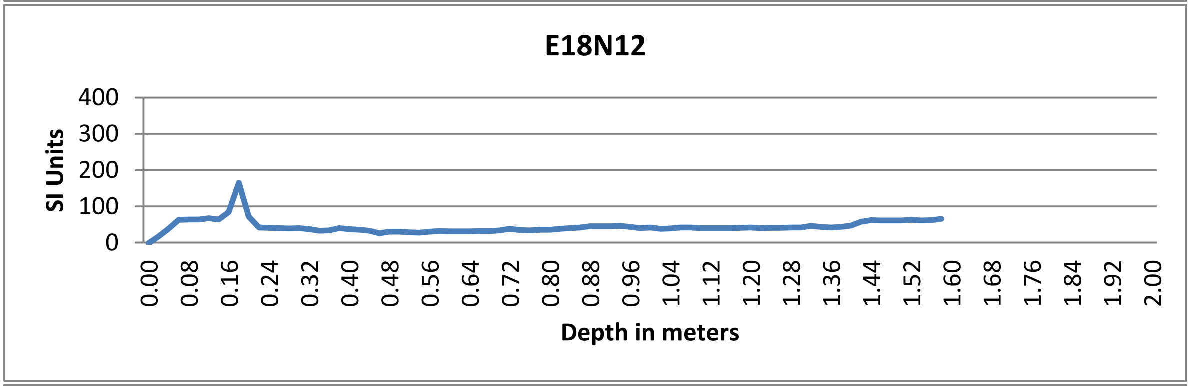
E18N12
SI Units
0
100
200
300
400
0.00
0.08
0.16
0.24
0.32
0.40
0.48
0.56
0.64
0.72
0.80
0.88
0.96
1.04
1.12
1.20
1.28
1.36
1.44
1.52
1.60
1.68
1.76
1.84
1.92
2.00
Depth in meters

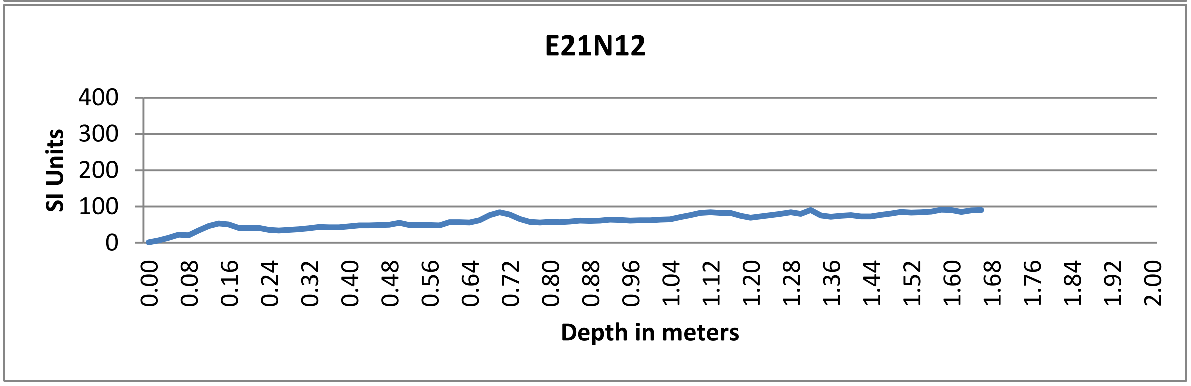
E21N12
SI Units
0
100
200
300
400
0.00
0.08
0.16
0.24
0.32
0.40
0.48
0.56
0.64
0.72
0.80
0.88
0.96
1.04
1.12
1.20
1.28
1.36
1.44
1.52
1.60
1.68
1.76
1.84
1.92
2.00
Depth in meters

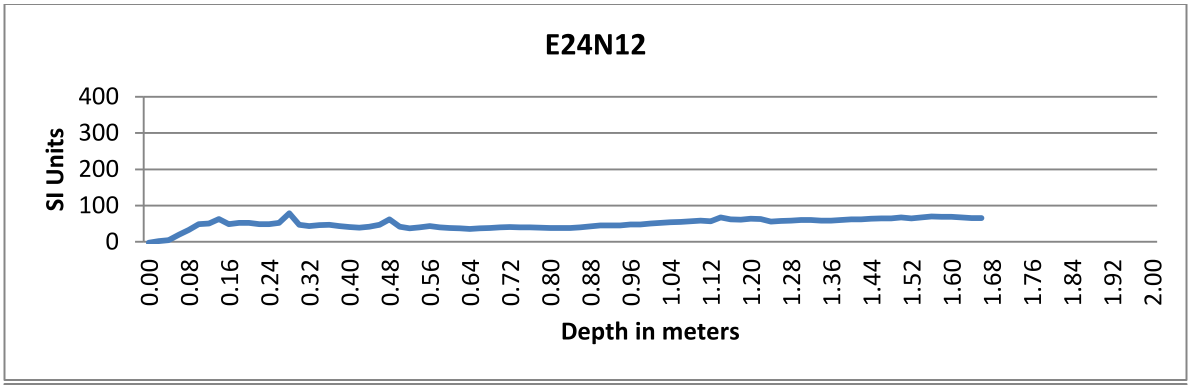
E24N12
SI Units
400
300
200
100
0
0.00 0.08 0.16 0.24 0.32 0.40 0.48 0.56 0.64 0.72 0.80 0.88 0.96 1.04 1.12 1.20 1.28 1.36 1.44 1.52 1.60 1.68 1.76 1.84 1.92 2.00
Depth in meters

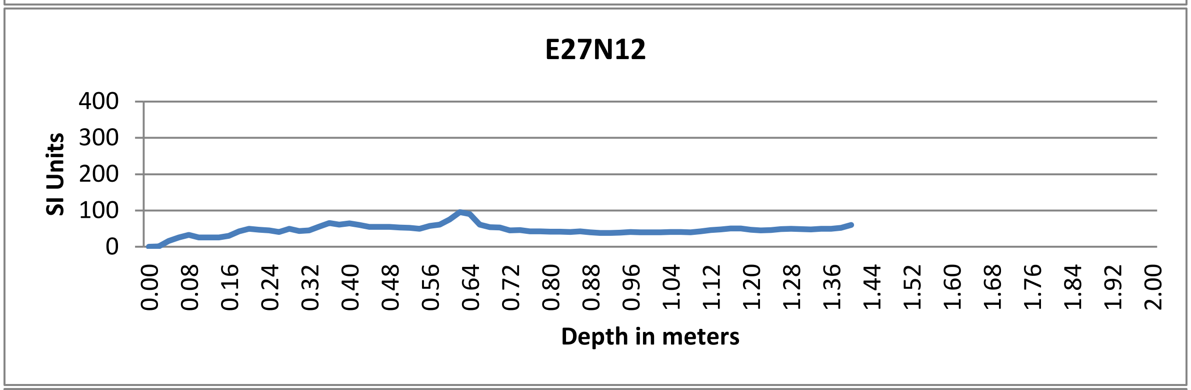
E27N12
SI Units
400
300
200
100
0
0.00 0.08 0.16 0.24 0.32 0.40 0.48 0.56 0.64 0.72 0.80 0.88 0.96 1.04 1.12 1.20 1.28 1.36 1.44 1.52 1.60 1.68 1.76 1.84 1.92 2.00
Depth in meters

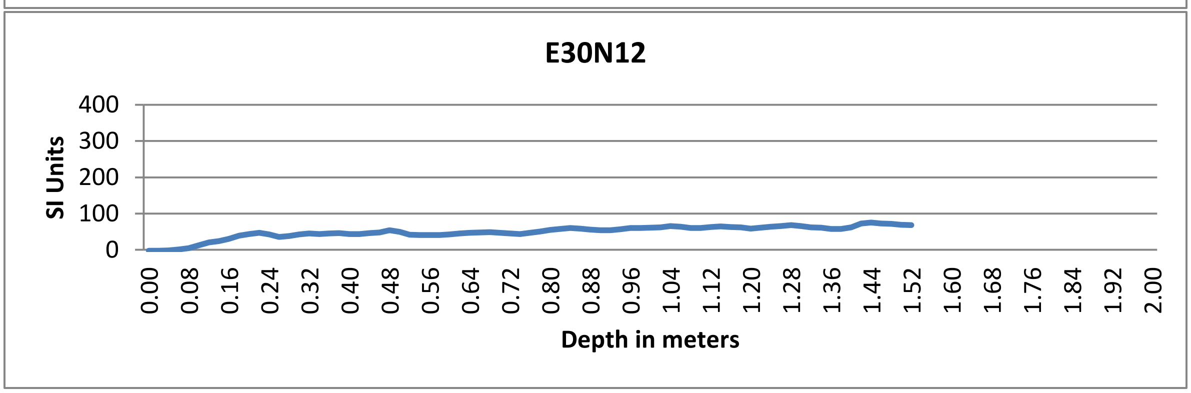
E30N12
SI Units
400
300
200
100
0
0.00 0.08 0.16 0.24 0.32 0.40 0.48 0.56 0.64 0.72 0.80 0.88 0.96 1.04 1.12 1.20 1.28 1.36 1.44 1.52 1.60 1.68 1.76 1.84 1.92 2.00
Depth in meters

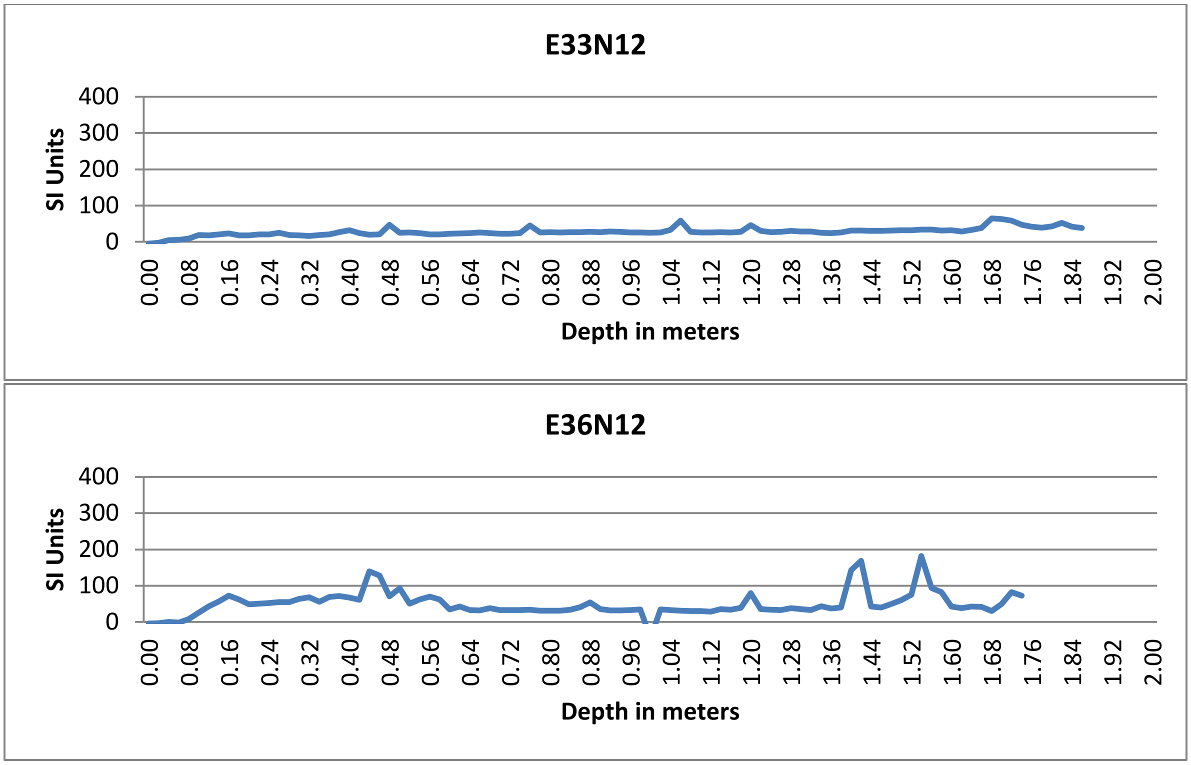

Figure 30 Hollywood downhole profiles, N12 line.

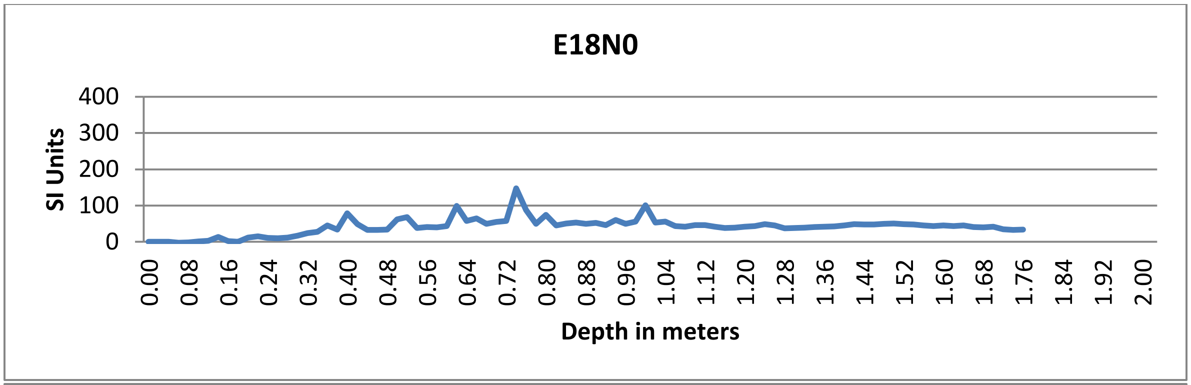
E18N0
SI Units
400
300
200
100
0
0.00
0.08
0.16
0.24
0.32
0.40
0.48
0.56
0.64
0.72
0.80
0.88
0.96
1.04
1.12
1.20
1.28
1.36
1.44
1.52
1.60
1.68
1.76
1.84
1.92
2.00
Depth in meters

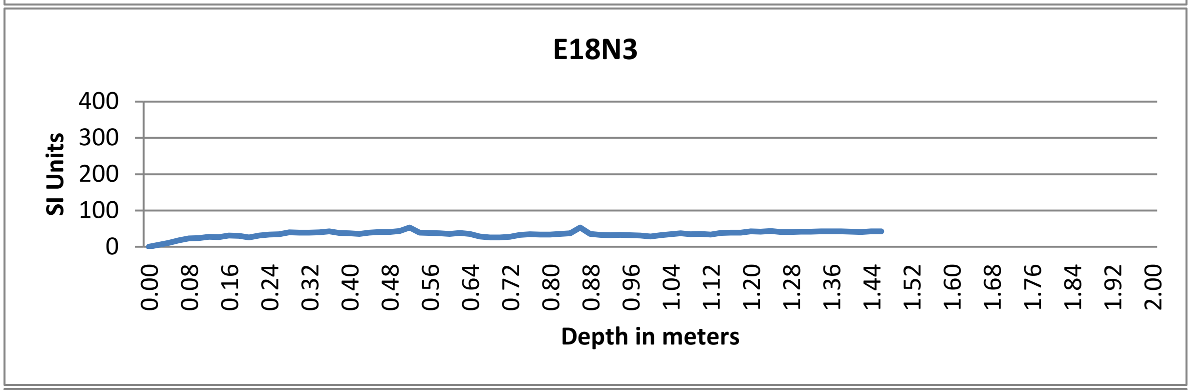
E18N3
SI Units
400
300
200
100
0
0.00
0.08
0.16
0.24
0.32
0.40
0.48
0.56
0.64
0.72
0.80
0.88
0.96
1.04
1.12
1.20
1.28
1.36
1.44
1.52
1.60
1.68
1.76
1.84
1.92
2.00
Depth in meters

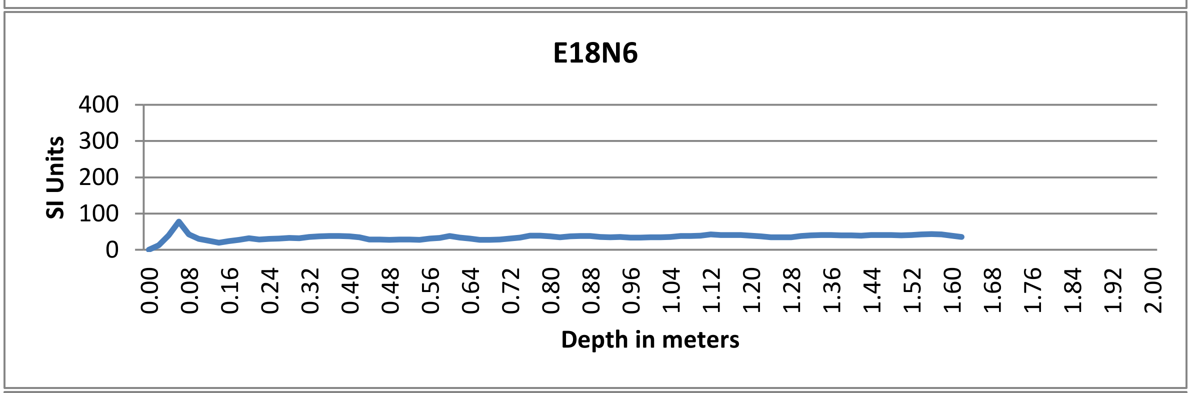
E18N6
SI Units
400
300
200
100
0
0.00
0.08
0.16
0.24
0.32
0.40
0.48
0.56
0.64
0.72
0.80
0.88
0.96
1.04
1.12
1.20
1.28
1.36
1.44
1.52
1.60
1.68
1.76
1.84
1.92
2.00
Depth in meters

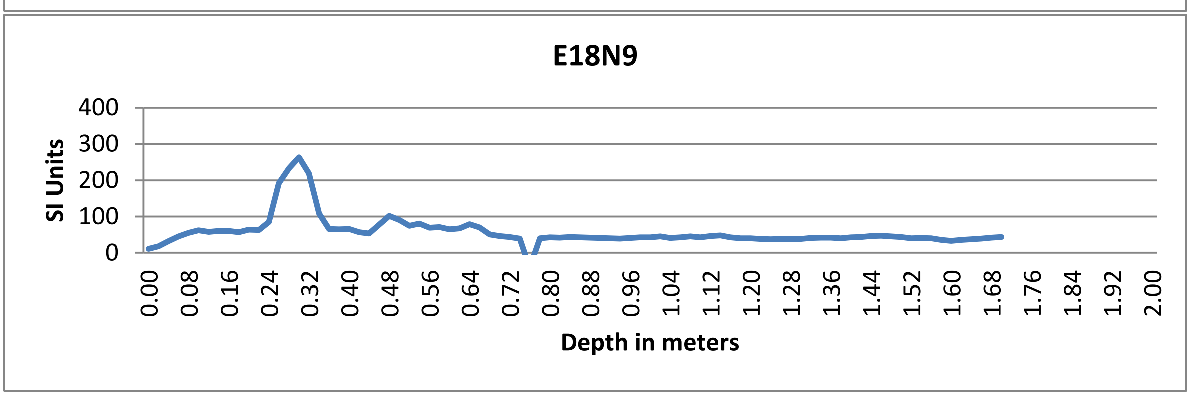
E18N9
SI Units
400
300
200
100
0
0.00
0.08
0.16
0.24
0.32
0.40
0.48
0.56
0.64
0.72
0.80
0.88
0.96
1.04
1.12
1.20
1.28
1.36
1.44
1.52
1.60
1.68
1.76
1.84
1.92
2.00
Depth in meters

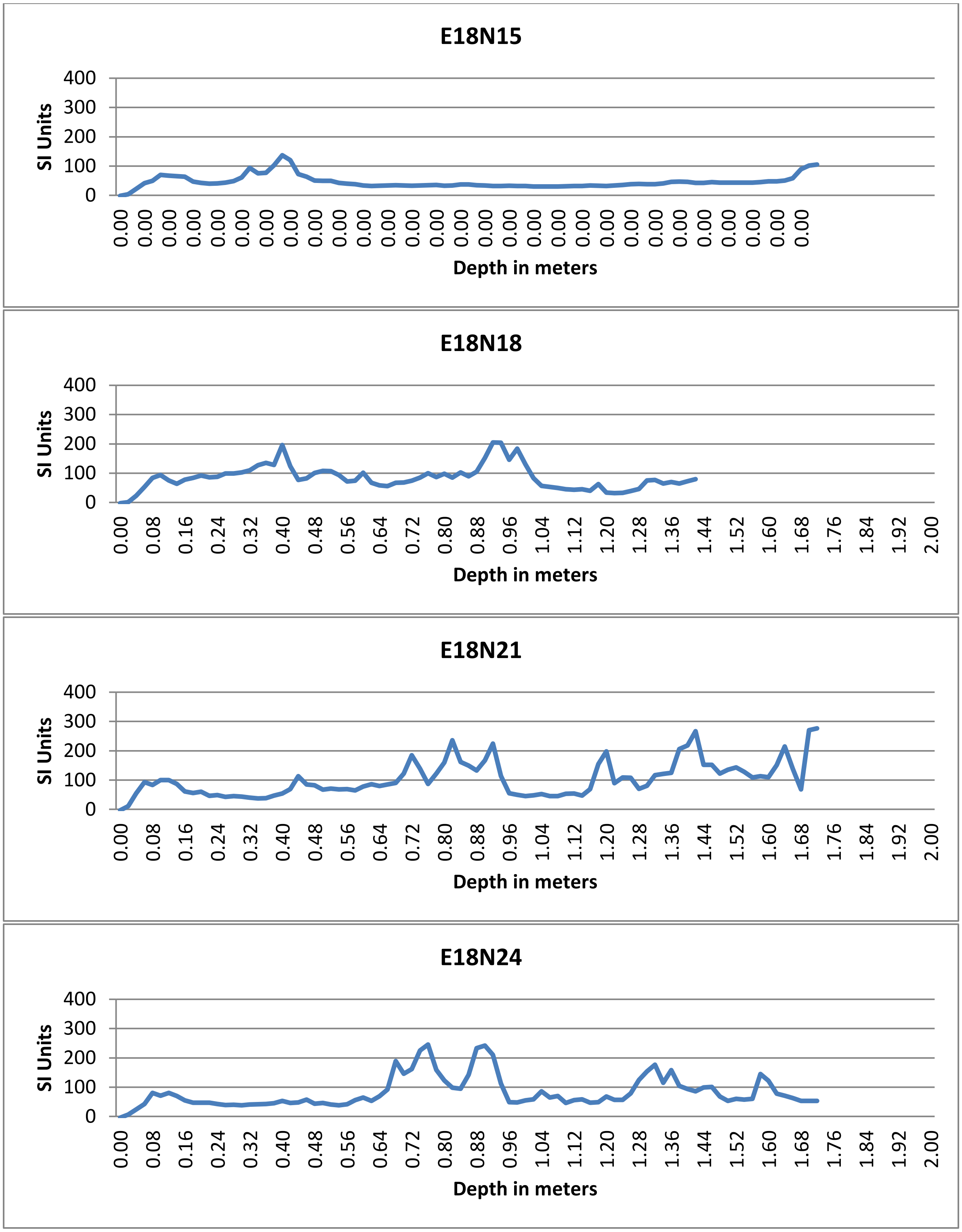

Figure 31 Hollywood downhole profiles, E18 line.

Beaverdam

The single mound at Beaverdam was the second downhole survey we did during the Phase III investigations, right after Hollywood in October of 2014. It still hadn't rained and we were still using the Oakfield. As a consequence, only one of the downhole surveys extended below a meter in depth (figs. 32-35; Table 5). We simply were not able to push or pound the Oakfield probe any deeper. Nothing that looked like a burned surface appeared in the solid cores and nothing that looked like a burned surface was evident in the downhole susceptibility readings. It may be that this relatively small mound was not a platform mound that was built to support a mound top structure. Haley's slope trench did expose burned surfaces deep in the trench but these are interpreted to be the remains of premound structures (Johnson et al. 2016).

Figure 32 Todd McLeod and Sam Butz taking GPS readings at Beaverdam.

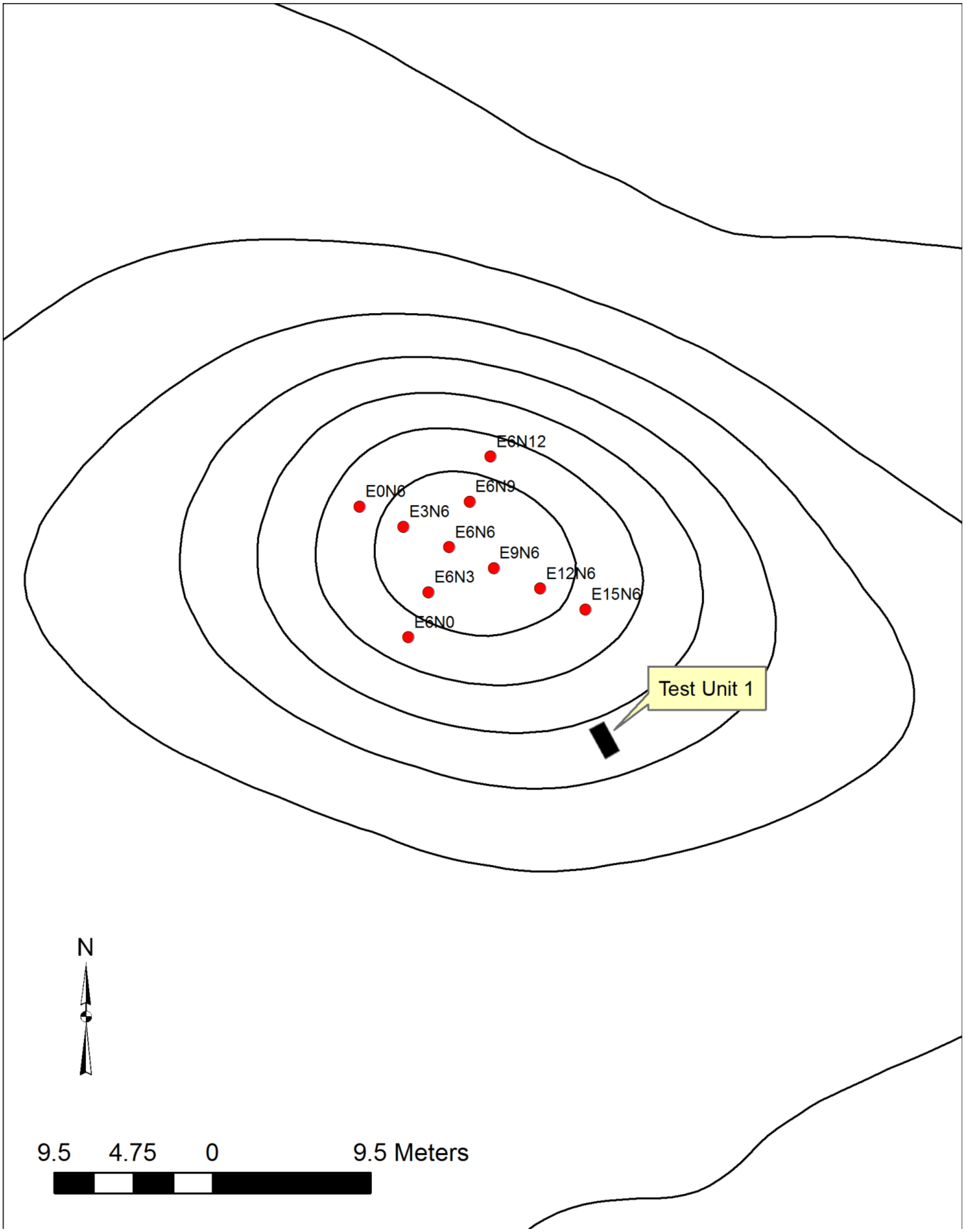

Figure 33 Downhole locations at Beaverdam.

Table 5 Downhole coordinates at Beaverdam, NAD 83

Coordinates	Easting	Northing
E0N6	738,855.47	3,834,988.61
E3N6	738,858.12	3,834,987.39
E6N6	738,860.86	3,834,986.16
E6N9	738,863.54	3,834,984.91
E12N6	738,866.32	3,834,983.68
E15N6	738,869.05	3,834,982.43
E6N0	738,858.41	3,834,980.75
E6N3	738,859.62	3,834,983.46
E6N9	738,862.09	3,834,988.90
E6N12	738,863.33	3,834,991.61

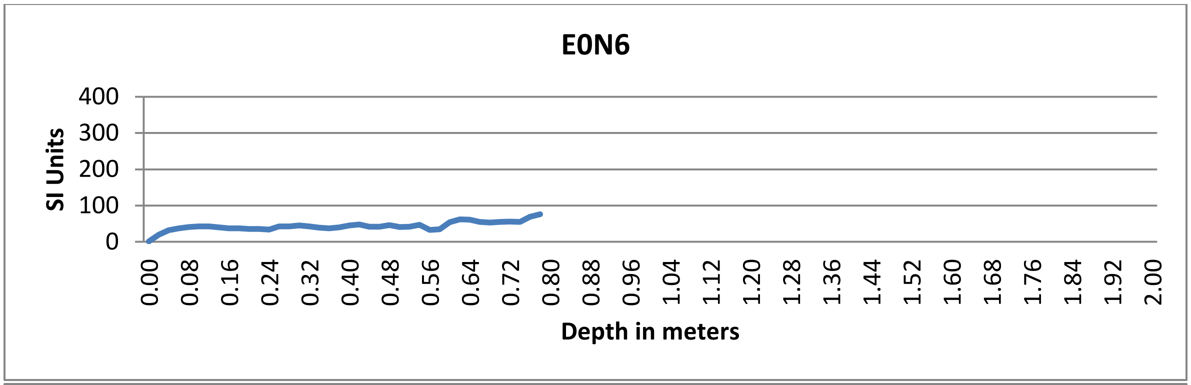
E0N6
SI Units
400
300
200
100
0
0.00 0.08 0.16 0.24 0.32 0.40 0.48 0.56 0.64 0.72 0.80 0.88 0.96 1.04 1.12 1.20 1.28 1.36 1.44 1.52 1.60 1.68 1.76 1.84 1.92 2.00
Depth in meters

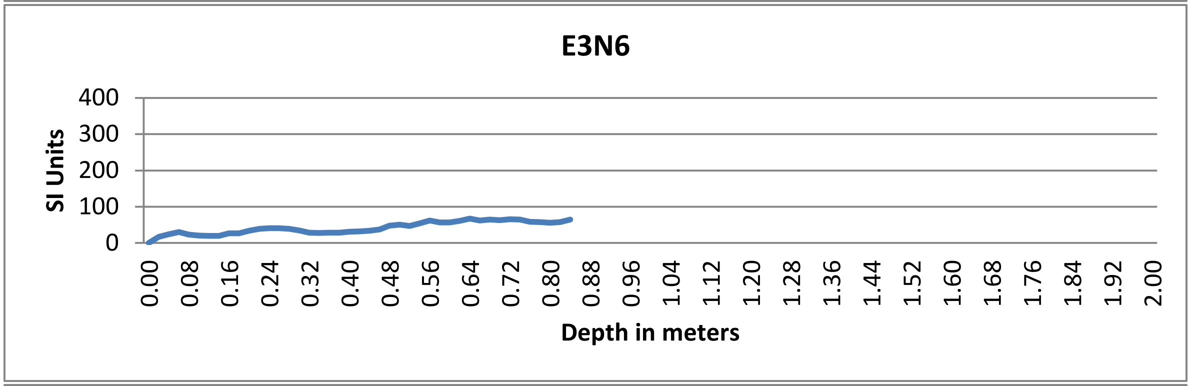
E3N6
SI Units
400
300
200
100
0
0.00 0.08 0.16 0.24 0.32 0.40 0.48 0.56 0.64 0.72 0.80 0.88 0.96 1.04 1.12 1.20 1.28 1.36 1.44 1.52 1.60 1.68 1.76 1.84 1.92 2.00
Depth in meters

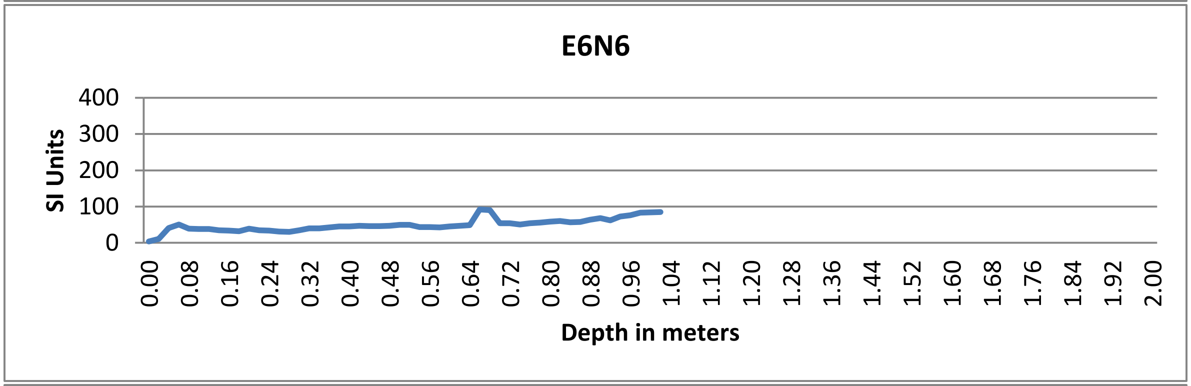
E6N6
SI Units
400
300
200
100
0
0.00 0.08 0.16 0.24 0.32 0.40 0.48 0.56 0.64 0.72 0.80 0.88 0.96 1.04 1.12 1.20 1.28 1.36 1.44 1.52 1.60 1.68 1.76 1.84 1.92 2.00
Depth in meters

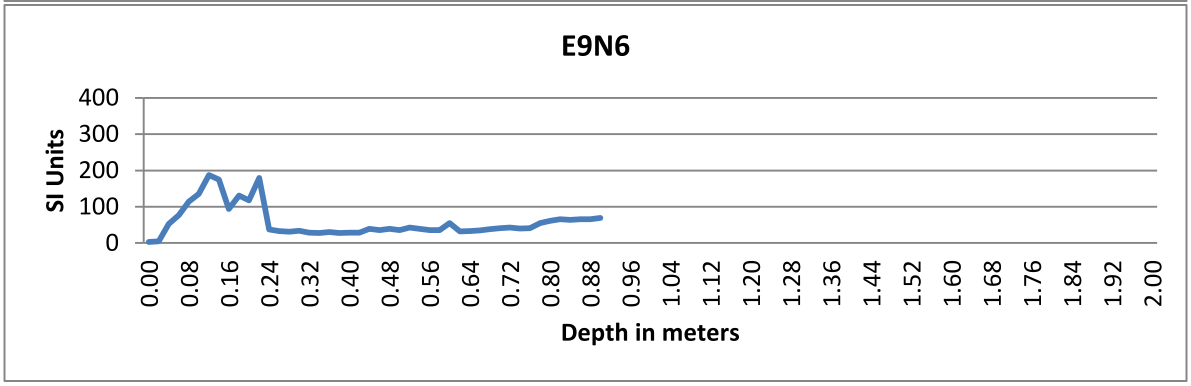
E9N6
SI Units
400
300
200
100
0
0.00 0.08 0.16 0.24 0.32 0.40 0.48 0.56 0.64 0.72 0.80 0.88 0.96 1.04 1.12 1.20 1.28 1.36 1.44 1.52 1.60 1.68 1.76 1.84 1.92 2.00
Depth in meters

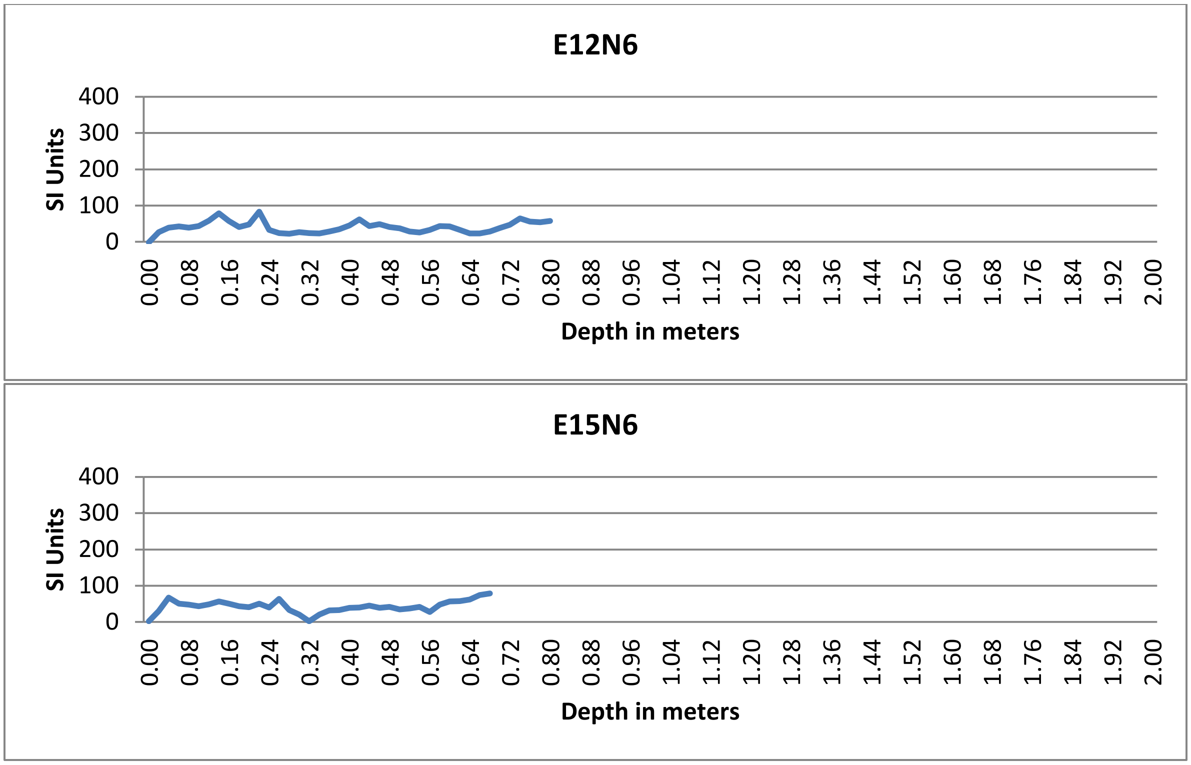

Figure 34 Beaverdam downhole profiles, N6 line.

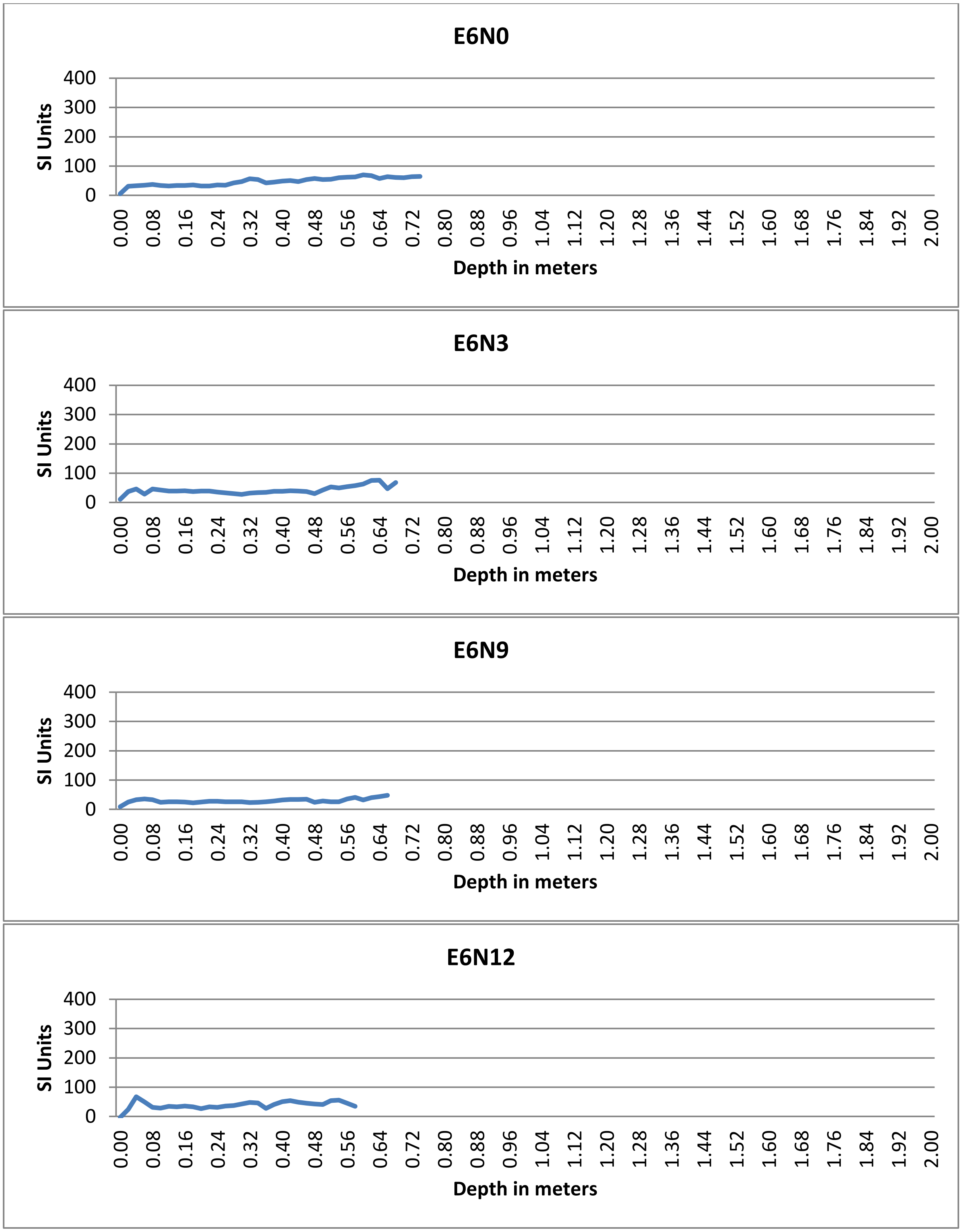

Figure 35 Beaverdam downhole profiles, E6 line.

Dunn

It actually took three trips to finish the downhole survey of the main mound at Dunn. It is fortunate that it is the closest of the Phase III sites to Oxford. Late in January of 2015, we cleared and shot in the sample transect, began the probe holes but had to quit when the battery finally failed on the laptop computer we were using to run the software that controlled the susceptibility probe and record the profiles. Multisus Fieldpro, the control program, runs best on Windows XP operating systems which dictates the use of an older computer. A second trip with a different computer had the same problem. We purchased an external battery pack designed specifically for portable computers and returned to Dunn in July of 2015 (fig. 36). By that time it was just Johnson and McLeod but we did finish. Another improvement on our field methods was the purchase of a different probe, the JMC T-Handle probe made it much easier to pound the cores deeper than we were able to go using the Oakfield. We actually purchased the JMC prior to our trip to begin the work on the Natchez sites in January of 2015.

Although, as the slope trenches demonstrated (Johnson et al. 2016) Mound A at Dunn is clearly a Mississippian structure, it is a very peculiar one, long and narrow with a relatively flat upper surface that is approximately 70m long but as little as 10m wide. We sampled the mound with a single line of downhole reading centering on the top of the mound (fig. 37; Table 6). Although several of the resulting susceptibility profiles show readings in the 200 to 300 SI range, no two adjacent profiles show elevated readings at the same depth (fig. 38). Several susceptibility profiles are nearly flat. It is likely that concentrations of daub caused the elevated readings. Not only was daub extremely common in the mound fill exposed in the slope tranches, it was encountered in several of the probe holes, often nearly stopping the probe and plugging it once we had punched through the concentrations of daub. The high density of daub suggests that there were mound top structures at Dunn. However, it appears that recent human and natural activity has destroyed any coherent evidence of those structures.

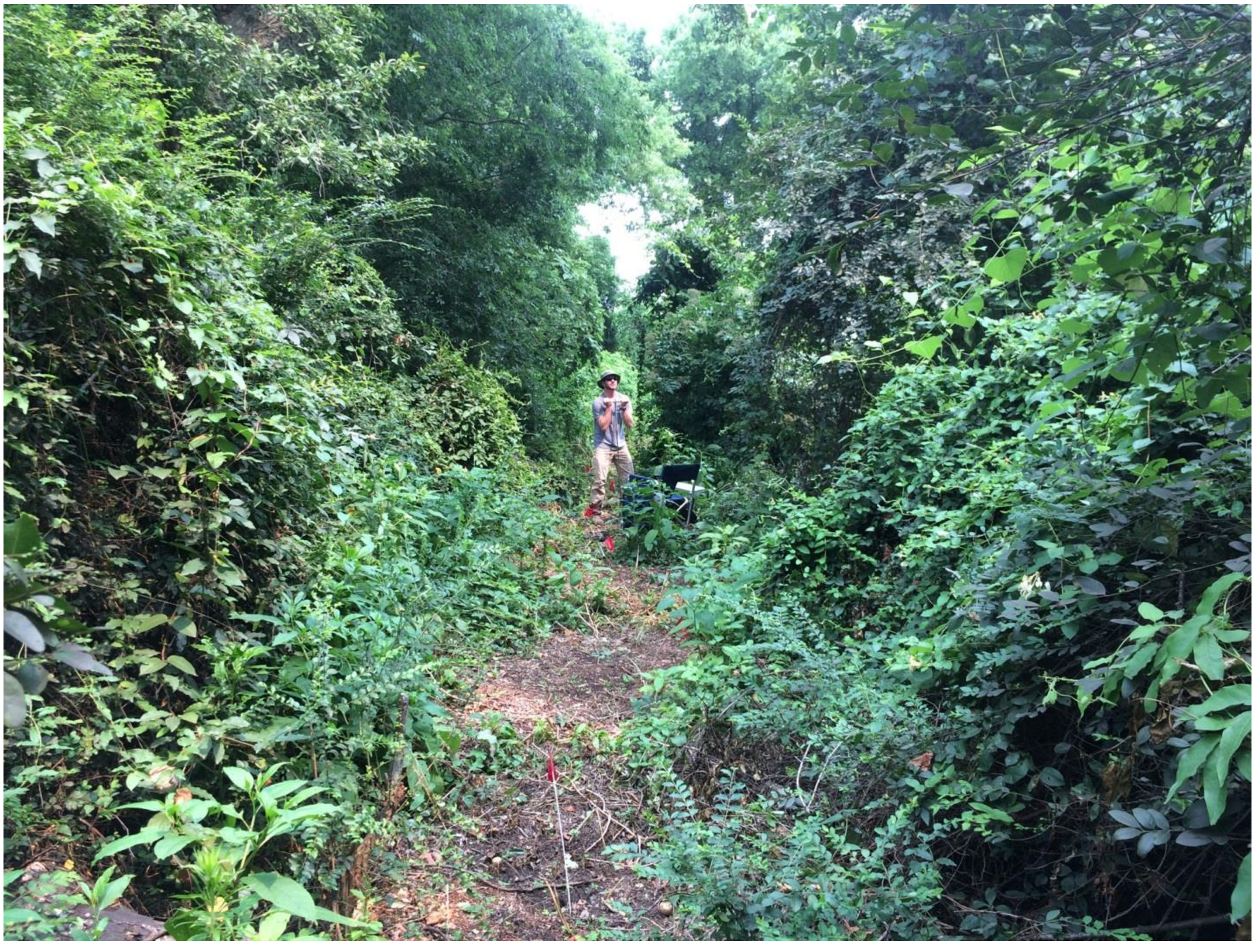
Figure 36 Downhole survey line at Dunn, Todd McLeod pulling the core.

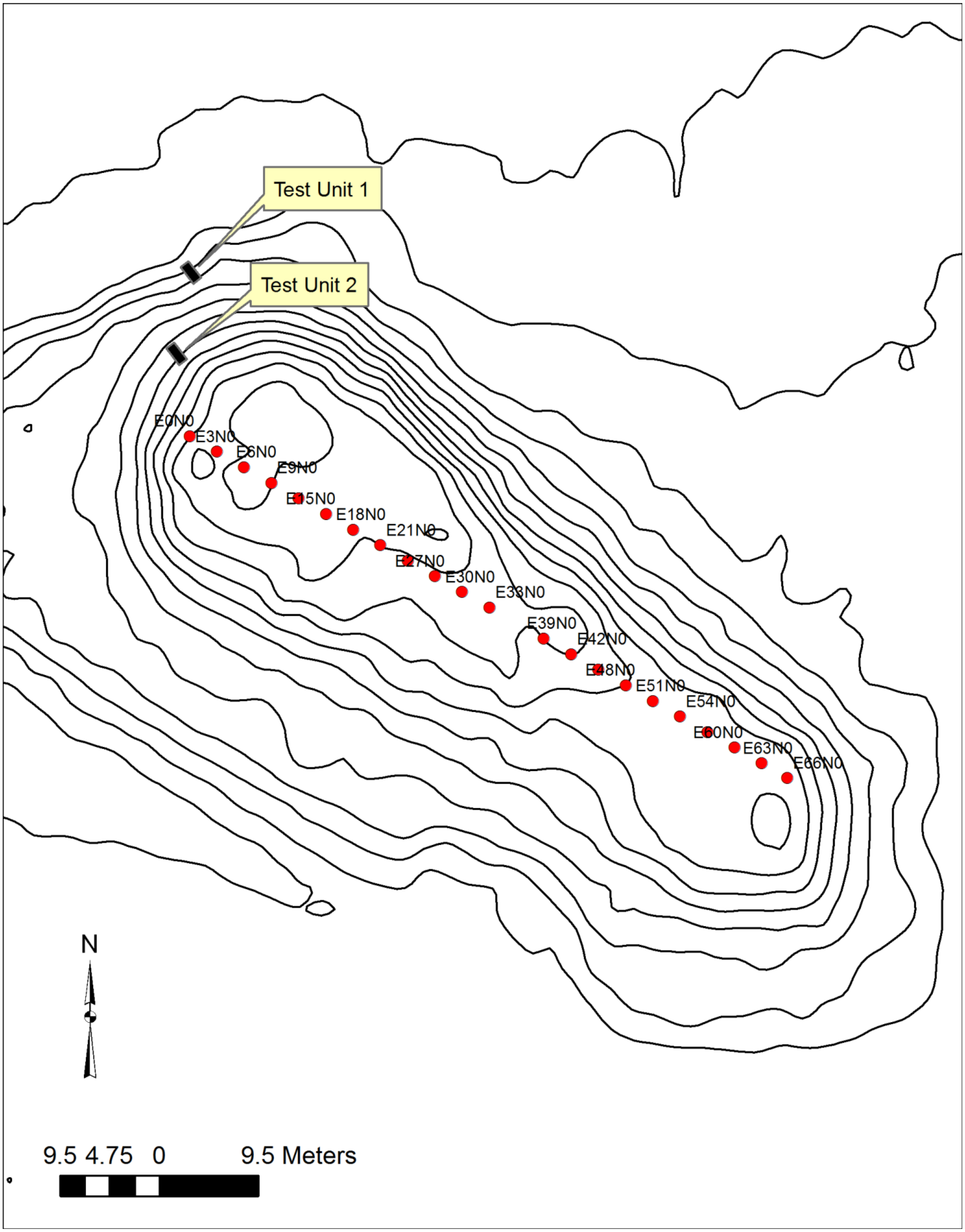

Figure 37 Downhole locations at Dunn.

Table 6 Downhole coordinates at Dunn, NAD 83.

Coordinates	Easting	Northing
E0N0	732,531.79	3,789,025.85
E3N0	732,534.40	3,789,024.36
E6N0	732,537.01	3,789,022.87
E9N0	732,539.62	3,789,021.38
E12N0	732,542.23	3,789,019.88
E15N0	732,544.85	3,789,018.39
E18N0	732,547.46	3,789,016.90
E21N0	732,550.07	3,789,015.41
E24N0	732,552.68	3,789,013.92
E27N0	732,555.29	3,789,012.42
E30N0	732,557.90	3,789,010.93
E33N0	732,560.52	3,789,009.44
E39N0	732,565.74	3,789,006.45
E42N0	732,568.35	3,789,004.96
E45N0	732,570.96	3,789,003.47
E48N0	732,573.58	3,789,001.98
E51N0	732,576.19	3,789,000.48
E54N0	732,578.80	3,788,998.99
E57N0	732,581.41	3,788,997.50
E60N0	732,584.02	3,788,996.01
E63N0	732,586.63	3,788,994.51
E66N0	732,589.09	3,788,993.09

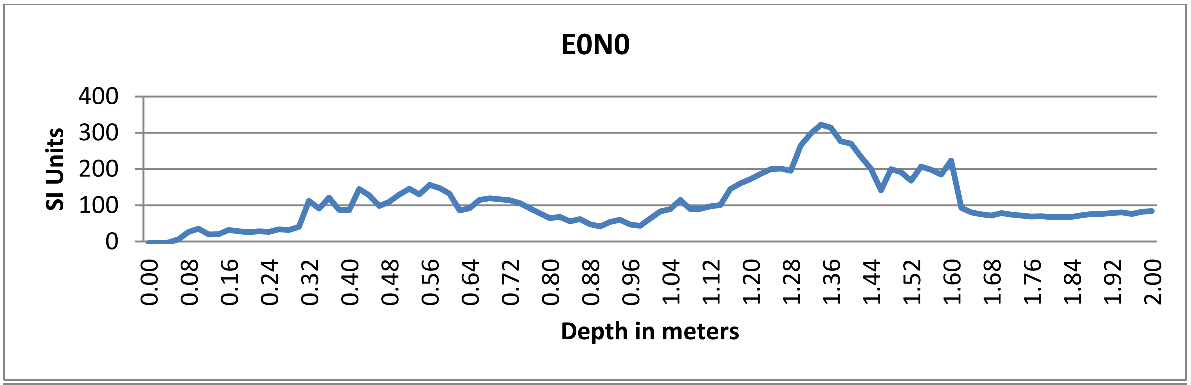
E0N0
SI Units
400
300
200
100
0
0.00 0.08 0.16 0.24 0.32 0.40 0.48 0.56 0.64 0.72 0.80 0.88 0.96 1.04 1.12 1.20 1.28 1.36 1.44 1.52 1.60 1.68 1.76 1.84 1.92 2.00
Depth in meters

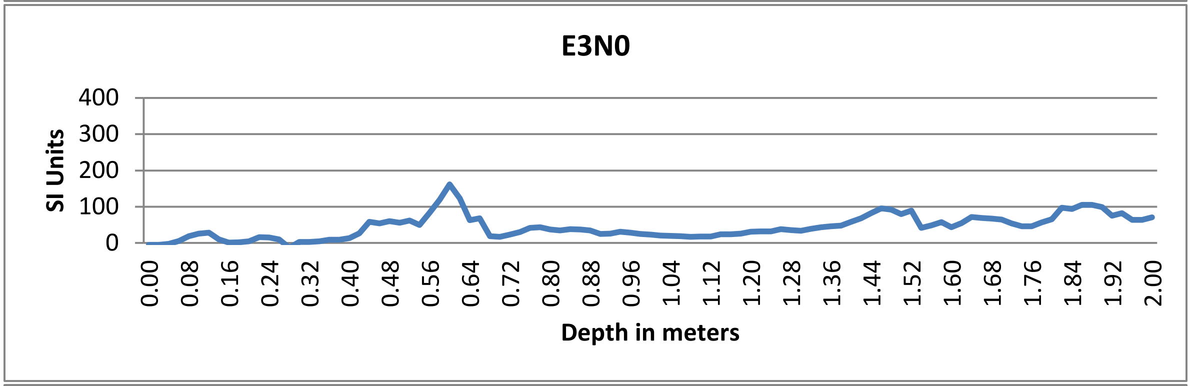
E3N0
SI Units
400
300
200
100
0
0.00 0.08 0.16 0.24 0.32 0.40 0.48 0.56 0.64 0.72 0.80 0.88 0.96 1.04 1.12 1.20 1.28 1.36 1.44 1.52 1.60 1.68 1.76 1.84 1.92 2.00
Depth in meters

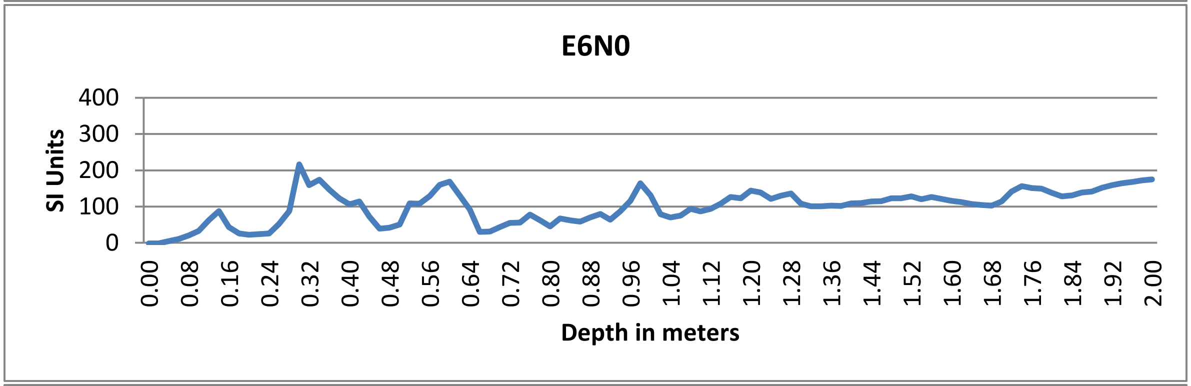
E6N0
SI Units
400
300
200
100
0
0.00 0.08 0.16 0.24 0.32 0.40 0.48 0.56 0.64 0.72 0.80 0.88 0.96 1.04 1.12 1.20 1.28 1.36 1.44 1.52 1.60 1.68 1.76 1.84 1.92 2.00
Depth in meters

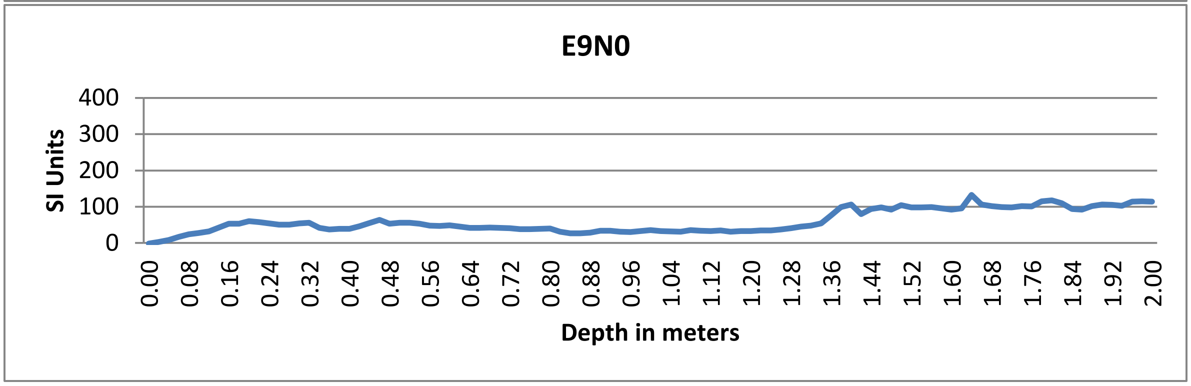
E9N0
SI Units
400
300
200
100
0
0.00 0.08 0.16 0.24 0.32 0.40 0.48 0.56 0.64 0.72 0.80 0.88 0.96 1.04 1.12 1.20 1.28 1.36 1.44 1.52 1.60 1.68 1.76 1.84 1.92 2.00
Depth in meters

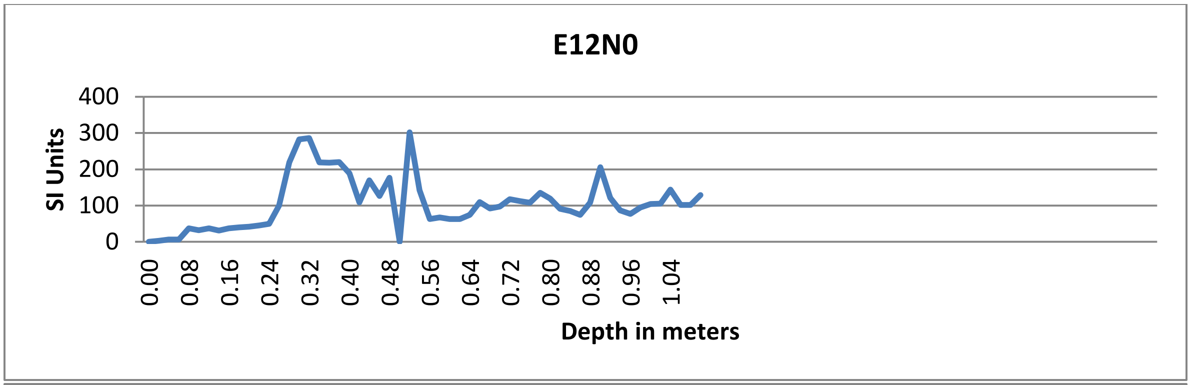
E12N0
SI Units
400
300
200
100
0
0.00 0.08 0.16 0.24 0.32 0.40 0.48 0.56 0.64 0.72 0.80 0.88 0.96 1.04
Depth in meters

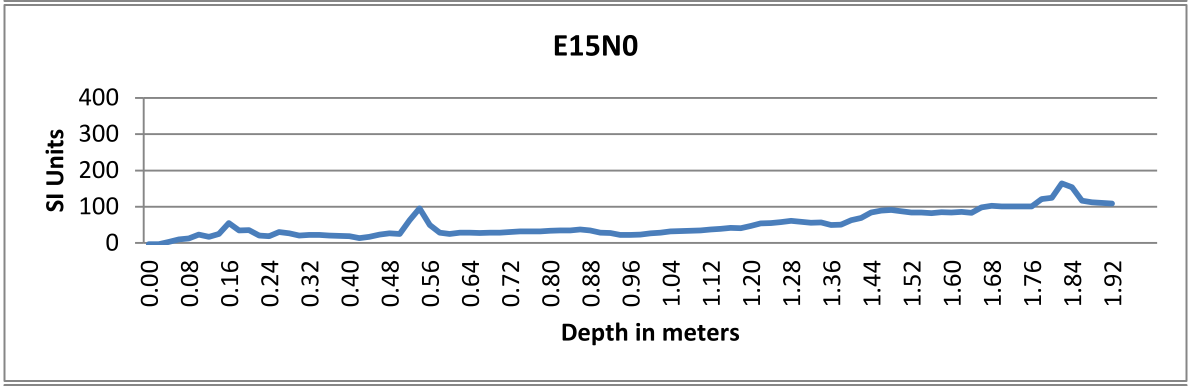
E15N0
SI Units
400
300
200
100
0
0.00 0.08 0.16 0.24 0.32 0.40 0.48 0.56 0.64 0.72 0.80 0.88 0.96 1.04 1.12 1.20 1.28 1.36 1.44 1.52 1.60 1.68 1.76 1.84 1.92
Depth in meters

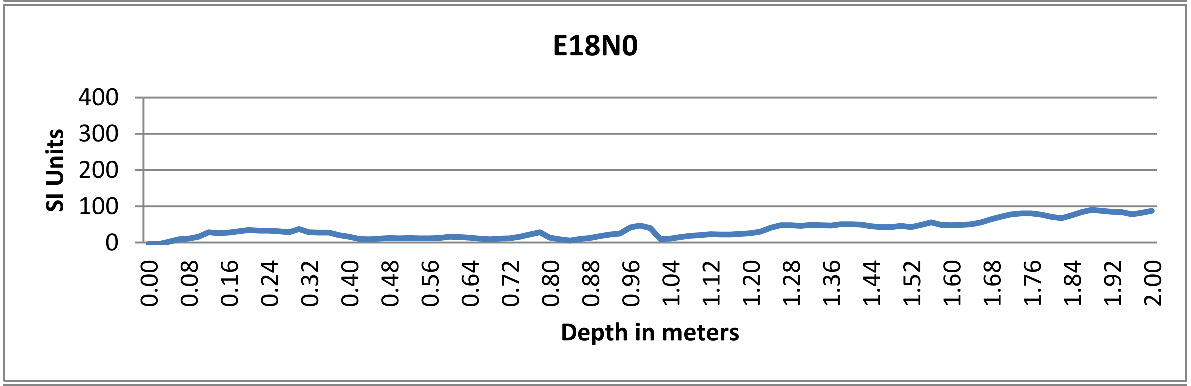
E18N0
SI Units
400
300
200
100
0
0.00 0.08 0.16 0.24 0.32 0.40 0.48 0.56 0.64 0.72 0.80 0.88 0.96 1.04 1.12 1.20 1.28 1.36 1.44 1.52 1.60 1.68 1.76 1.84 1.92 2.00
Depth in meters

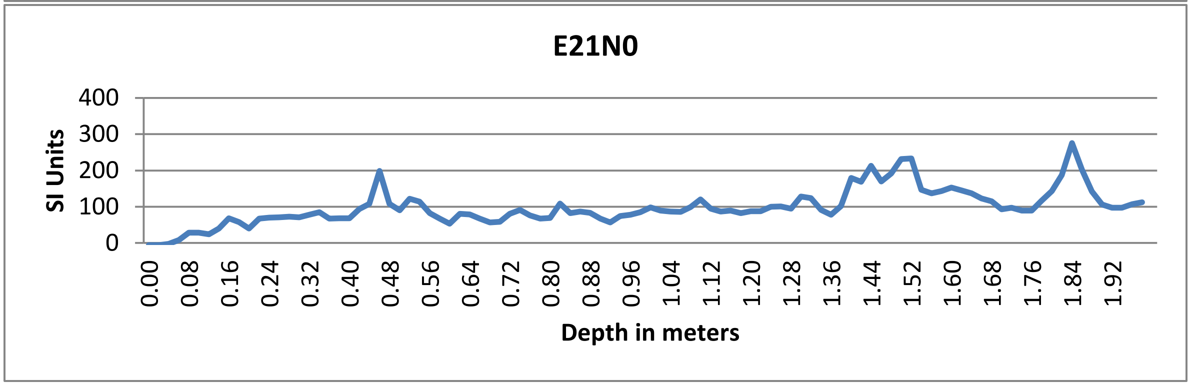
E21N0
SI Units
400
300
200
100
0
0.00 0.08 0.16 0.24 0.32 0.40 0.48 0.56 0.64 0.72 0.80 0.88 0.96 1.04 1.12 1.20 1.28 1.36 1.44 1.52 1.60 1.68 1.76 1.84 1.92
Depth in meters

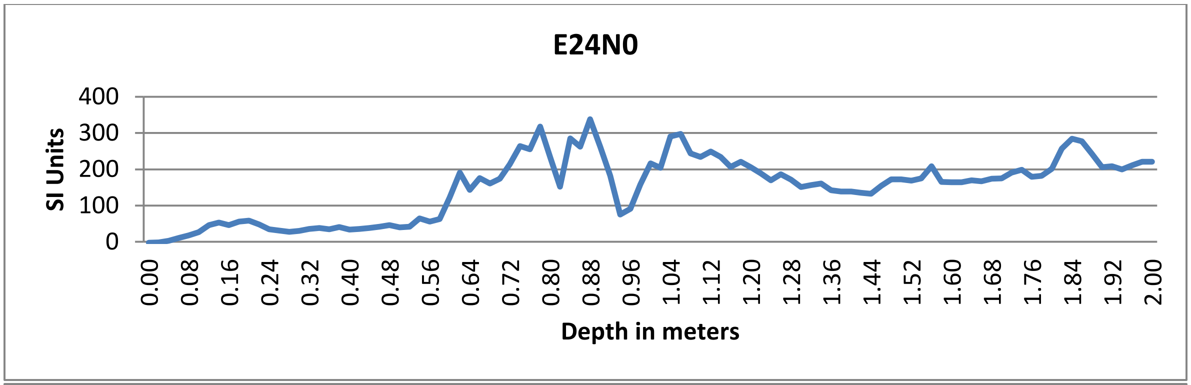
E24N0
SI Units
400
300
200
100
0
0.00 0.08 0.16 0.24 0.32 0.40 0.48 0.56 0.64 0.72 0.80 0.88 0.96 1.04 1.12 1.20 1.28 1.36 1.44 1.52 1.60 1.68 1.76 1.84 1.92 2.00
Depth in meters

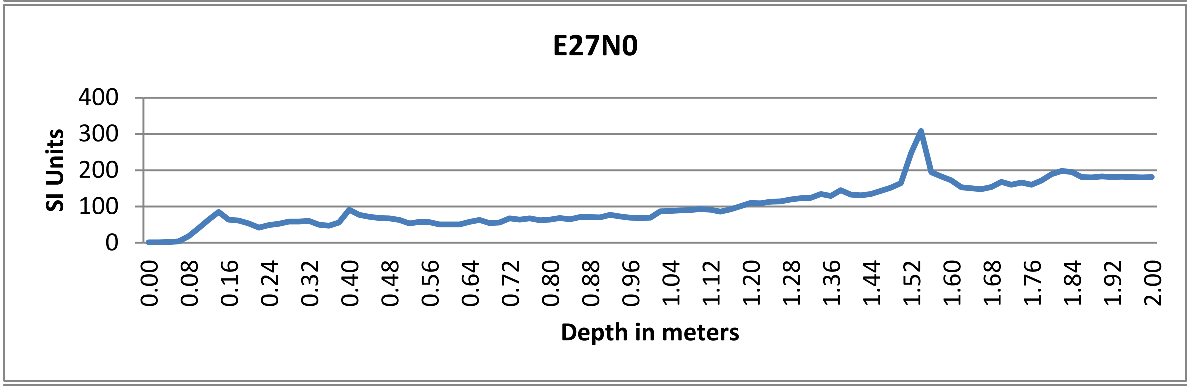
E27N0
SI Units
400
300
200
100
0
0.00 0.08 0.16 0.24 0.32 0.40 0.48 0.56 0.64 0.72 0.80 0.88 0.96 1.04 1.12 1.20 1.28 1.36 1.44 1.52 1.60 1.68 1.76 1.84 1.92 2.00
Depth in meters

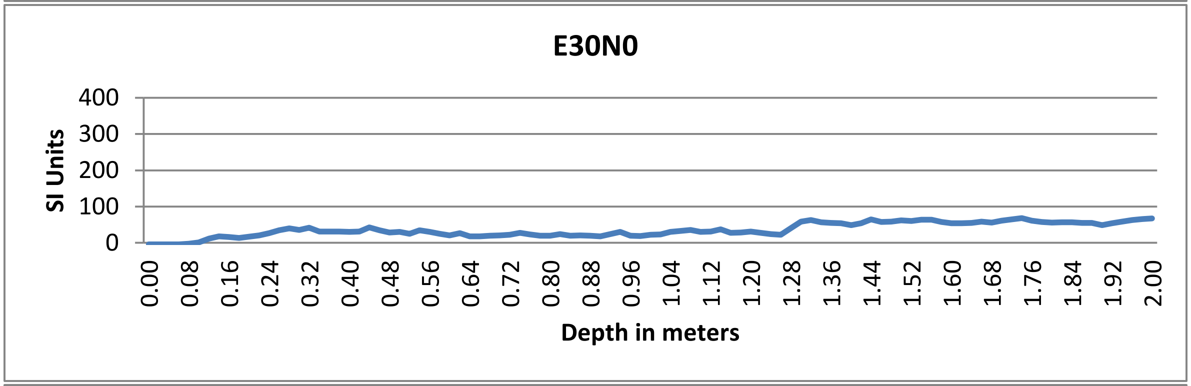
E30N0
SI Units
400
300
200
100
0
0.00 0.08 0.16 0.24 0.32 0.40 0.48 0.56 0.64 0.72 0.80 0.88 0.96 1.04 1.12 1.20 1.28 1.36 1.44 1.52 1.60 1.68 1.76 1.84 1.92 2.00
Depth in meters

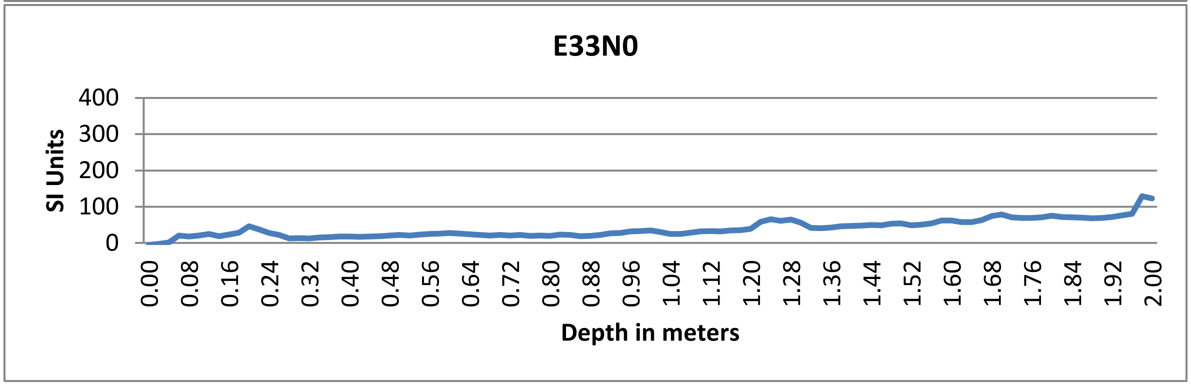
E33N0
SI Units
400
300
200
100
0
0.00 0.08 0.16 0.24 0.32 0.40 0.48 0.56 0.64 0.72 0.80 0.88 0.96 1.04 1.12 1.20 1.28 1.36 1.44 1.52 1.60 1.68 1.76 1.84 1.92 2.00
Depth in meters

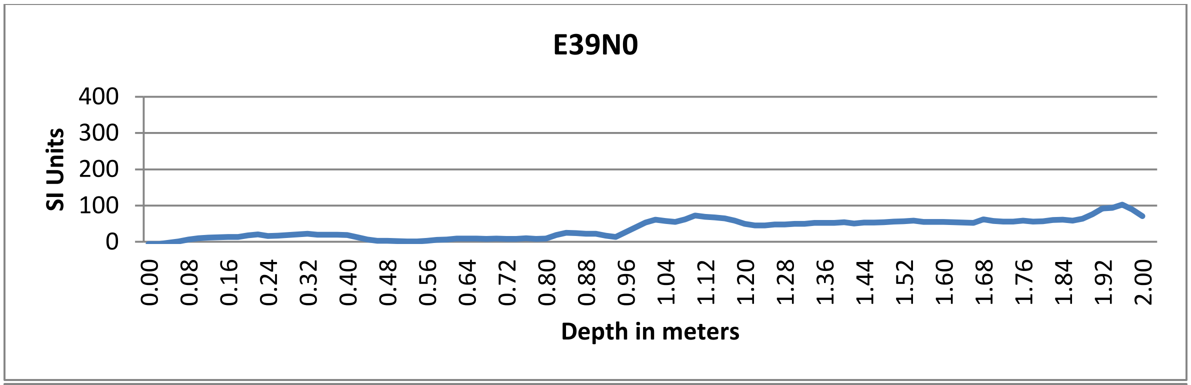
E39N0
SI Units
400
300
200
100
0
0.00 0.08 0.16 0.24 0.32 0.40 0.48 0.56 0.64 0.72 0.80 0.88 0.96 1.04 1.12 1.20 1.28 1.36 1.44 1.52 1.60 1.68 1.76 1.84 1.92 2.00
Depth in meters

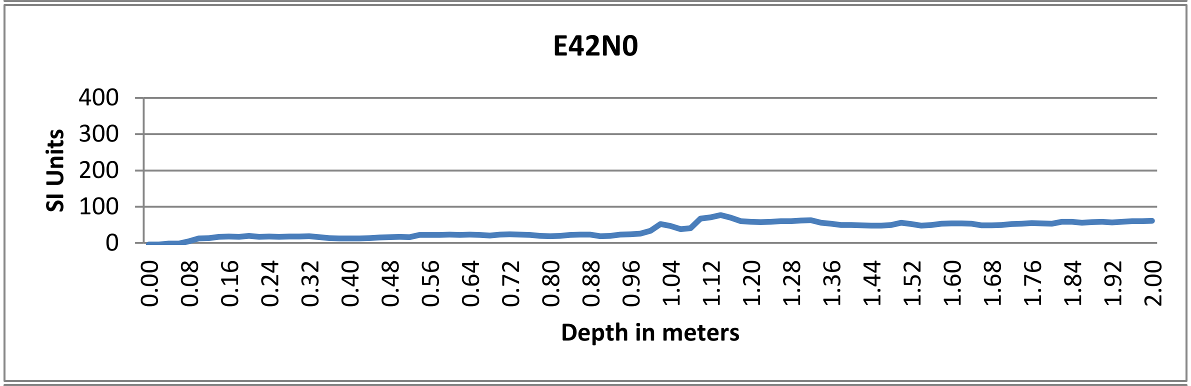
E42N0
SI Units
400
300
200
100
0
0.00 0.08 0.16 0.24 0.32 0.40 0.48 0.56 0.64 0.72 0.80 0.88 0.96 1.04 1.12 1.20 1.28 1.36 1.44 1.52 1.60 1.68 1.76 1.84 1.92 2.00
Depth in meters

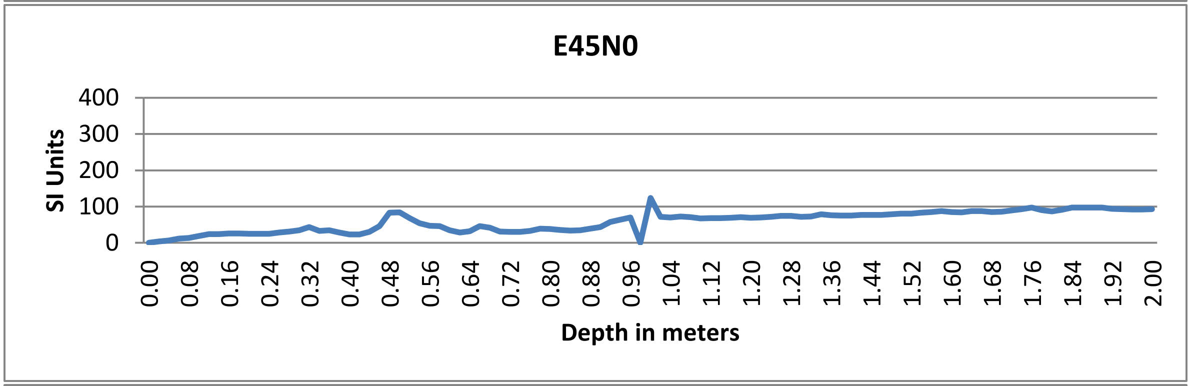
E45N0
SI Units
400
300
200
100
0
0.00 0.08 0.16 0.24 0.32 0.40 0.48 0.56 0.64 0.72 0.80 0.88 0.96 1.04 1.12 1.20 1.28 1.36 1.44 1.52 1.60 1.68 1.76 1.84 1.92 2.00
Depth in meters

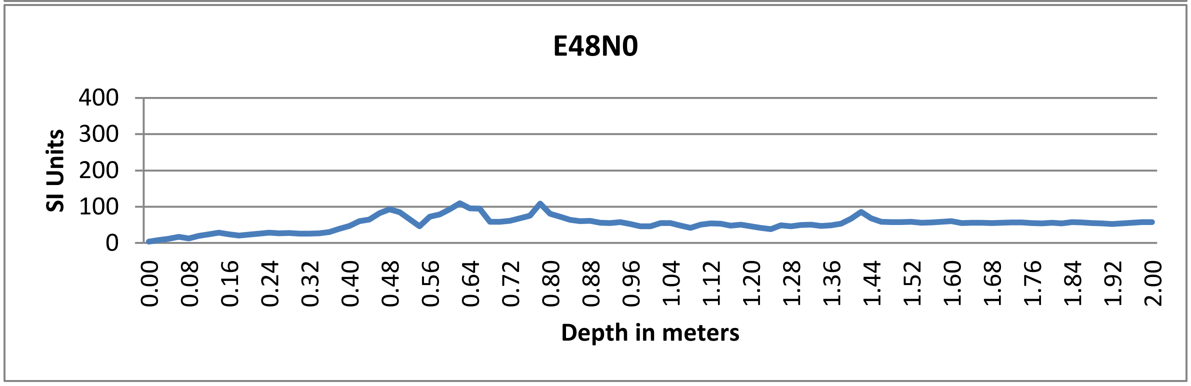
E48N0
SI Units
400
300
200
100
0
0.00 0.08 0.16 0.24 0.32 0.40 0.48 0.56 0.64 0.72 0.80 0.88 0.96 1.04 1.12 1.20 1.28 1.36 1.44 1.52 1.60 1.68 1.76 1.84 1.92 2.00
Depth in meters

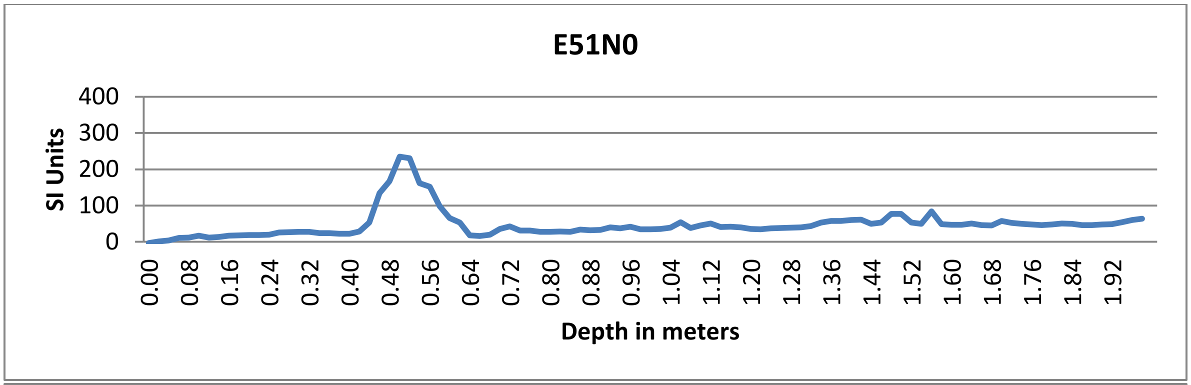
E51N0
SI Units
400
300
200
100
0
0.00
0.08
0.16
0.24
0.32
0.40
0.48
0.56
0.64
0.72
0.80
0.88
0.96
1.04
1.12
1.20
1.28
1.36
1.44
1.52
1.60
1.68
1.76
1.84
1.92
Depth in meters

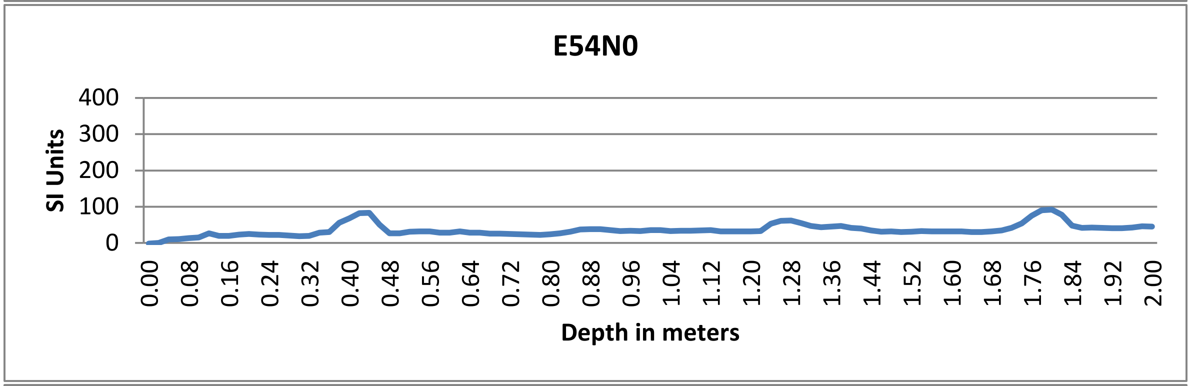
E54N0
SI Units
400
300
200
100
0
0.00
0.08
0.16
0.24
0.32
0.40
0.48
0.56
0.64
0.72
0.80
0.88
0.96
1.04
1.12
1.20
1.28
1.36
1.44
1.52
1.60
1.68
1.76
1.84
1.92
2.00
Depth in meters

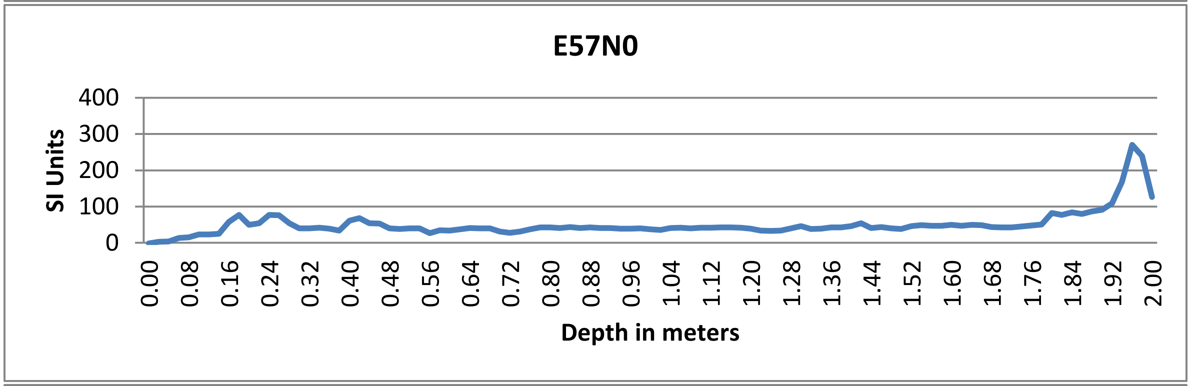
E57N0
SI Units
400
300
200
100
0
0.00
0.08
0.16
0.24
0.32
0.40
0.48
0.56
0.64
0.72
0.80
0.88
0.96
1.04
1.12
1.20
1.28
1.36
1.44
1.52
1.60
1.68
1.76
1.84
1.92
2.00
Depth in meters

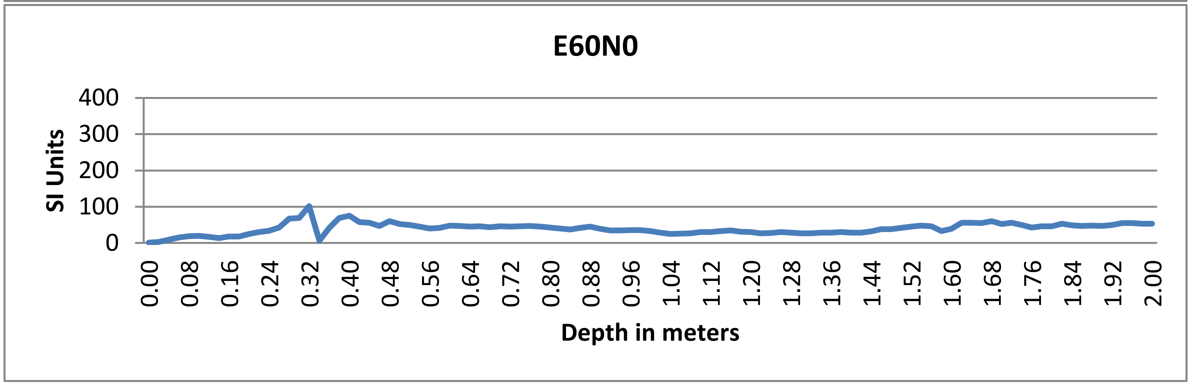
E60N0
SI Units
400
300
200
100
0
0.00
0.08
0.16
0.24
0.32
0.40
0.48
0.56
0.64
0.72
0.80
0.88
0.96
1.04
1.12
1.20
1.28
1.36
1.44
1.52
1.60
1.68
1.76
1.84
1.92
2.00
Depth in meters

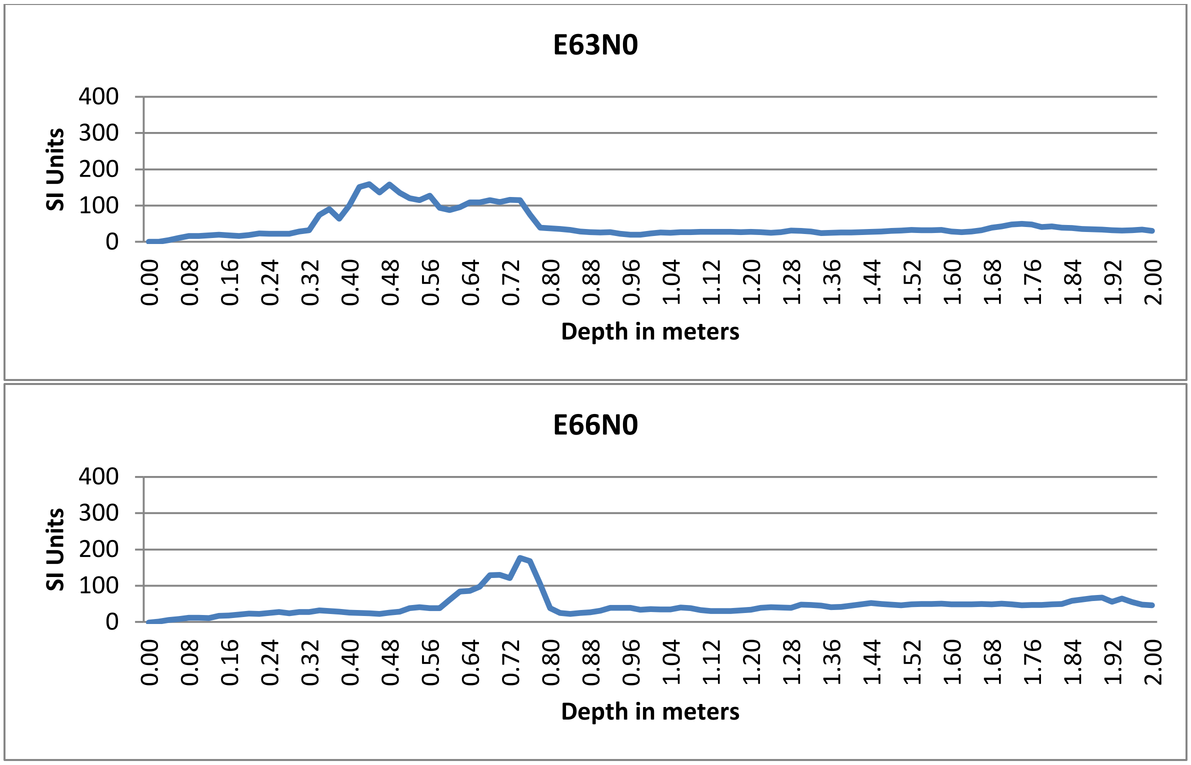

Figure 38 Dunn downhole profiles, N0 line.

Arcola

In addition to the gradiometer survey were did at Arcola, we conducted a downhole susceptibility survey of the top of Mound A in hopes of located a burned floor that Jessica Kowalski could test during her thesis research (figs 39, 40; Table 7). This was the last survey we did in 2014 and we were still using the Oakfield probe but were able to go a little deeper than we did at Hollywood and Beaverdam, reaching depths of nearly 1.7m. The majority of the profiles are relatively flat with readings around 50 SI (figs. 41, 42). The only exceptions are the profile recorded at E0N12 and E9N15, each of which had a single, isolated peak. The first peaked at slightly more than 400 SI and may have been a piece of daub although that is generally higher than the daub readings we got a Dunn. The second peak was more than 1,000 SI and is almost certainly metal. Kowalski recounted a long tradition of Boy Scout campouts on top of Mound A which may account for the probable metal reading. There was nothing in the profiles that we could relate to prehistoric activity at the site.

Figure 39 Jessica Kowalski and Sam Butz taking downhole readings on Mound A at Arcola.

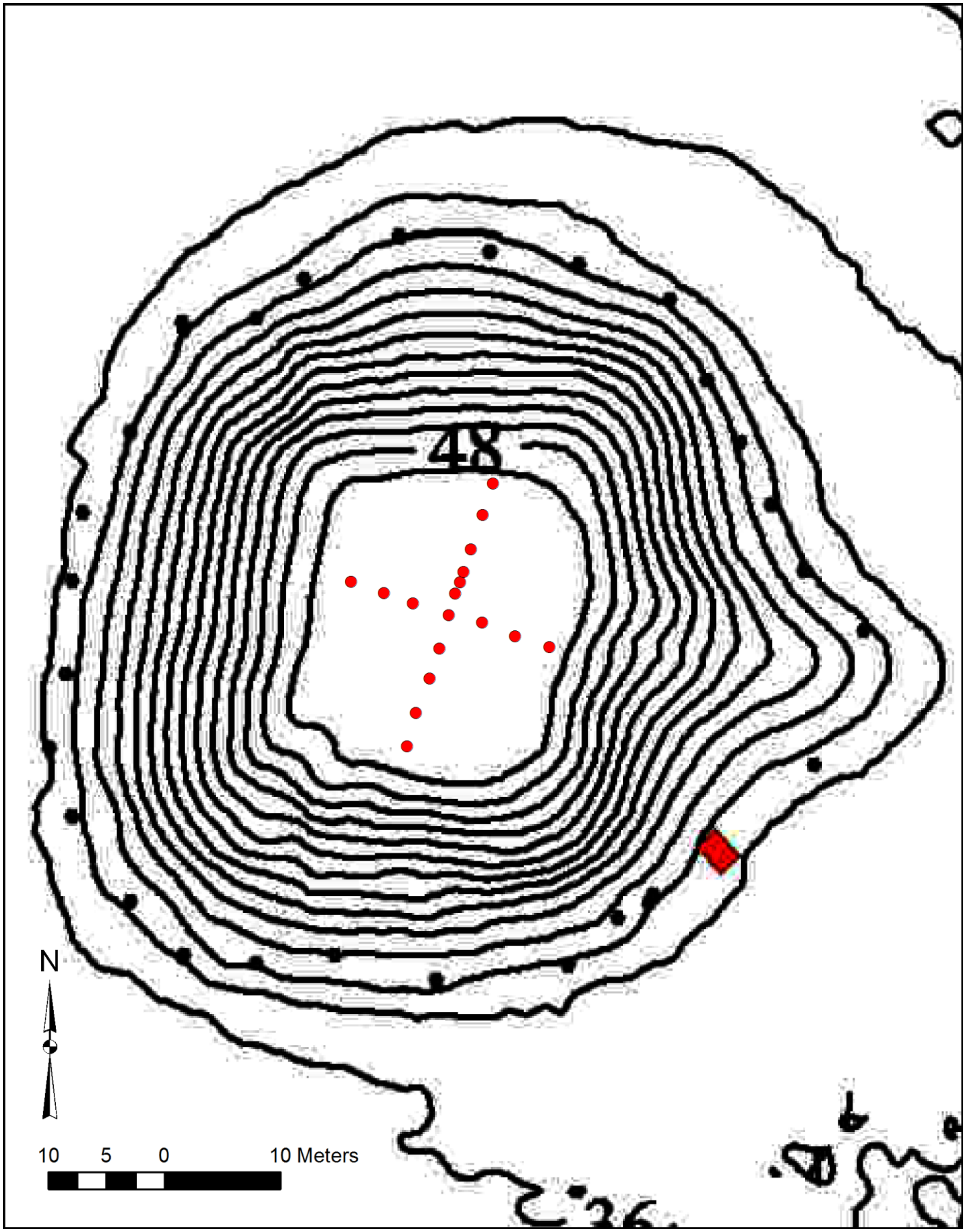

Figure 40 Arcola, downhole locations on Mound A summit.

Table 7 Downhole coordinate on Mound A at Arcola, NAD83

ID	Easting	Northing
E9N0	697,229.52	3,680,451.11
E9N3	697,230.26	3,680,454.00
E9N6	697,231.45	3,680,456.94
E9N9	697,232.29	3,680,459.55
E9N12	697,233.12	3,680,462.40
E9N15	697,234.10	3,680,465.24
E9N18	697,235.03	3,680,468.08
E9N21	697,236.04	3,680,471.07
E9N24	697,236.94	3,680,473.76
E0N12	697,224.68	3,680,465.28
E3N12	697,227.51	3,680,464.33
E6N12	697,230.03	3,680,463.41
E12N12	697,235.97	3,680,461.79
E15N12	697,238.85	3,680,460.59
E18N12	697,241.80	3,680,459.66

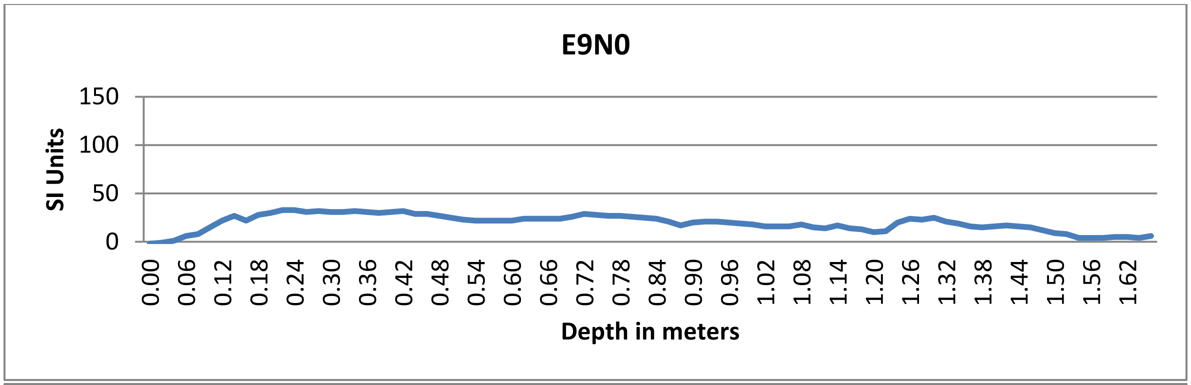
E9N0
SI Units
150
100
50
0
0.00
0.06
0.12
0.18
0.24
0.30
0.36
0.42
0.48
0.54
0.60
0.66
0.72
0.78
0.84
0.90
0.96
1.02
1.08
1.14
1.20
1.26
1.32
1.38
1.44
1.50
1.56
1.62
Depth in meters

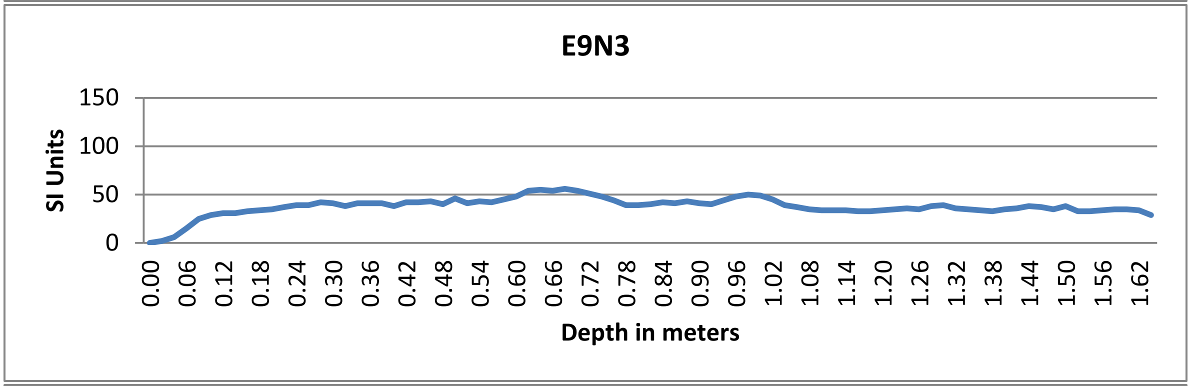
E9N3
SI Units
150
100
50
0
0.00
0.06
0.12
0.18
0.24
0.30
0.36
0.42
0.48
0.54
0.60
0.66
0.72
0.78
0.84
0.90
0.96
1.02
1.08
1.14
1.20
1.26
1.32
1.38
1.44
1.50
1.56
1.62
Depth in meters

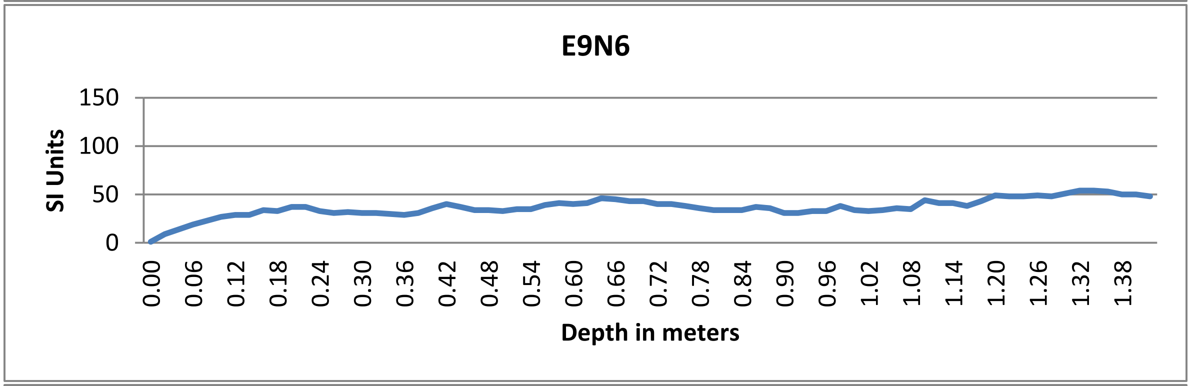
E9N6
SI Units
150
100
50
0
0.00
0.06
0.12
0.18
0.24
0.30
0.36
0.42
0.48
0.54
0.60
0.66
0.72
0.78
0.84
0.90
0.96
1.02
1.08
1.14
1.20
1.26
1.32
1.38
Depth in meters

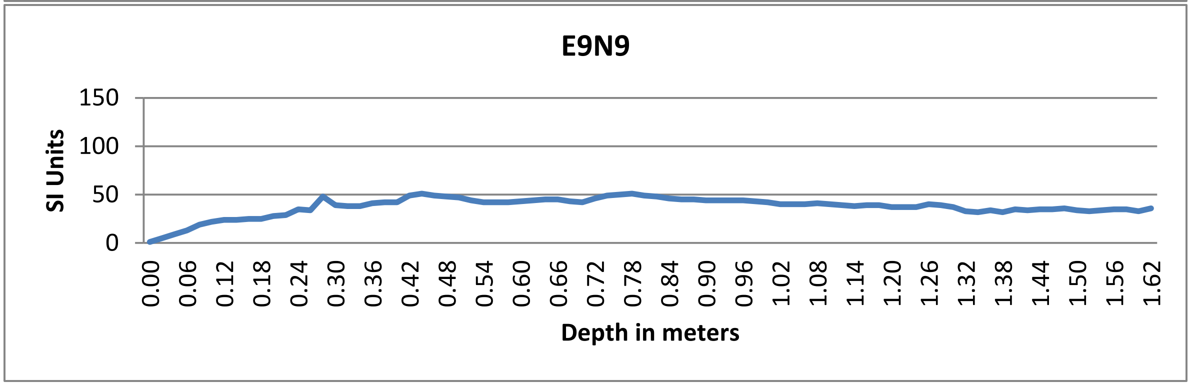
E9N9
SI Units
150
100
50
0
0.00
0.06
0.12
0.18
0.24
0.30
0.36
0.42
0.48
0.54
0.60
0.66
0.72
0.78
0.84
0.90
0.96
1.02
1.08
1.14
1.20
1.26
1.32
1.38
1.44
1.50
1.56
1.62
Depth in meters

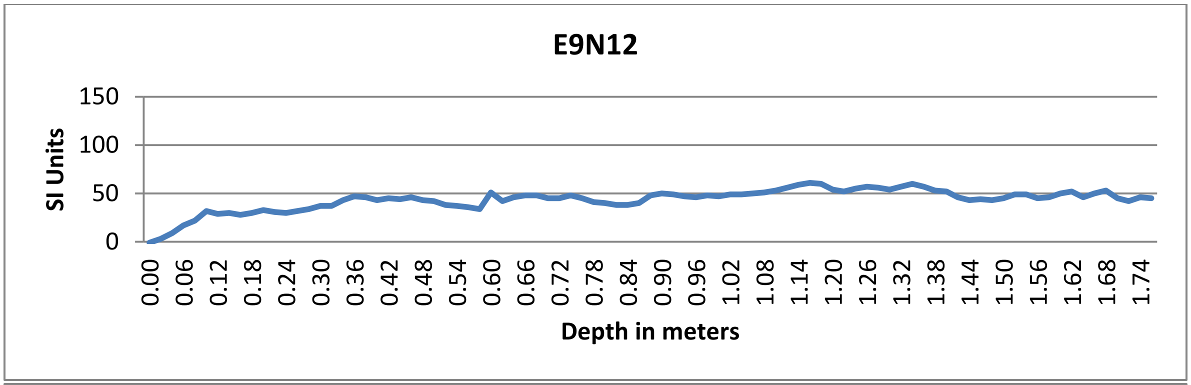
E9N12
SI Units
Depth in meters

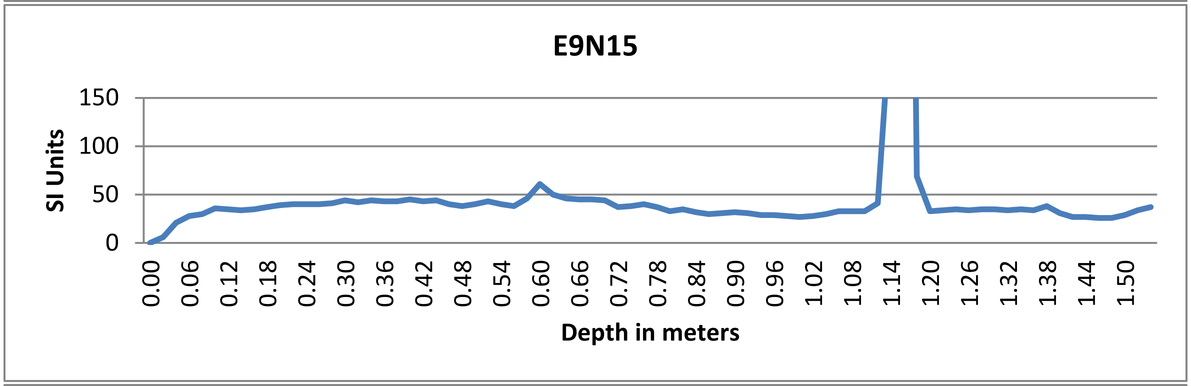
E9N15
SI Units
Depth in meters

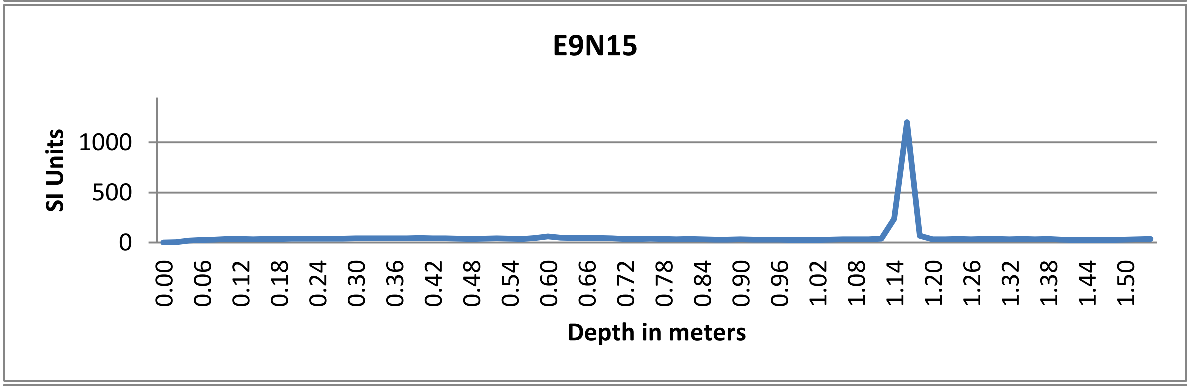
E9N15
SI Units
Depth in meters

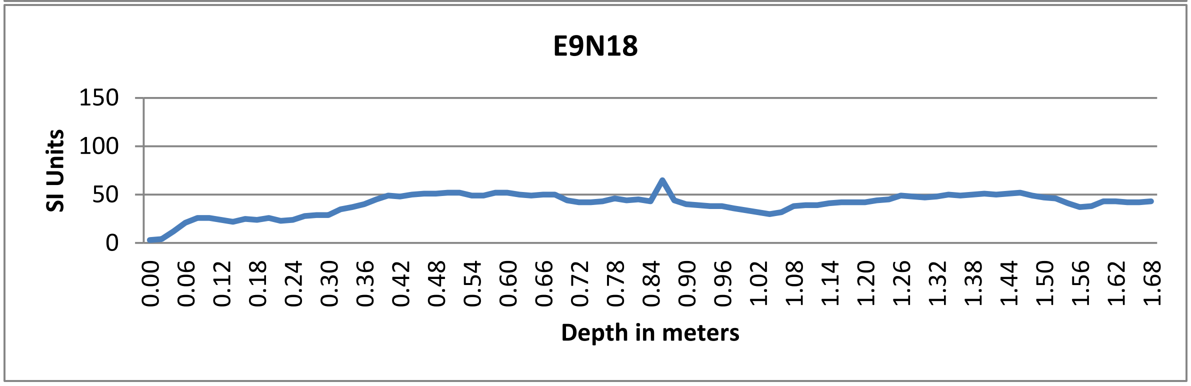
E9N18
SI Units
Depth in meters

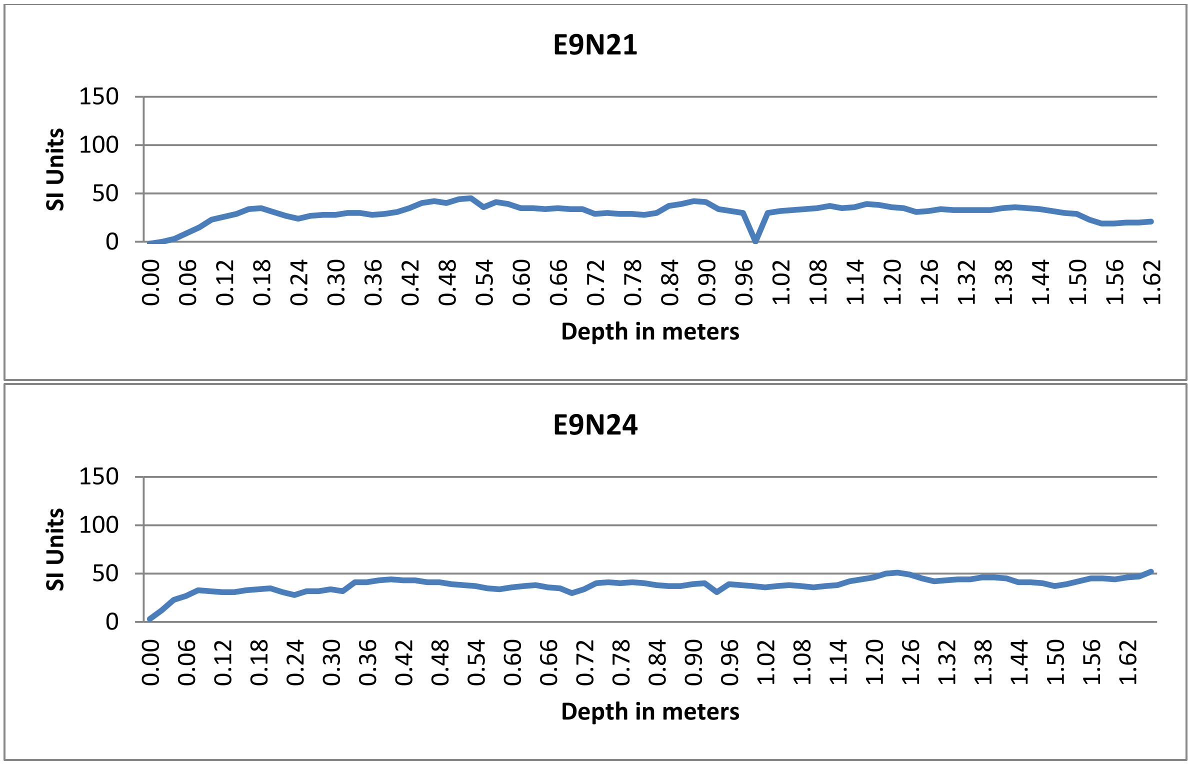

Figure 41 Arcola downhole profiles, E9 line.

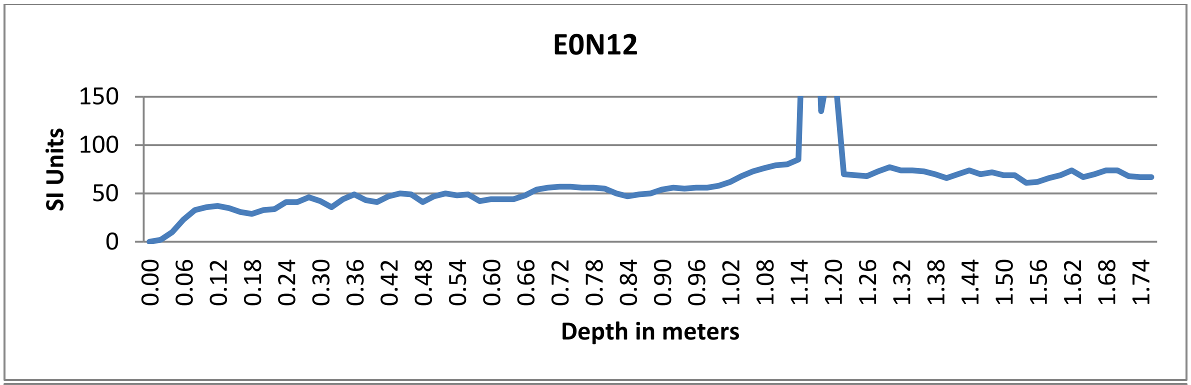
E0N12
SI Units
150
100
50
0
0.00 0.06 0.12 0.18 0.24 0.30 0.36 0.42 0.48 0.54 0.60 0.66 0.72 0.78 0.84 0.90 0.96 1.02 1.08 1.14 1.20 1.26 1.32 1.38 1.44 1.50 1.56 1.62 1.68 1.74
Depth in meters

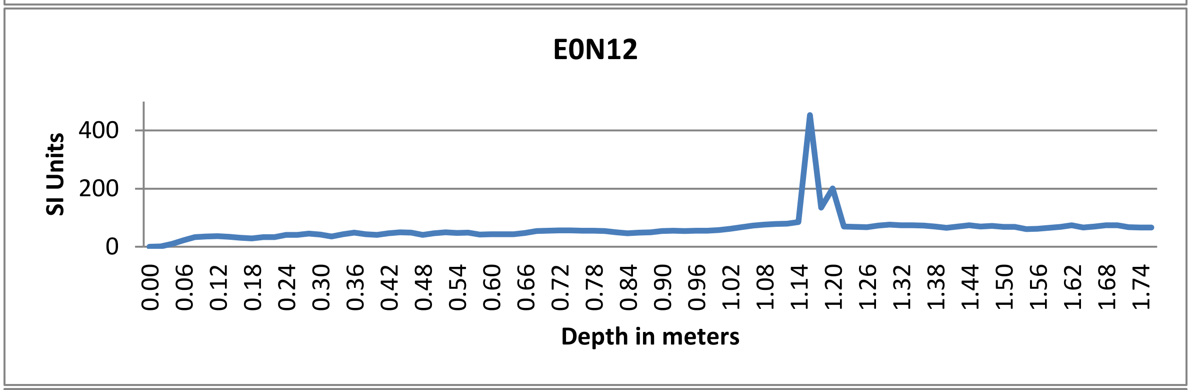
E0N12
SI Units
400
200
0
0.00 0.06 0.12 0.18 0.24 0.30 0.36 0.42 0.48 0.54 0.60 0.66 0.72 0.78 0.84 0.90 0.96 1.02 1.08 1.14 1.20 1.26 1.32 1.38 1.44 1.50 1.56 1.62 1.68 1.74
Depth in meters

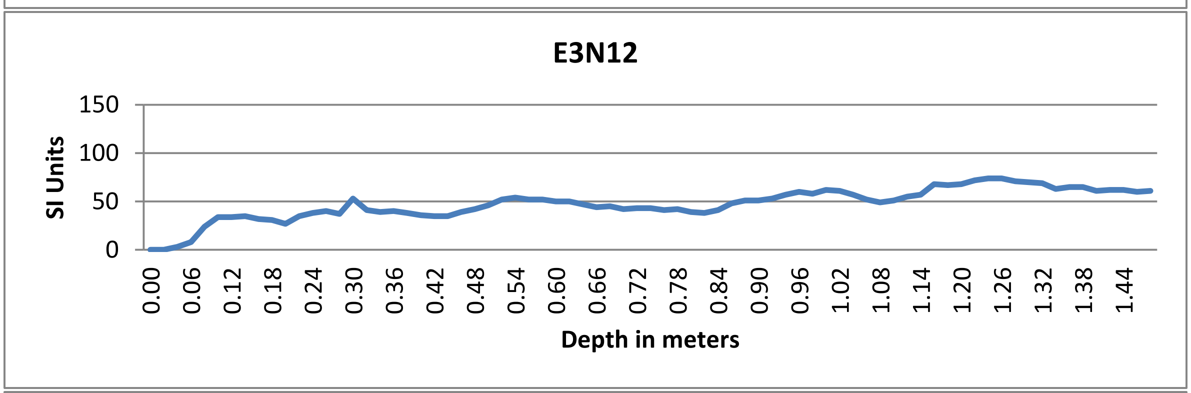
E3N12
SI Units
150
100
50
0
0.00 0.06 0.12 0.18 0.24 0.30 0.36 0.42 0.48 0.54 0.60 0.66 0.72 0.78 0.84 0.90 0.96 1.02 1.08 1.14 1.20 1.26 1.32 1.38 1.44
Depth in meters

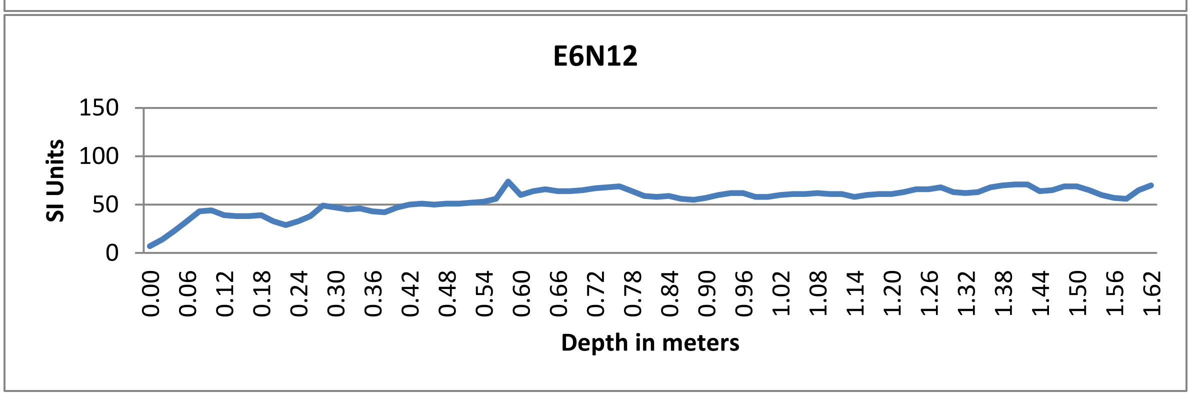
E6N12
SI Units
150
100
50
0
0.00 0.06 0.12 0.18 0.24 0.30 0.36 0.42 0.48 0.54 0.60 0.66 0.72 0.78 0.84 0.90 0.96 1.02 1.08 1.14 1.20 1.26 1.32 1.38 1.44 1.50 1.56 1.62
Depth in meters

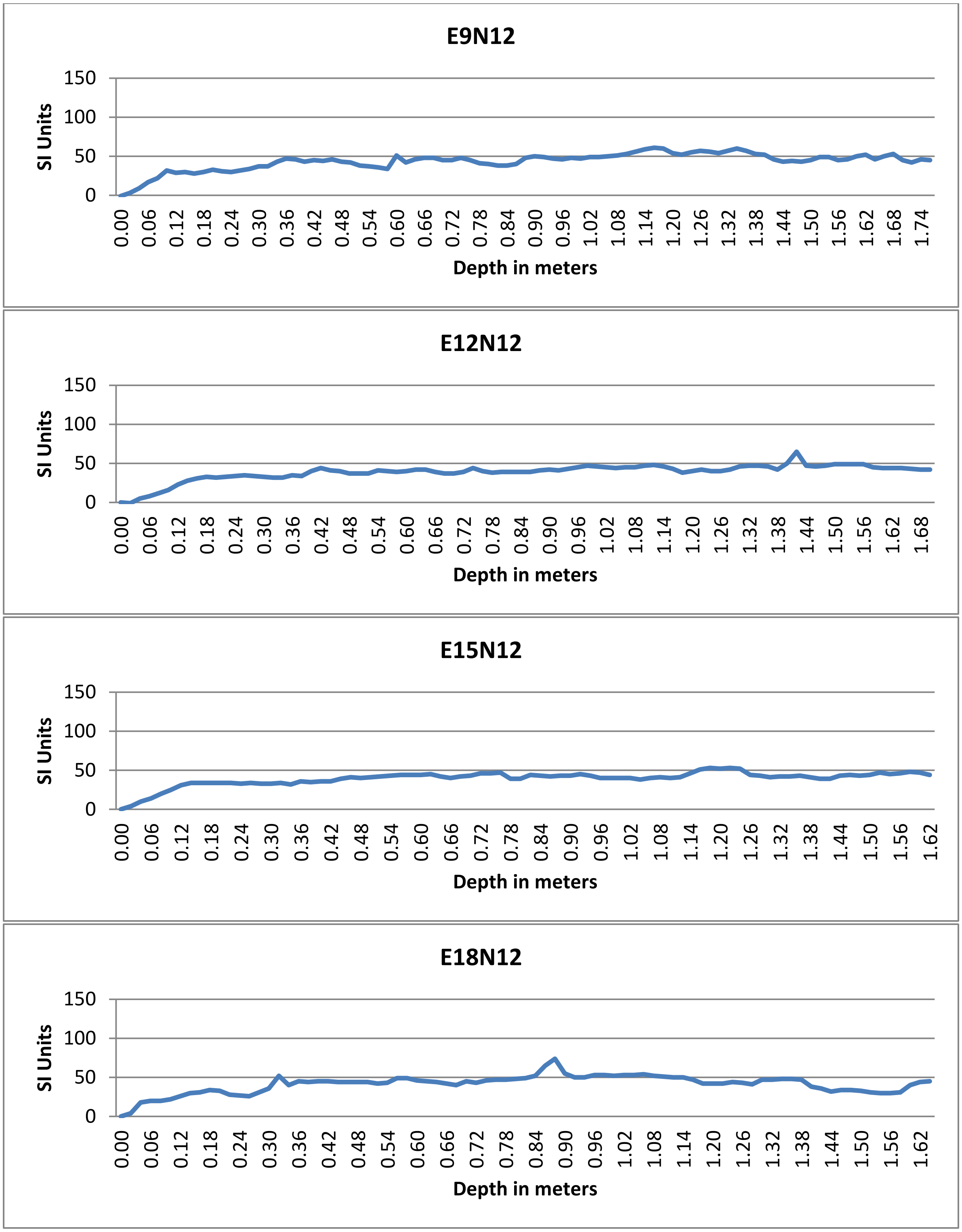

Figure 42 Arcola downhole profiles, N12 line.

Lessley

Our first visit to Lessley took place during the January 2015 trip to the Natchez Bluffs region. We collected gradiometer data from the field to the northeast of the mound and set out the transects for the downhole survey. Unfortunately, the battery on the computer failed so we were unable to take any readings. We returned again in June of 2015 with an external battery pack for the computer and the JMC probe. The southwest half of the mound is taken up by a 19th century cemetery with several large monuments and was obviously disturbed (fig. 43). We restricted out survey to the other half of the mound (fig. 44: Table 8). Like Arcola, most of the susceptibility profiles were low amplitude and relatively flat (figs. 45, 46). Most had readings that were barely more than 50 SI. The one exception, E9N6 had a single peak reading of 859 SI. The readings 2cm above and below this elevation were less than 100 SI and the readings above and below those were less than 50 SI. This has all the hallmarks of a single point reading. As a test, we placed the probe against a portion of the wrought iron fence which ran along the southwest side of the cemetery and got a reading of more than 1000 SI. It is likely that the reading at 1.48m below the surface at E9N6 was a piece of coffin hardware or a nail. This leads to the suggestion that there are unmarked, historic burials on the mound. There is, however, no indication of intact, burned surfaces. In fact, if the present of daub can be used to mark the location of prehistoric structures, the low amplitude returns of the downhole survey indicate that there were no structures on the mound at Lessley. At least, there were none that had burned.

Figure 43 Jay Johnson and Gabby Coggin taking downhole readings at Lessley using external battery pack.

Figure 44 Downhole locations at Lessley (after Nelson et. al 2013:170).

Table 8 Downlhole coordinates at Lessley, NAD83.

Coordinate	Easting	Northing
E9N3	648,634.62	3,448,192.30
E9N6	648,636.29	3,448,194.81
E9N9	648,637.97	3,448,197.32
E9N12	648,639.64	3,448,199.78
E9N15	648,641.24	3,448,202.32
E9N18	648,642.95	3,448,204.74
E9N21	648,644.69	3,448,207.24
E9N24	648,646.24	3,448,209.74
E0N15	648,633.86	3,448,207.24
E3N15	648,636.28	3,448,205.61
E6N15	648,638.82	3,448,203.98
E12N15	648,643.75	3,448,200.60

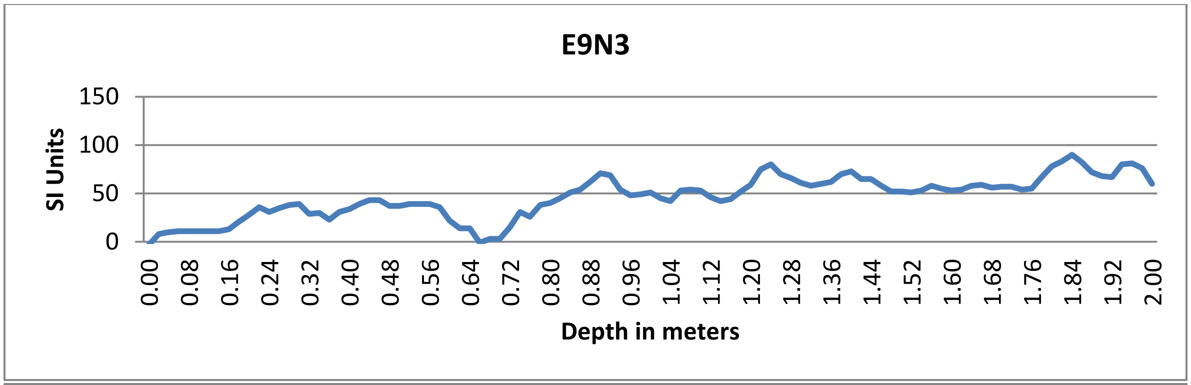
E9N3
SI Units
150
100
50
0
0.00
0.08
0.16
0.24
0.32
0.40
0.48
0.56
0.64
0.72
0.80
0.88
0.96
1.04
1.12
1.20
1.28
1.36
1.44
1.52
1.60
1.68
1.76
1.84
1.92
2.00
Depth in meters

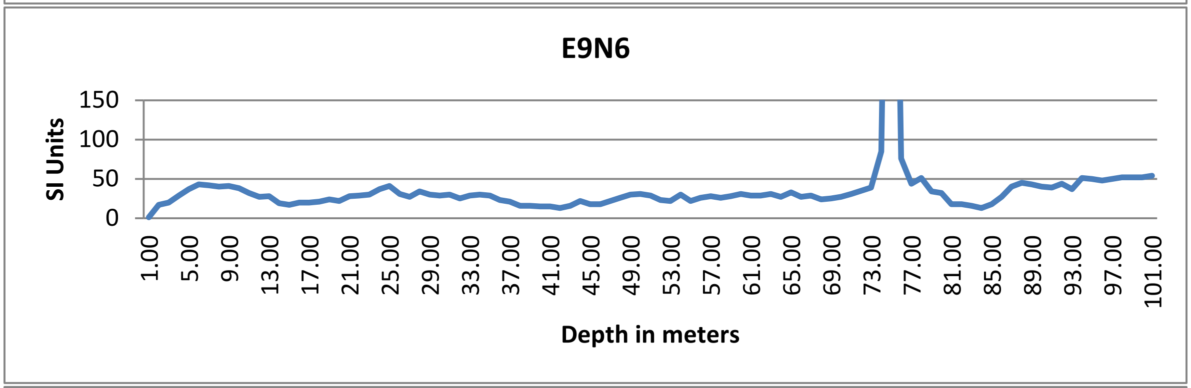
E9N6
SI Units
150
100
50
0
1.00
5.00
9.00
13.00
17.00
21.00
25.00
29.00
33.00
37.00
41.00
45.00
49.00
53.00
57.00
61.00
65.00
69.00
73.00
77.00
81.00
85.00
89.00
93.00
97.00
101.00
Depth in meters

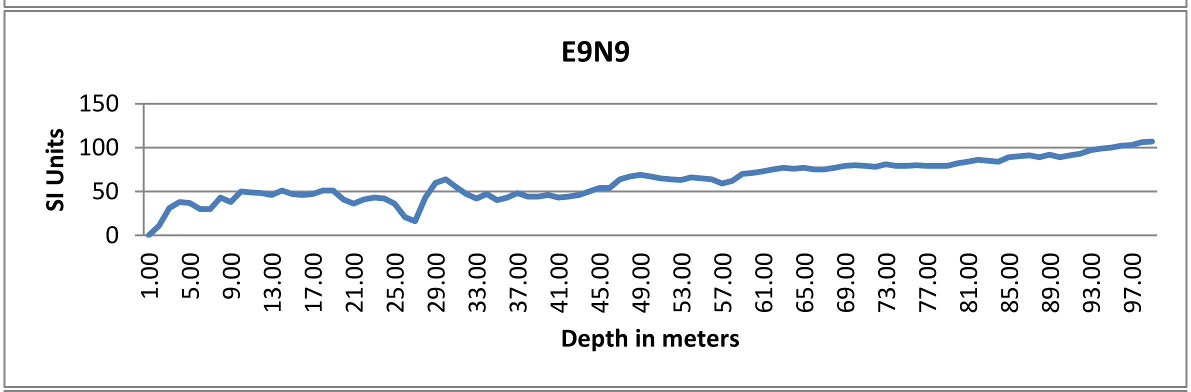
E9N9
SI Units
150
100
50
0
1.00
5.00
9.00
13.00
17.00
21.00
25.00
29.00
33.00
37.00
41.00
45.00
49.00
53.00
57.00
61.00
65.00
69.00
73.00
77.00
81.00
85.00
89.00
93.00
97.00
Depth in meters

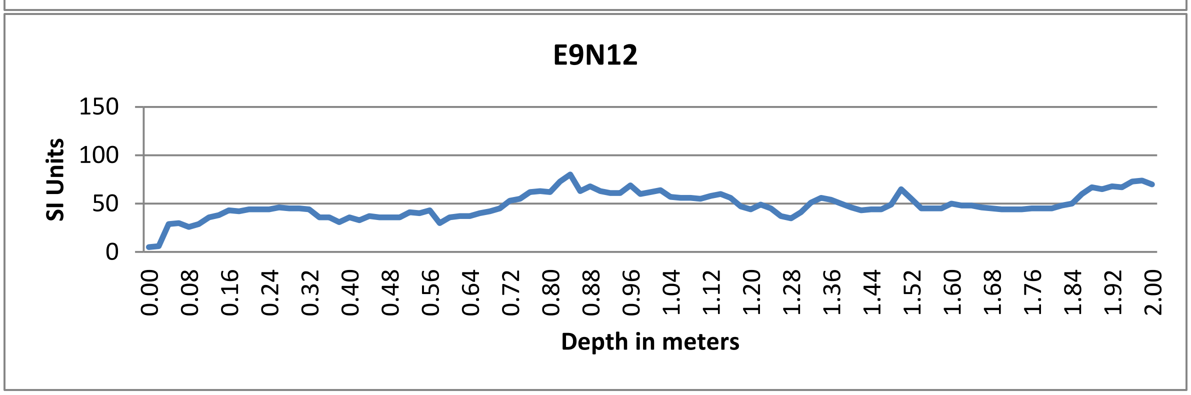
E9N12
SI Units
150
100
50
0
0.00
0.08
0.16
0.24
0.32
0.40
0.48
0.56
0.64
0.72
0.80
0.88
0.96
1.04
1.12
1.20
1.28
1.36
1.44
1.52
1.60
1.68
1.76
1.84
1.92
2.00
Depth in meters

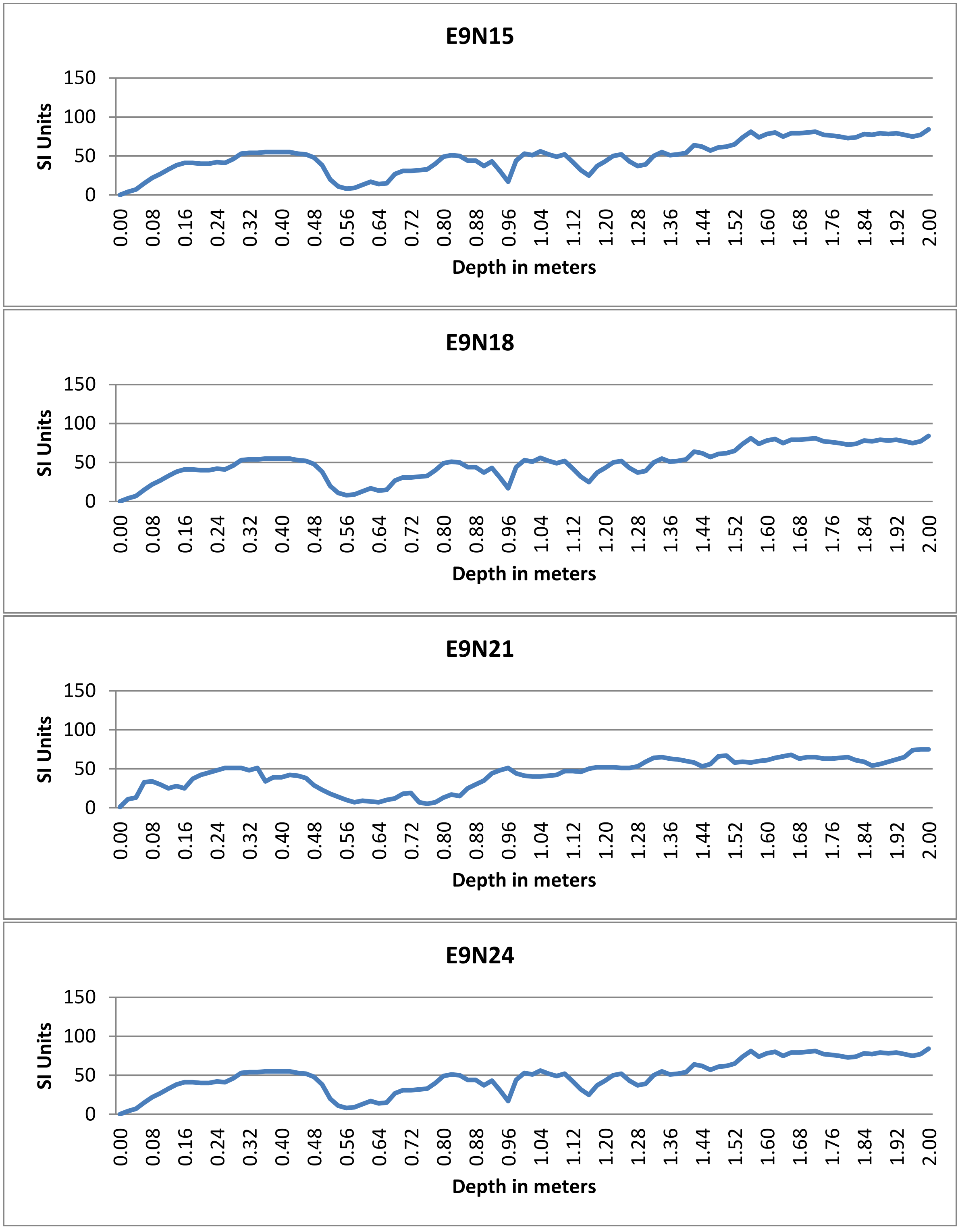

Figure 45 Lessley downhole profiles, E 9 line.

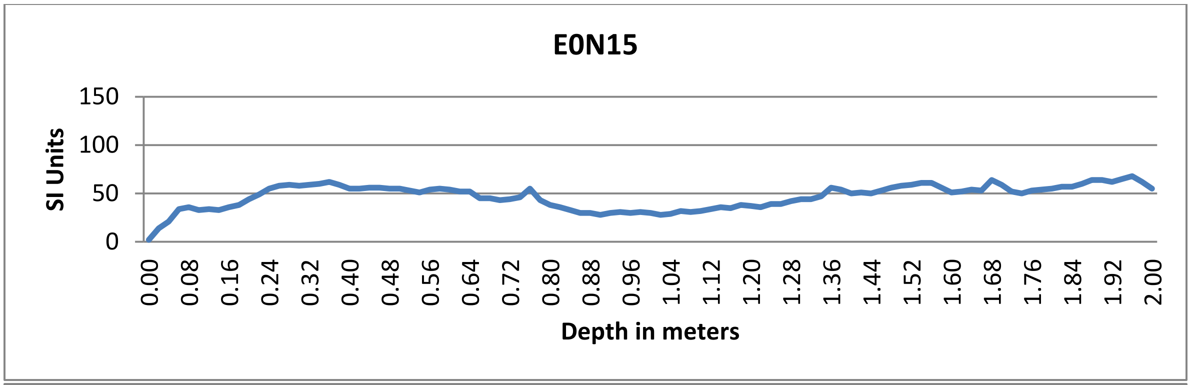
E0N15
SI Units
150
100
50
0
0.00
0.08
0.16
0.24
0.32
0.40
0.48
0.56
0.64
0.72
0.80
0.88
0.96
1.04
1.12
1.20
1.28
1.36
1.44
1.52
1.60
1.68
1.76
1.84
1.92
2.00
Depth in meters

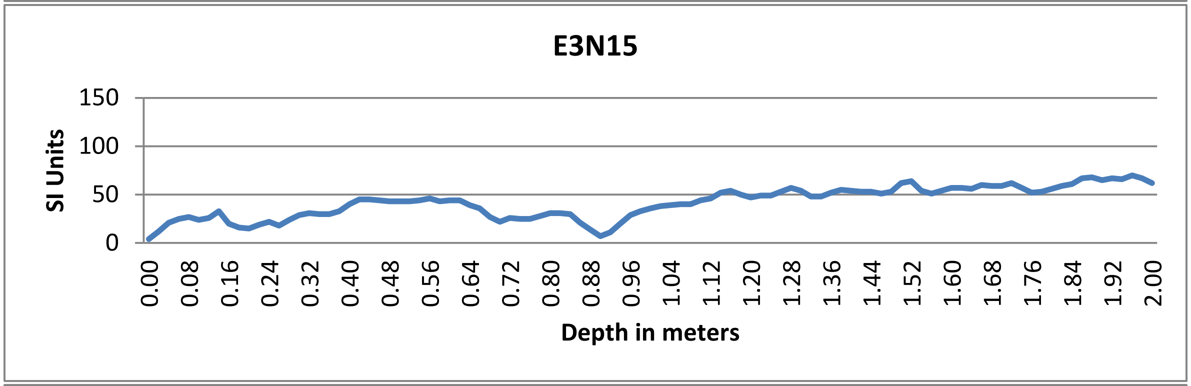
E3N15
SI Units
150
100
50
0
0.00
0.08
0.16
0.24
0.32
0.40
0.48
0.56
0.64
0.72
0.80
0.88
0.96
1.04
1.12
1.20
1.28
1.36
1.44
1.52
1.60
1.68
1.76
1.84
1.92
2.00
Depth in meters

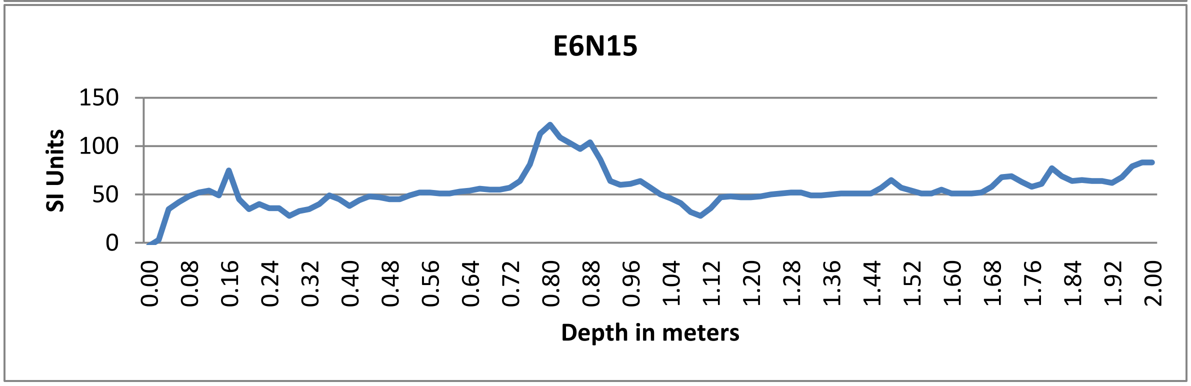
E6N15
SI Units
150
100
50
0
0.00
0.08
0.16
0.24
0.32
0.40
0.48
0.56
0.64
0.72
0.80
0.88
0.96
1.04
1.12
1.20
1.28
1.36
1.44
1.52
1.60
1.68
1.76
1.84
1.92
2.00
Depth in meters

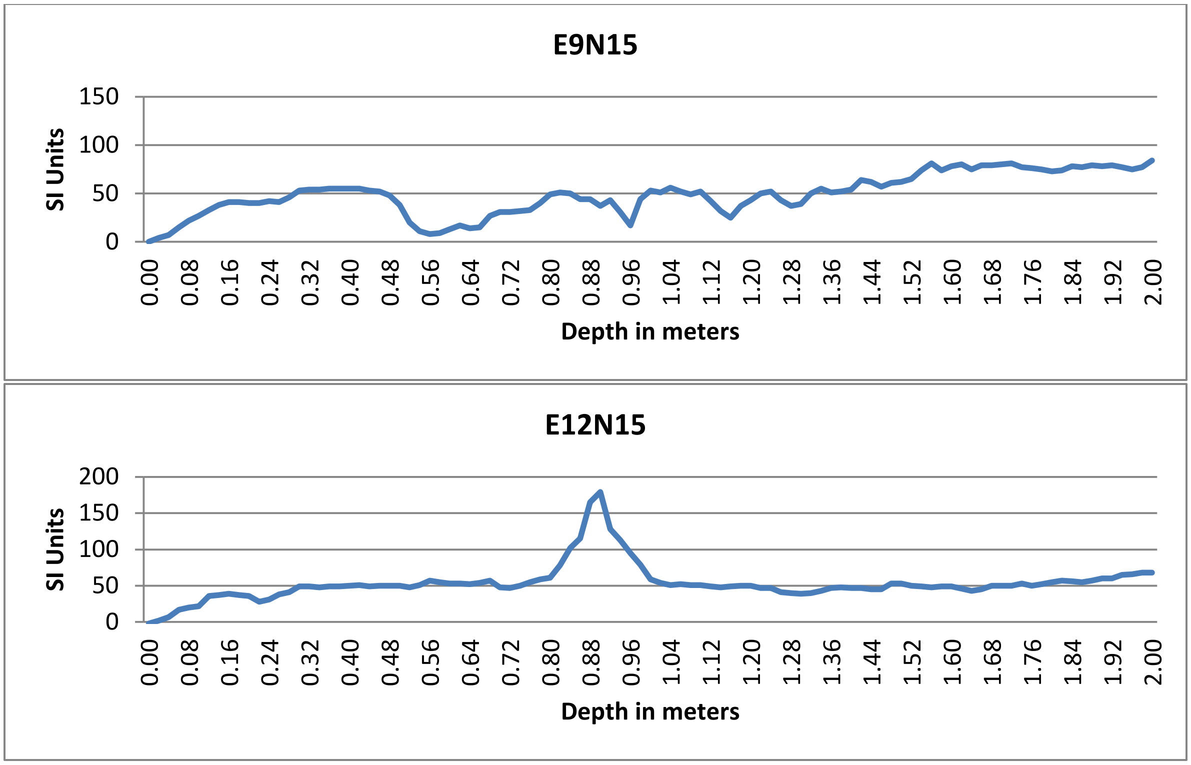

Figure 46 Lessley downhole profiles, N15 line.

Smith Creek

We visited Smith Creek at the end of our January 2015 trip to the Natchez Bluff region. It is the southernmost site on the Mound Trail. Since there was what appeared to be a midden deposit exposed in the road cut that removed the southwest corner of Mound A, we planned to see if it could be detected in the downhole susceptibility readings. Two cores were driven into a narrow bench just above the road cut on the eastern side of the mound (figs. 47-49). Their locations were shot in using the Mound Trail reference point on the top of the mound using a total station (Table 9). Meg Kassabaum located one of the test pits she dug during her 2015 field school at the site on that same bench which actually fell between the two cores, less than a half a meter from the southern one. The profile of that test pit shows a clearly defined boundary at about 1.38m below stake at the southwestern corner of the test pit (E641466, N3446026) which has an elevation of 36.194m. This artifact rich deposit continued to the bottom of the test pit at about 2.5m below surface (fig. 49). The elevation of the top of the midden deposit is about 34.796m which means it would have been encountered in the SC1 downhole at 1.127m down. SC2 would have encountered the top of the midden deposit at 1.650m below surface. We expected to see a dramatic increase in the susceptibility readings at these depths in both cores which should have continued to the bottom of the core. There is no such pattern (figs. 51, 52). In fact, the readings rarely exceed 100 SI. Smith Creek has eroded the eastern side of Mound C, leaving a narrow strip of what was probably the top of the mound. A single downhole survey was placed in that mound remnant in order to see if we could detect any burned surfaces. Once again, we record readings in the 0 to 100SI range with no evident patterning (fig. 53).

Figure 47 Sam Butz and Gabby Coggin preparing to take downhole readings on Mound A at Smith Creek.

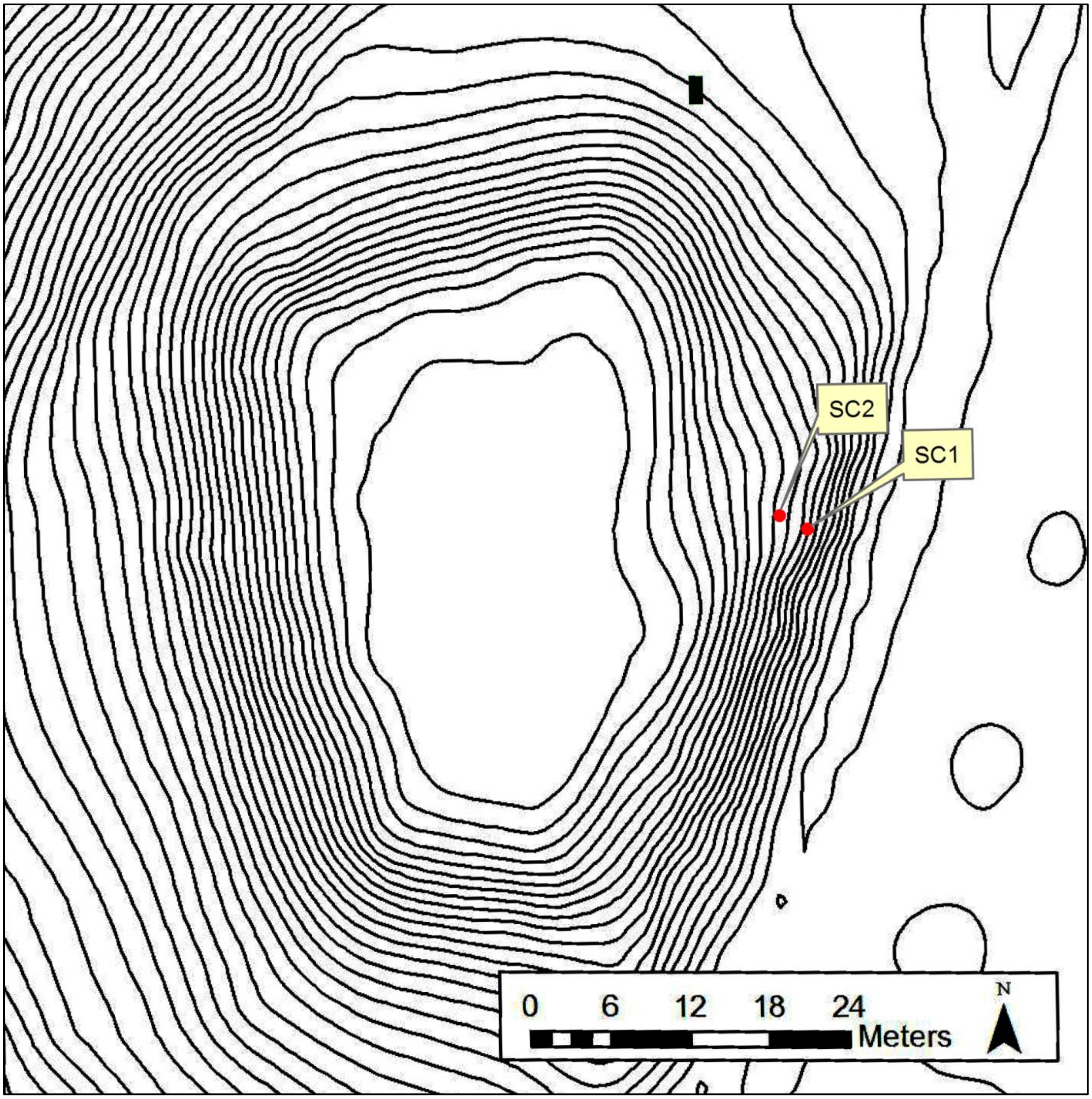

Figure 48 Downhole locations in Mound A at Smith Creek (after Kassabaum et. al 2014:fig10.2).

Table 9 Downhole coordinates at Smith Creek, NAD83.

ID	Easting	Northing	Elevation
SC1	641467.42	3446026.33	35.924
SC2	641465.38	3446027.40	36.414
SC3	641637.31	3446072.96	32.943

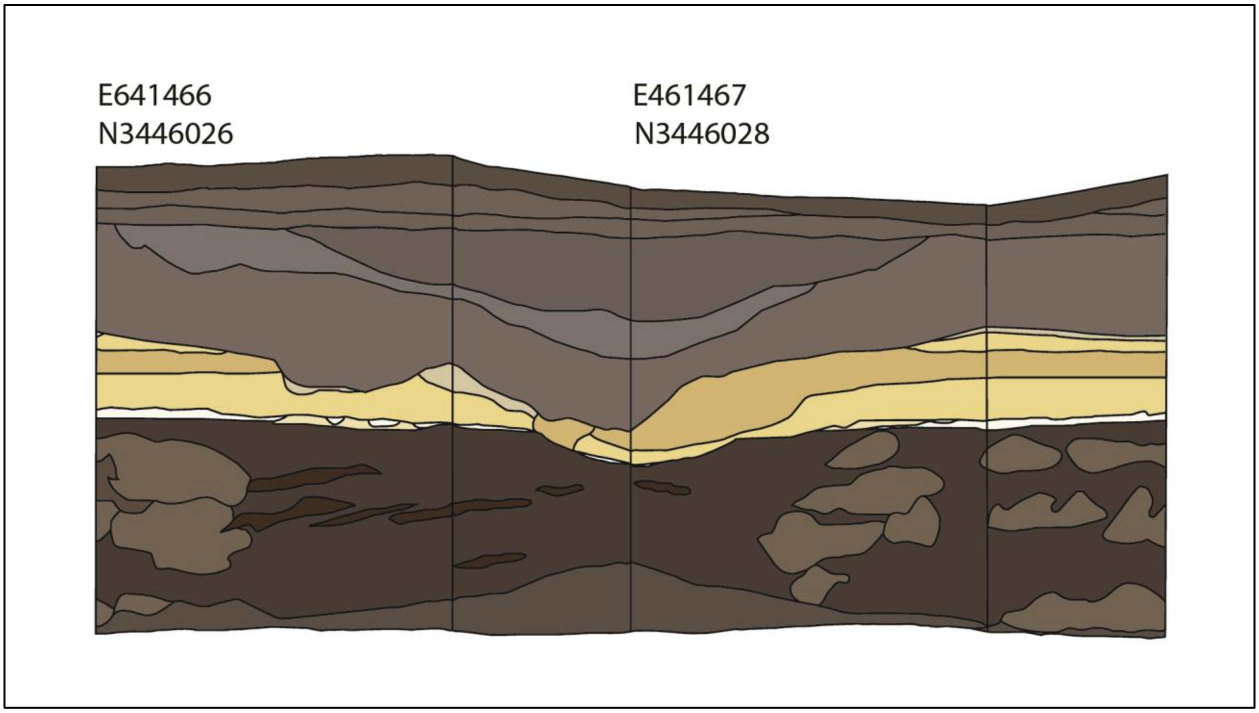

Figure 49 Mound A test pit profile courtesy of Meg Kassabaum.

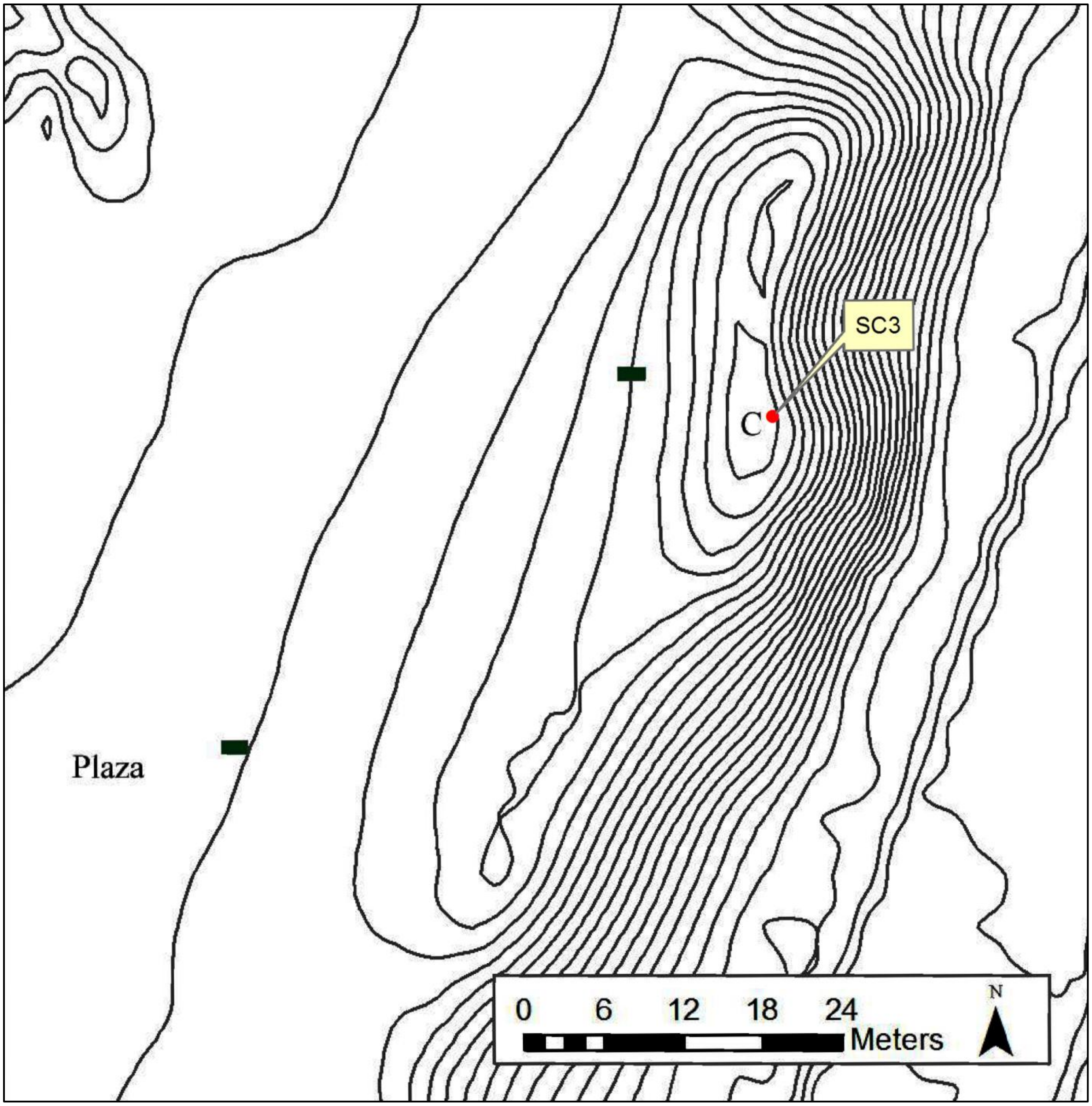

Figure 50 Downhole location in Mound C at Smith Creek (after Kassabaum et. al 2014:fig10.3).

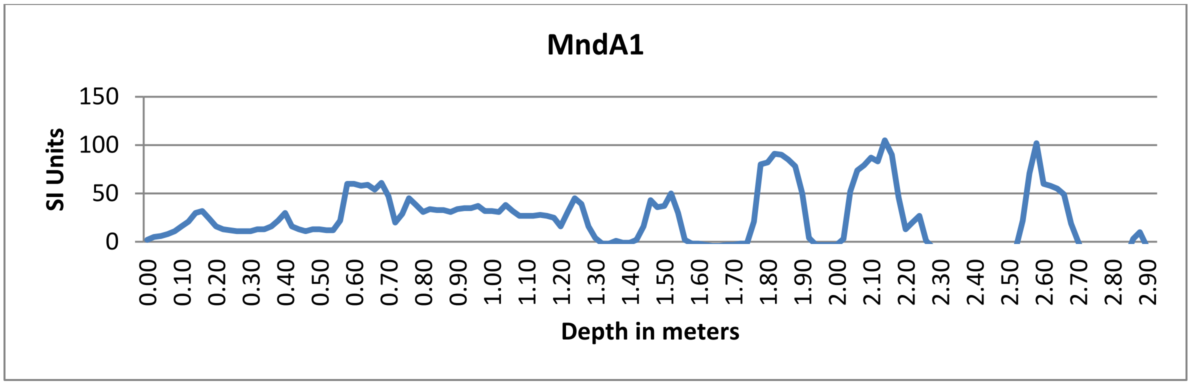

Figure 51 Smith Creek downhole profile, Mound A1.

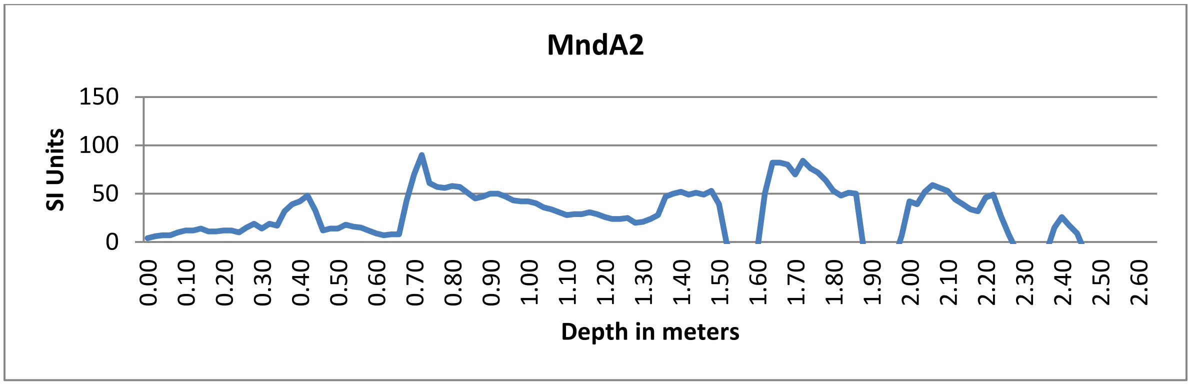

Figure 52 Smith Creek downhole profile, Mound A2.

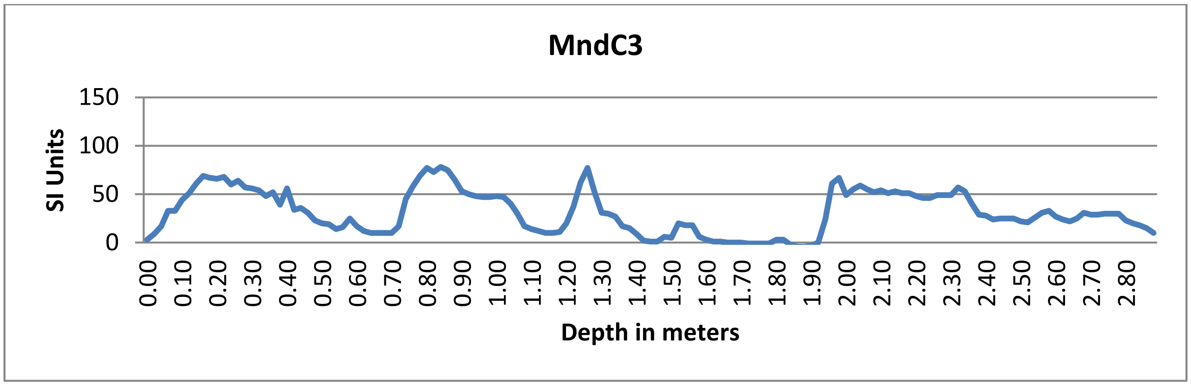

Figure 53 Smith Creek downhole profile, Mound C3

Summary and Conclusions

There are, of course, two kinds of conclusions that can be reached based on our research. In the first place, we can talk about results that are specific to each site and useful in interpreting the prehistory of that site. We can also talk about the methodological implications of our research.

Prehistory

In terms of providing data useful for future archaeological work at the site, the gradiometer surveys were clearly more productive than the downhole magnetic susceptibility surveys. The features identified at Arcola have already been explored by Kowalski in her dissertation research. Without the geophysical survey, she would have had to rely on controlled surface collections to identify areas of interest. Likewise, although there are no immediate plans to do additional fieldwork at Aden, the large circular feature located east of Mound B would be an excellent place to start.

On the other hand, the gradiometer surveys of Foster and Lessley produced nothing that can be of use in future archaeological research at the site. There are a couple of possible explanations. In the first place, because of the nature of modern land use in the Natchez Bluffs, large, open fields adjacent to prehistoric mounds are not common. It is always easier to pick out patterns in gradiometer imagery where you are looking at large areas. Perhaps if we had been able to survey larger areas, we would have seen something.

It is also possible that the loess soils of the Natchez Bluffs are less suitable for gradiometer surveys. The success of the surveys at Aden and Arcola was not surprising given our results in the northern Yazoo Basin where similar sites are located on similar soils. In fact, we intentionally did not plan to do any gradiometer survey in the northern segment of the Mound Trail. First because our surveys at sites like Hollywood, Parchman, and Carson have demonstrated the utility of the technique there and secondly because the middle and southern segments are relatively under-represented in terms of gradiometer surveys. However, the one large scale gradiometer survey that has been conducted in the plaza of a site located in the Natchez Bluffs, the survey at Feltus, did detect large pit features, just not structures. It is clearly too early to discount the utility of gradiometer prospection on prehistoric sites in the Natchez Bluffs region.

If we had not done the downhole magnetic susceptibility survey at Winterville, our assessment of the utility this technique would be far less positive. The Winterville survey did demonstrate that it is possible to map burned surfaces using susceptibility. It also allows us to conclude that there are no intact burned surfaces at any of the other mounds, at least in the areas covered by our survey. Although we did not encounter a burned surface at Lessley, we did detect a metal artifact at a depth which makes it clear that in addition to the numerous marked burials on one half of the mound top, there are likely to be more, unmarked burials on the other half. Our results from Dunn indicate that the relative horizontal and vertical density of daub can be mapped using susceptibility. It also allows us to conclude that there are no intact burned surfaces at any of the other mounds, at least in the areas covered by our survey.

Methodology

The primary methodological lesson to be learned from the gradiometer survey is the flexibility of the technique, especially when using the Bartington Grad601 instrument. Although most of the discussions of the layout of a gradiometer survey indicate that the transects should run north-south in order to minimize bearing errors, we have found that not to be necessary. Because of the deep furrows and Arcola and the rows of corn at Aden, we had to run the transects east-west. There was no appreciable impact on the quality of the data. The second lesson that was demonstrated at both sites is that while it is preferable to have square survey grids, in a GIS environment, it not essential. Because we had to walk between the rows and the spacing between the transects at Arcola and Aden was less than a meter, our survey grid were not square. This was not a problem. All we had to do was take GPS readings on the corners of the survey area to use in locating the survey and the probable cultural features it revealed in space.

While it may seem to be a trivial improvement, the replacement of the Oakfield soil probe with the JMC T-Handle probe made it much easier to achieve the target depth for the downhole survey. It was simply not possible to push the probe through the dry, clay-rich mound fill. The sample tube and shafts are interchangeable between the two brands but JMC probe was designed to be driven into the ground. JMC also offers a hand tool designed to clear the bit when daub or roots plug it which we enjoyed.

The downhole susceptibility survey of Mound A at Hollywood suggests an improvement it the survey design. Although, as Bryan Haley's excavation at the site have demonstrated, there are burned surfaces on top of Mound A, we missed them because the two survey transects followed the main axes of the mound top, intersecting at the center. Implicit in this survey design was the idea that mound top structures were centered on the mound. The major implication is that rather than transects, the distribution of downhole survey sample should probably be determined using a grid in order to cover the entire mound top.

References Cited

Burks, Jerod A.

2014 Geophysical Survey at Ohio Earthworks: updating Nineteenth Century Maps and Filling the 'Empty' Spaces. *Archaeological Prospection* 21(1):5-13.

Burks, Jerod A. and Robert A. Cook

2011 Beyond Squier and Davis: Rediscovering Ohio's Earthworks Using Geophysical Remote Sensing. *American Antiquity* 76(4):667-689.

Clark, Anthony

1996 *Seeing Beneath the Soil, Prospecting Methods in Archaeology*. 2nd Ed. B. T. Batsford Ltd., London.

Clay, R. Burle

2001 Complementary geophysical survey techniques: why two ways are always better than one. *Southeastern Archaeology* 20(1):31-43.

Dalin, Rinita A.

2001 A magnetic susceptibility logger for archaeological application. *Geoarchaeology* 16(3):263-273.

2006 Magnetic susceptibility. In *Remote Sensing in Archaeology: An Explicitly North American Perspective*, edited by Jay K. Johnson, pp. 161-203. The University of Alabama Press, Tuscaloosa.

Gaffney, Christopher and John Gater

2003 *Revealing the Buried Past: Geophysics for Archaeologists*. Tempus Publishing Ltd, Stroud, Gloucestershire.

Haley, Bryan S.

2014 The big picture at Hollywood: Geophysical and archaeological investigations at a Mississippian mound centre. *Archaeological Prospection* 21(1):39-47.

Harris, Stephen

2011 The Use of Space at the Late Woodland Shady Grove Site (22-QU-525). Unpublished Master's Thesis, Department of Sociology and Anthropology, University of Mississippi.

Henry, Edward R.
2009 Geophysical Prospection and Excavation at an Early Woodland Ceremonial Circle in Bourbon County, KY. Unpublished Master's Thesis, Department of Sociology and Anthropology, University of Mississippi.

Henry, Edward R. and Jay K. Johnson
2012 Geophysical Investigations at Feltus Mounds (22Je568), Jefferson County, MS. Report Prepared for the Mississippi Department of Archives and History, Center for Archaeological Research, University of Mississippi.

Henry, Edward R., Nicholas R. Laracuente, Jared S. Case, and J.K. Johnson
2014 Incorporating multistaged geophysical data into regional-scale models: A case study from an Adena burial mound in central Kentucky. *Archaeological Prospection* 21(1):15-26.

Jackson, H.Edwin and Jessica Kowalski
2015 Report of Investigations for the Southern Yazoo Portion of the Mississippi Mound Trail Project, 2014 Season, Issaquena, Washington, Sharkey, and Warren Counties, Mississippi. Report submitted to the Mississippi Department of Archives and History, University of Southern Mississippi.

Kassabaum, Megan C., Edward R. Henry, Vincas P. Steponaitis, and John W. O'Hear
2014 Between Surface and Summit: the Process of Mound Construction at Feltus . *Archaeological Prospection* 21(1):27-37.

Kassabaum, Megan C., Vincas P. Steponaitis, and Mallory A. Melton
2014 Mississippi Mound Trail, Southern Region: Phase 2 Investigations. Report submitted to the Mississippi Department of Archives and History, Research Laboratories of Archaeology, University of North Carolina at Chapel Hill.

Kowalski, Jessica, Cecilia. Henderson, H. Edwin Jackson
2014 Excavation Summary and Ceramic Analysis for the Southern Yazoo Portion of the Mississippi Mound Trail Project; Issaquena, Sharkey, and Washington Counties, Mississippi, 2013 Field Season. Report submitted to the Mississippi Department of Archives and History, University of Southern Mississippi.

Kvamme, Kenneth
2006 Magnetometry: Nature's Gift to Archaeology. In *Remote Sensing in Archaeology: An Explicitly North American Perspective*, edited by Jay K. Johnson, pp. 205-234. University of Alabama Press, Tuscaloosa.

Mehta, Jayur M.
2015 Native American Monuments and Landscape in the Lower Mississippi Valley. Unpublished Ph.D. dissertation, Department of Anthropology, Tulane University, New Orleans.

Nelson, Erin Stevens
2014 Intimate landscapes: the social nature of the spaces between. *Archaeological Prospection* 21(1):49-57.

2016 Community Identity in the Late Prehistoric Yazoo Basin: The Archaeology of Parchmann Place, Coahoma County, Mississippi. Unpublished PhD Dissertation, Department of Anthropology, University of North Carolina, Chapel Hill.

Nelson, Erin Stevens., R.P.Steven Davis, Vincas P. Steponaitis, Andrius Valiunas
2013 Mississippi Mound Trail, Southern Region: Phase 1 Investigations. Report submitted to the Mississippi Department of Archives and History, Research Laboratories of Archaeology, University of North Carolina at Chapel Hill.

Reynolds, Mathew
2002 Magnetic Remote Sensing and Ground Truth: Some Example from the Hollywood Site, Tunica County, Mississippi. Unpublished Master's Thesis, Department of Sociology and Anthropology, University of Mississippi.

Stevens, Erin
2006 The Making of a Monument: Investigating Mound Stratigraphy in the Yazoo Basin. Unpublished Master's Thesis, Department of Sociology and Anthropology, University of Mississippi.